Universidade de Aveiro Departamento de Química
Ano 2013

Renato Manuel Pereira Alves

Estudos da resposta epitelial à hiperglicemia induzida por estreptozotocina

Studies of epithelial response to streptozotocin-induced hyperglycemia

Universidade de Aveiro Departamento de Química
Ano 2013

Renato Manuel Pereira Alves

Estudos da resposta epitelial à hiperglicemia induzida por estreptozotocina

Studies of epithelial response to streptozotocin-induced hyperglycemia

Tese apresentada à Universidade de Aveiro para cumprimento dos requisitos necessários à obtenção do grau de Doutor em Bioquímica, realizada sob a orientação científica do Doutor Francisco Manuel Lemos Amado, Professor Associado da Escola Superior de Saúde da Universidade de Aveiro

Apoio financeiro da FCT e do FSE no âmbito do Quadro de Referência Estratégico Nacional.

o júri

presidente

Doutor João de Lemos Pinto
professor catedrático da Universidade de Aveiro

Doutor José Alberto Ramos Duarte
professor catedrático da Faculdade de Desporto da Universidade do Porto

Doutor Fernando Manuel Gomes Remião
professor associado da Faculdade de Farmácia da Universidade do Porto

Doutor Francisco Manuel Lemos Amado
professor associado da Universidade de Aveiro

Doutor Armando José Cerejo Caseiro
professor adjunto da Escola Superior de Tecnologia da Saúde de Coimbra

Doutora Maria do Rosário Gonçalves dos Reis Marques Domingues
professora auxiliar da Universidade de Aveiro

Doutora Luísa Alejandra Helguero
Investigadora auxiliar da Universidade de Aveiro

agradecimentos

Embora uma tese tenha uma natureza individual, qualquer trabalho resulta sempre da interacção com as pessoas que me rodearam durante estes anos. Assim, ao concluir mais esta etapa, não posso deixar de agradecer:

- ao Prof. Francisco Amado e ao grupo de Espectrometria de Massa do Departamento de Química, pelas condições que proporcionaram para a realização deste trabalho.

- ao Prof. José Alberto Duarte da FADEUP, e ao Daniel, pelo apoio na elaboração e manutenção do protocolo animal.

- ao Prof. Fernando Remião do grupo de Toxicologia da FFUP, e muito especialmente à Renata e à Vânia pela preciosa ajuda na obtenção e análise dos dados de citometria de fluxo.

- aos meus colegas e amigos que me acompanharam no laboratório: Alex, André, Ana Isabel, Catarina, Cláudia, Cristina, Miguel, Susana, Zita e em especial ao Armando, pelo apoio nesta recta final. Obrigado a todos pelos bons momentos passados, fossem em trabalho ou em lazer!

- à Rita, Amandine e Virginia pelos já longos anos de especial amizade, em contacto quase diário e repletos de excelentes momentos passados em conjunto, que tornaram esta etapa muito mais agradável!

- aos meus amigos que, pessoalmente ou à distância, estiveram sempre disponíveis para me ouvir e aconselhar. Não teria espaço para vos nomear a todos, e seria imperdoável correr o risco de me esquecer de alguém, mas sem dúvida que ao lerem isto vão saber que ocuparão sempre um lugar especial pela vossa amizade.

- à minha família pelo apoio e por também serem um “porto seguro” nos bons e nos maus momentos com que a vida nos presenteia.

Finalmente, agradeço também à Fundação para a Ciência e Tecnologia pelo financiamento através da bolsa de doutoramento SHRH/BD/46829/2008, sem o qual este trabalho não teria sido possível.

palavras-chave Diabetes, hiperglicemia, glândulas salivares, endotélio, proteómica

resumo

A hiperglicemia é a principal característica da diabetes mellitus (DM), uma das causas de morte que mais cresce em Portugal, e cujas complicações a longo prazo são mais debilitantes e mais sobrecarregam os sistemas de saúde. No entanto, os mecanismos subjacentes à resposta fisiológica de alguns tecidos à hiperglicemia não estão completamente esclarecidos.

Este estudo teve como objetivo avaliar de que forma o tempo de exposição à hiperglicemia afeta dois tecidos epiteliais, o endotélio e as glândulas salivares, que são frequentemente associados a complicações da DM, utilizando um modelo animal. Adicionalmente, procurou-se encontrar novos biomarcadores para avaliar a suscetibilidade a complicações orais em diabéticos, analisando as modificações pós-traducionais (PTMs) da família de proteínas mais representativa na saliva humana: proteínas ricas em prolina (PRPs).

A disfunção vascular está na origem de várias complicações da diabetes. Neste sentido, observou-se uma progressiva disfunção endotelial com o aumento do tempo de exposição à hiperglicemia, que resulta do aumento de danos no endotélio e da diminuição da capacidade de mobilização de células progenitoras. Simultaneamente, o aumento observado na atividade da via de ativação do sistema de complemento mediada por lectinas (MBL), sugere um envolvimento do sistema de imunidade inata na patogénese da disfunção vascular.

Outra complicação comum da DM é o desenvolvimento de doenças orais, nomeadamente as relacionadas com a redução da secreção salivar. Na análise às glândulas submandibulares, observou-se uma resposta inicial à hiperglicemia com fortes variações na expressão de proteínas, mas a longo prazo, estas variações foram atenuadas, sugerindo um mecanismo de adaptação à hiperglicemia crónica. Adicionalmente, as proteínas relacionadas com a secreção, como as anexinas, apresentaram-se sobre-expressas, enquanto as calicreinas e proteínas metabólicas estavam sub-expressas. Estas variações sugerem que, apesar de uma diminuição da capacidade de regeneração, as células tentam superar a perda de tecido por meio do aumento da secreção, embora sem êxito.

O comprometimento funcional das glândulas salivares tem consequências na composição e funções da saliva. Analisando as PTMs das PRPs salivares humanas, observou-se um aumento da frequência de péptidos com ciclização de resíduos N-terminais de glutamina a piroglutamato, o que confere uma resistência à atividade proteolítica que, por sua vez, se encontra aumentada em diabéticos. Assim, a presença de péptidos com N-piroglutamato poderá ser um potencial biomarcador da suscetibilidade a complicações orais em diabéticos.

keywords Diabetes, hiperglycemia, salivary glands, endothelium, proteomics

abstract

Hyperglycemia is the major hallmark of diabetes mellitus, which is one of the fastest growing causes of death in Portugal and whose long-term complications are more debilitating and burden health-care systems. However, the mechanisms underlying the physiological response of some tissues to hyperglycemia are not fully understood.

This study aimed to understand how the time of exposure to hyperglycemia affects two epithelial tissues, the endothelium and the salivary glands tissue, that are often associated with diabetes mellitus complications, using an animal model. Complementarily, post translational modifications of the most representative family of human salivary proteins, salivary proline-rich proteins (PRPs), were evaluated to propose novel biomarkers to assess the susceptibility of diabetic patients to oral complications.

Vascular dysfunction is on the genesis of several diabetes complications. In this sense, it was observed a progressive endothelial dysfunction over time, due to the increase of endothelial damage and diminished capacity for the mobilization of progenitor cells. Concomitantly, it was observed an increased activity of the MBL pathway of activation of the complement system, suggesting an involvement of the innate immune system in the pathogenesis of vascular dysfunction.

Another common complication of diabetes is the development of oral diseases, namely related to the reduction of saliva secretion. Submandibular glands presented an early-phase response with strong variations in protein expression, which were attenuated in long-term exposure, suggesting an adaptive mechanism to chronic hyperglycemia. Moreover, proteins related to secretion, such as annexins, were found up-regulated, while kallikreins and metabolic proteins were down-regulated. This suggests that, despite a reduction of the regeneration ability, cells may try to overcome the apoptotic loss of tissue, though unsuccessfully, through the increase of secretion.

Impairment of salivary gland function has consequences in saliva composition and functions. Analysing the PRPs of human salivary proteins, it was observed an increase in the frequency of peptides bearing N-terminal cyclization of glutamine residues to pyroglutamate, which confers some resistance to the increased activity of proteases observed in diabetic patients, making it a potential biomarker for susceptibility to oral complications among diabetic patients.

Man may be the captain of his fate, but he is also the victim of his blood sugar

Wilfrid Oakley [Trans. Med. Soc. Lond. 78, 16 (1962)]

Table of Contents

List of Figures

List of Abbreviations

a/bPRPs	Acidic/basic proline-rich proteins
AAI	Anti-insulin autoantibodies
ADA	American Diabetes Association
AGEs	Advanced-glycation endproducts
BMP	Bone morphogenetic protein
BrdU	Bromo deoxy-Uridine
BSA	Bovine serum albumin
CEC	Circulating mature endothelial cells
CVD	Cardiovascular disease
DAF	Decay-accelerating factor
DM	Diabetes mellitus
EDHF	Endothelium-derived hyperpolarizing factors
EDTA	Ethylenediaminetetraacetic acid
ELAM	Endothelial leucocyte adhesion molecule
eNOS	Endothelial nitric oxide synthase
EPC	Circulating progenitor endothelial cells
ET-1	Endothelin-1
FACS	Fluorescence-activated cell sorting
FGF	Fibroblast growth factor
FPG	Fasting plasma glucose
GABA	Gamma-aminobutyric acid
GAD	Glutamic acid decarboxylase
GDM	Gestational diabetes mellitus
HGF	Hepatocyte growth factor
HIF	Hypoxia-inducible factor
ICAM	Intercellular adhesion molecule
IDF	International Diabetes Federation
IFN-gamma	Interferon gamma
IgA	Immunoglobulin A
IGF	Insulin-like growth factor
IGFR	Insulin-like growth factor receptor
IgG	Immunoglobulin G
IR	Insulin receptor
MAC	Membrane attack complex
MAPK/Erk1/2	Mitogen-activated protein kinase/Extracellular signal-regulated kinases 1/2

MASP	MBL-associated serine protease
NAD	Nicotinamide adenine dinucleotide
NCDs	Non-communicable diseases
OGTT	Oral glucose tolerance test
PAD	Peripheral artery disease
PBS	Phosphate-buffered saline
PTMs	Post-translational modifications
ROS	Reactive oxygen species
SOPF	Specific and opportunistic pathogens free
SPF	Specific pathogens free
STZ	Streptozotocin
T1DM	Type 1 Diabetes mellitus
T2DM	Type 2 Diabetes mellitus
TBS	Tris-buffered saline
TNF-alpha	Tumour necrosis factor alpha
VCAM	Vascular cell adhesion molecule
VEGF	Vascular endothelial growth factor
VEGFR	Vascular endothelial growth factor receptor
WHO	World Health Organization

Other abbreviations will be defined when used in the text

I. GENERAL INTRODUCTION

1. Introduction

Hyperglycaemia is the major hallmark of diabetes mellitus (DM). In fact, DM is clinically defined as a syndrome of disordered metabolism where, due to a deficiency in insulin production and/or its action, patients present inappropriate hyperglycemia (Gardner, Shoback et al. 2011). Thus, the study of its mechanisms and effects in the organism is essential to fully understand the disease and further advance in the search for more effective treatments and even a cure.

2. Diagnosis and classification of diabetes mellitus

The criteria for the diagnosis and classification of diabetes have evolved with the accumulation of new knowledge since, in 1979, a new definition was proposed by the (American) National Diabetes Data Group Committee, and was generally accepted by the major health organizations in America and Europe, including the World Health Organization (WHO). An updated report is published annually by the American Diabetes Association (ADA), as a supplement to the journal Diabetes Care, summarizing the latest clinical practice recommendations (American Diabetes Association 2013).

The classical diagnosis of DM has been based in measuring the fasting plasma glucose (FPG) or with an oral glucose tolerance test (OGTT). The current WHO diagnostic criteria for DM are FPG ≥7.0 mmol/l (126 mg/dl) or 2–h plasma glucose ≥11.1 mmol/l (200 mg/dl) during an OGTT (World Health Organization. 2006). However, other tests have been used, especially to detect early stages of the disease where glycemia levels do not fulfil the requirements for a diagnosis of DM, but are still higher than normal. The measurement of glycated hemoglobin (HbA_{1c}) is another widely used marker for chronic hyperglycemia, as it reflects the average blood glucose levels over the previous 2-3 months. It is not recommended as a suitable diagnostic tool by the WHO, due to the lack of a standardization of the assay and hence the definition of a threshold (World

Health Organization. 2006). Nonetheless, the ADA has included it in the latest review for the diagnosis and classification of DM, following the publication of a report from an International Expert Committee recommending its use with a threshold of ≥6.5%, if using a method certified by the (American) National Glycohemoglobin Standardization Program (NGSP). As the ADA points out, there are obvious advantages of using a chronic marker (HbA_{1c}) instead of a more acute (FPG or OGTT), nevertheless, the advantages must be balanced with the higher cost per test, its limited availability worldwide and the influence of other physiological conditions such as anemia or hemoglobinopathies (International Expert Committee 2009).

As from 2013, DM is classified into 4 major categories: Type 1, Type 2, Gestational and Other Specific Types (American Diabetes Association 2013).

Type 1 diabetes mellitus (T1DM) is the result of the partial or complete absence of insulin production originated by the destruction of pancreatic beta-cells (Patterson, Dahlquist et al. 2009). Consequently, patients rely on insulin therapy to survive. The aetiology of beta-cell destruction may be an autoimmune mechanism or an undeterminable cause, resulting in “autoimmune T1DM” or “idiopathic T1DM” respectively (Deshpande, Harris-Hayes et al. 2008; Jurysta, Nicaise et al. 2013). As a result of the lack of insulin, glycemic control is impaired and may result in periods of hyperglycemia, as well as hypoglycemia. Due to the dependency of insulin therapy to survive, T1DM was formerly known as insulin-dependent DM. In a similar manner, because of its early onset it could also be referred as juvenile-onset DM.

Type 2 diabetes mellitus (T2DM) is by far the most frequent type of diabetes; approximately 90%-95% of the cases reported. It often starts with the development of insulin resistance by muscle cells and adipocytes, thus preventing the intake of glucose by these cells and keeping them in a permanent fasting metabolism. Although initially the pancreas tries to overcome this by secreting more insulin, over time the secretion capacity

is also affected. Due to the later onset when compared with T1DM, T2DM was also known as adult-onset diabetes or noninsulin-dependent diabetes, as it usually does not require insulin therapy.

When hyperglycemia is detected during pregnancy, it is named Gestational diabetes mellitus (GDM). This type of diabetes is usually diagnosed during prenatal screening tests but its symptoms are very similar to T2DM. It occurs in 7% of pregnancies worldwide and usually disappears after delivery; however both women and their children have increased risk of developing T2DM later in life. Left untreated, it may carry risks to both mother and child (IDF guidelines).

The cases of DM that cannot be included in any of the other categories are referred to as other types of DM and may include cases ranging from genetic defects to infections, or drug-induced forms. The American Diabetes Association has classified them into 8 sub-categories, which are further subdivided, according to their aetiology.

When FPG or OGTT values are still out of the normal range but not enough to be diagnosed as DM, individuals are considered to be in a state of prediabetes. Individuals presenting FPG <7.0 mmol/l (126 mg/dl) and 2–h plasma glucose ≥7.8 and <11.1 mmol/l (140 mg/dl and 200 mg/dl) are diagnosed with impaired glucose tolerance (IGT), while individuals presenting FPG >6.1 and ≤6.9 mmol/l (110 mg/dl and 125 mg/dl) and 2-h plasma glucose <7.8 mmol/l (140 mg/dl) are diagnosed with impaired fasting glucose (World Health Organization. 2006)

3. Physiological and molecular mechanisms for regulation of glycemia

3.1. Glucose transporters

Glucose is a water soluble simple monosaccharide; hence it does not cross the lipid bilayer by simple diffusion and needs carrier proteins to facilitate the diffusion along the concentration gradient, from the bloodstream into the cells. In mammalian cells, glucose is transported by

a family of transport facilitators, the GLUT transporters, although these may transport sugars and polyols other than glucose. The 13 members of this family are structurally divided into 3 classes: Class I (GLUT1-4), Class II (GLUT5, 7, 8 and 11) and Class III (GLUT6, 8, 10 and 12 and HMIT) (Joost and Thorens 2001).

Class I contains the most well characterized and widely distributed members. GLUT1 is expressed in fetal tissues, erythrocytes and endothelial cells, namely from the blood-brain barrier. GLUT2 is expressed especially in pancreatic beta-cells, liver and kidney, as well as in the basolateral membrane of small intestine cells, and has the lowest affinity for glucose ensuring that transporter saturation is not rate limiting and rapidly reaches the equilibrium of the intracellular/extracellular glucose concentration. GLUT3 is mainly present in brain and nervous tissue but is also detected in lower levels in kidney, liver and heart; its distribution in tissues with a high glucose demand together with the high affinity presented for glucose, suggests it is essential to allow glucose intake in those cells even in the case of hypoglycemia. Finally, GLUT4 is the primary transporter in adipose tissue, skeletal muscle and heart; the expression and translocation of this transporter to the plasma membrane is regulated by insulin and it is essential in the rapid removal of blood glucose into the body's glycogen and triacylglycerol storage tissues (Bell, Kayano et al. 1990; Gould and Holman 1993; Joost and Thorens 2001; Jurysta, Nicaise et al. 2013).

Classes II and III members are structurally distinct from Class I members, some of which are not fully characterized (Joost and Thorens 2001; Uldry and Thorens 2004).

3.2. Endocrine regulation of glycemia

The pancreas is an abdominal organ that comprises both exocrine and endocrine cell types, as well as ductal cells. The exocrine function is performed by acinar cells that secrete digestive enzymes and bicarbonate ions, releasing them through the ducts into the duodenum, and represent

the bulk (70%-90%) of the pancreas volume. These secretions play important roles in both food digestion and neutralization of the acidic chymus released by the stomach. The endocrine function is performed by the numerous cell clusters evenly scattered throughout the organ, named islets of Langerhans, which secrete directly into the bloodstream and represent only 3-5% of pancreatic volume, although they can reach 1 million islets in a human pancreas (Novak 2008). The islets of Langerhans are composed of five main types of cells (Clark, Wells et al. 1988; Wieczorek, Pospischil et al. 1998; Andralojc, Mercalli et al. 2009):

- Alpha cells: secrete glucagon and represent approximately 15-20% of islet cells;
- Beta cells: secrete insulin and amylin and cover 70-80% of islet cells;
- Delta cells: secrete somatostatin and are 5% of islet cells;
- Gamma cells (or PP cells): secrete pancreatic polypeptide (PP) and are less than 1% of islet cells;
- Epsilon cells: secrete ghrelin and the less abundant cells with roughly 1 cell/islet.

The regulation of glycemia is performed by the joint action of glucagon and insulin (Figure 1).

When glycemia rises, the pathway of glucose-stimulated insulin secretion (CSIS) is activated. Glucose enters beta-cells through the GLUT2 transporters, this leads to an increase in the ATP/ADP ratio, through the stimulation of glycolysis and the Krebs cycle. This increase, in turn, leads to the closure of ATP-sensitive K^+ channels and subsequent membrane depolarization, which promotes the opening of voltage-dependent Ca^{2+} channels. The resulting increase in the levels of cytosolic free Ca^{2+} is the trigger for insulin secretion (Henquin 2000; Henquin, Ravier et al. 2003; Bensellam, Laybutt et al. 2012). Glucagon secretion, on the other hand, is achieved by intrinsic and paracrine regulation (Walker, Ramracheya et al. 2011). Like in insulin secretion, the regulation of ion-channels and

subsequent membrane depolarization is the key event to promote glucagon secretion (Wang, Liang et al. 2012). Insulin itself has been shown to inhibit glucagon secretion, together with the simultaneously secreted amylin and GABA from beta-cells and somatostatin from delta-cells, through the Akt-mediated translocation of $GABA_A$ receptors and subsequent membrane hyperpolarization and closure of Ca^{2+} channels (Aronoff, Berkowitz et al. 2004; Walker, Ramracheya et al. 2011; Wang, Liang et al. 2012). When glucose levels are low, beta- and delta-cells secretion is inhibited, lowering the levels of insulin, amylin, GABA and somatostatin, and the inhibitory effect of these in alpha-cells secretion is ceased. The increase in amino acids and free fatty acids, together with paracrine and epinephrine stimuli, may lead to the activation of K^+_{ATP} and Ca^{2+} channels, triggering the depolarization cascade and the release of glucagon (Walker, Ramracheya et al. 2011; Wang, Liang et al. 2012).

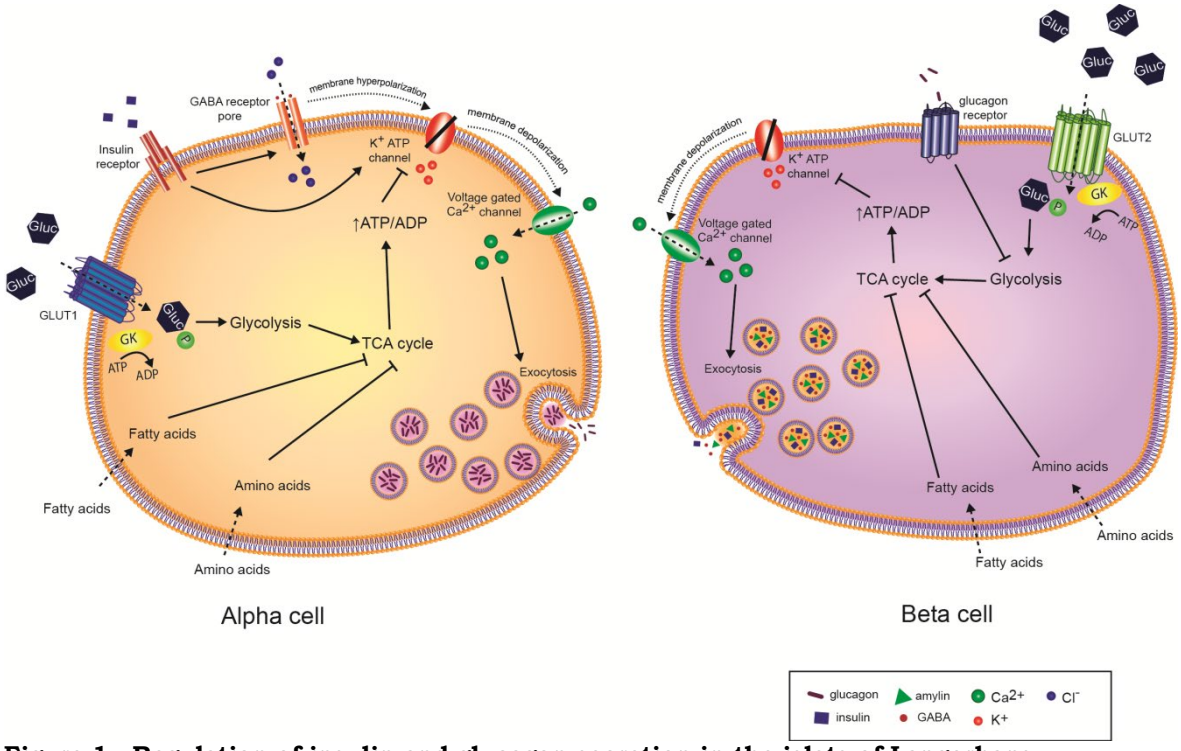

Figure 1 - Regulation of insulin and glucagon secretion in the islets of Langerhans.
In alpha-cells, the entry of glucose through the high affinity GLUT1 transporters activates ATP synthesis, increasing the ATP/ADP ratio. This closes the ATP sensitive K^+ channels, causing membrane depolarisation, which opens Ca^{2+} channels. The Ca^{2+} influx promotes exocytosis of glucagon vesicles. If there is a high level of insulin stimulation, the K^+ channels are open, not causing membrane depolarization and Ca^{2+} entry. Additionally, GABA stimulation of its receptors allow the passage of Cl^- and causing membrane hyperpolarization, further blocking the

Ca^{2+}-stimulated exocytosis. In beta-cells, glucose entry through the low affinity GLUT2 transporters has a similar effect on the promotion of Ca^{2+}-stimulated exocytosis of insulin/amylin/GABA vesicles. However, if glucagon receptors are stimulated, glycolysis is inhibited and the ATP/ADP ratio lowers, inhibiting exocytosis. High levels of circulating fatty acids and certain amino acids may also inhibit secretion through the inhibition of the TCA cycle and the reduction of the ATP/ADP ratio. Adapted from Wang, Liang et al. (2012) and Walker, Ramracheya et al. (2011)

3.3. Intracellular response to insulin and glucagon signalling

Upon release in the bloodstream, insulin major targets are liver, adipose tissue and skeletal muscle. These tissues express insulin receptors (IRs), type 1 insulin-like growth factor receptors (IGFR) or an hybrid form of these, although such receptors have also been found in brain, heart, kidney tubules and glomeruli, pulmonary alveoli, pancreatic acini, vascular endothelium, monocytes, granulocytes, erythrocytes and fibroblasts. This multitude of tissues expressing IRs suggests that the role of insulin may be more diverse than the traditional metabolic action it is attributed to (Kaplan 1984; Belfiore, Frasca et al. 2009). In the traditionally referred to as "insulin main targets", the binding to IRs triggers a signalling cascade that starts with the activation of IR tyrosine kinase, which will phosphorylate several substrates, namely IR substrates (IRS-1, -2, -3 and -4), generating binding sites for Src homolog 2 (SH2) domain proteins, such as regulatory subunits of class 1A phosphatidylinositol 3-kinase (PI3K), leading to the activation of the Akt/PKB and PKCζ cascades. The Akt/PKB is involved in: the regulation of glycogen synthesis, through GSK-3; the regulation of glucose transport, through the Rab GTPase activating protein AS160/TBC1D4; the regulation of mTOR and protein synthesis, through the Rheb GTPase activating complex TSC1/2; the regulation of the expression of gluconeogenic and other genes, through Forkhead box (Fox) transcription factors; and also apoptosis, through BAD (Siddle 2011).

In muscle cells and adipocytes, one of the most important features of Akt activation is the translocation of GLUT4-containing vesicles to the plasma membrane; additionally, the stimulation of glycogen synthesis and

lipid synthesis, respectively, further enhances glucose uptake from the bloodstream (Figure 2).

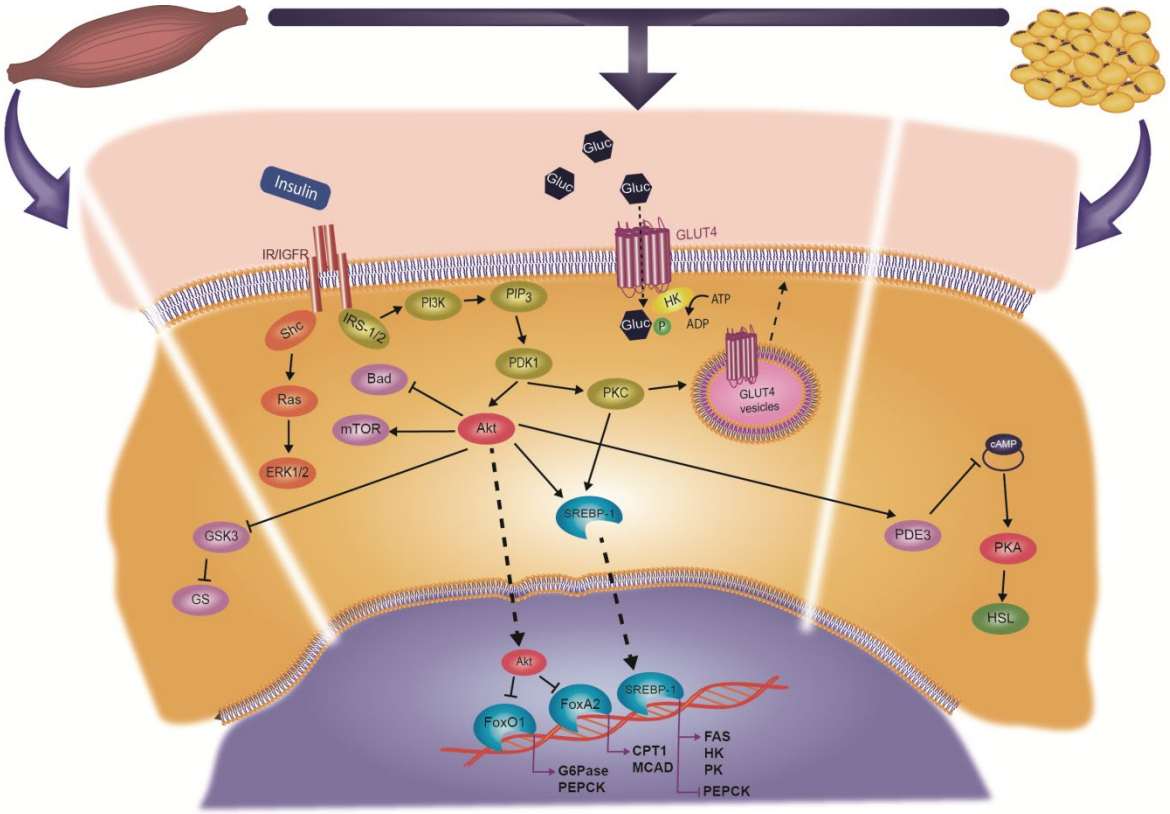

Figure 2 – Insulin signalling cascade in muscle cells and adipocytes
The activation of insulin receptors (IR/IGFR) leads to proliferation stimuli through the ERK1/2 pathways. Additionally, the activation of insulin-receptor substrate (IRS-1/2) activates protein kinase C (PKC), which promotes the translocation of GLUT4 vesicles to the membrane, and Akt, which activates the Sterol Regulatory Element-Binding Protein 1 (SREBP-1) transcription factor, promoting the transcription of fatty acid synthase (FAS), hexokinase (HK), pyruvate kinase (PK) and inhibiting transcription of phosphoenolpyruvate carboxykinase (PEPKC), and the inactivation of FoxA1 and FoxA2 transcription factors that promote the transcription of glucose-6-phosphatase, PEPCK, carnitine palmitoyltransferase 1 (CPT1) and medium-chain acyl-CoA dehydrogenase (MCAD). In muscle cells, Akt also has a pivotal role in the inhibition of GSK3, activating glycogen synthase, while in adipocytes, the activation of phosphodiesterase 3 (PDE3), inhibits lypogenolisis through the Hormone sensitive Lipase (HSL) by inhibiting the synthesis of cAMP. Adapted from Fritsche, Weigert et al. (2008)

Liver cells express GLUT2 as the main glucose transporter, but the activation of the Akt/PKB pathway is important for the inhibition of gluconeogenesis and fatty acid oxidation and the stimulation glycolysis and glycogen synthesis both directly and through transcriptional regulation (Figure 3). Liver, however, also expresses glucagon receptors. Glugagon receptors are G-protein coupled and, upon stimulation, induce the activation of adenylate cyclase, increasing the levels of cAMP and

activating protein kinase A (PKA). PKA activates glycogen phosphorylase promoting glycogenolysis. Additionally, PKA inhibits glycogen synthase and pyruvate kinase, reducing glycogenesis and glycolysis. Glugagon also mediates transcriptional regulation through PKA-activation of the cAMP response element-binding protein (CREB), increasing the expression of phosphoenolpyruvate carboxykinase (PEPCK) promoting gluconeogenesis (Jiang and Zhang 2003).

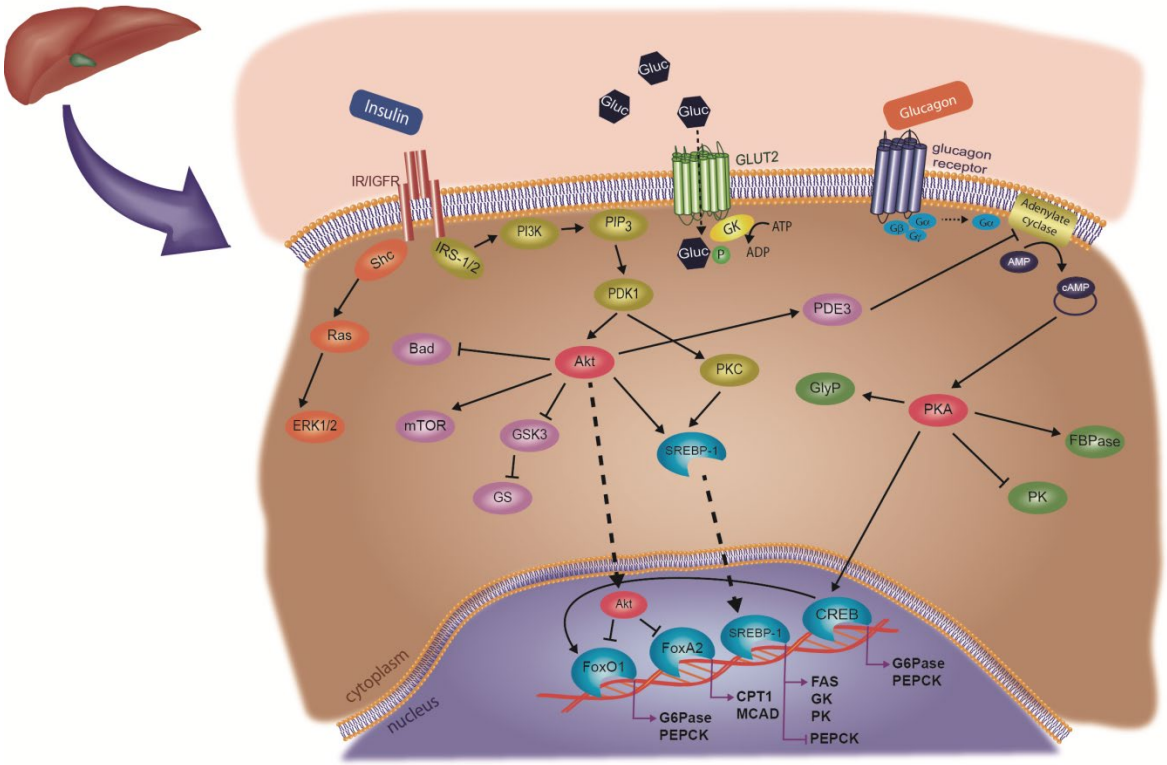

Figure 3 - Insulin and glucagon signalling cascade in hepatocytes.
The activation of insulin receptors (IR/IGFR) leads to proliferation stimuli through the ERK1/2 pathways. Additionally, the activation of insulin-receptor substrate (IRS-1/2) activates the Akt pathway, in which the Sterol Regulatory Element-Binding Protein 1 (SREBP-1) transcription factor, promotes the transcription of fatty acid synthase (FAS), hexokinase (HK), pyruvate kinase (PK) and inhibiting transcription of phosphoenolpyruvate carboxykinase (PEPKC), and the inactivation of forkhead box protein (FoxA1 and FoxA2) transcription factors that promote the transcription of glucose-6-phosphatase, PEPCK, carnitine palmitoyltransferase 1 (CPT1) and medium-chain acyl-CoA dehydrogenase (MCAD). The activation of the G-protein coupled glucagon receptors, activates adenylate cyclase promoting the activation of protein kinase A (PKA), responsible for the activation of glycogen phosphorylase (GlyP) and fructose-1,6 bisphosphatase (FBPase) and inhibition of pyruvate kinase (PK). The activation of cAMP response element binding protein (CREB), activates the transcription of G6Pase and PEPCK directly and through the activation of FoxO1. Adapted from Fritsche, Weigert et al. (2008)

4. Pathogenesis of diabetes mellitus

In T1DM, there is a destruction of beta-cells, resulting in the absence of insulin secretion and subsequent impairment of glycemic control. The aetiology of diabetes is not fully understood, despite decades of research, but some possible factors have been identified and are summarized in Table 1. Genetic predisposition may be the result of a complex interaction between several genes and the environment (Henquin, Anello et al. 2000).

Table 1 – List of possible etiological factors for T1DM (Adapted from Zimmet, Alberti et al. 2001)

Non-genetic	Genetic
Viral infections Early infant diet Perinatal infections Toxins	Human leucocyte antigen (HLA) associated Non-HLA associated

In the case of autoimmune diabetes, autoantibodies are currently the best biomarkers (Dang, Rockell et al. 2011) and approximately 85-90% of individuals present one or more markers of pancreatic islets β-cells autoimmune destruction, following the detection of fasting hyperglycemia. These markers include anti-insulin autoantibodies (AAI), anti-islets of Langerhans (Islet Cell Antibody-ICA), anti-glutamic acid decarboxylase (GAD65), anti-zinc transporter 8 (ZnT8) and anti-tyrosine phosphatases insulinoma antigen IA-2 and IA-2β (Wilkin, Hoskins et al. 1985; Goldstein, Little et al. 2003; Orban, Sosenko et al. 2009; Tsirogianni, Pipi et al. 2009; Sorensen, Vaziri-Sani et al. 2012). Conversely, when such autoimmune antibodies are not present, as well as any other evidence of an autoimmune disorder, we are in presence of an idiopathic T1DM. This form of T1DM is strongly inherited and is more frequent in non-Caucasian individuals (American Diabetes Association 2013).

T2DM, although more prevalent, has a more complex and diverse aetiology. The understanding of the disease has suffered significant changes over time. It is now recognized an important set of risk factors for the development of T2DM and most of them can be prevented by acting many years before the onset of the disease (Table 2) (Zimmet, Alberti et al. 2001).

Table 2 – Aetiological determinants and risk factors of T2DM (Adapted from Zimmet, Alberti et al. 2001)

Genetic factors
Genetic markers
Family history
Thrifty gene(s)
Demographic characteristics
Sex
Age
Ethnicity
Behavioural- and lifestyle-related risk factors
Obesity
Physical inactivity
Diet
Stress
Westernization, urbanization, modernization
Metabolic determinants and intermediate risk categories
Impaired glucose tolerance
Insulin resistance
Pregnancy-related determinants

The evolution of the T2DM is thus a gradual process, unlike the abrupt onset of T1DM. Similarly, T2DM patients do not present signs of autoimmune destruction of beta-cells. Glucose intolerance in T2DM is said to result from a "triumvirate" of interacting factors: impaired insulin secretion, muscle insulin resistance and hepatic insulin resistance (Bays, Mandarino et al. 2004). Which of the events comes first, and whether it is determinant for the progression to overt T2DM, is still a matter of extensive discussion. It is recognized that both impaired insulin secretion and insulin resistance begin very early, even when there is a normal glucose tolerance, and are equally important for the progression to T2DM

(Leahy 2005). The need for accurate prognostic tools is thus of paramount importance to contain this pandemic. The course to the disease state follows a state of prediabetes, where the first signals of glucose intolerance, IFG or IGT, are presented. Subjects with this signals have increased risk of developing diabetes or cardiovascular diseases and should be monitored, especially if other risk factors such as obesity, dyslipidemia or hypertension are concomitant, according to the recommendations of the ADA (Leahy 2005; American Diabetes Association 2013). Prediabetes is also characterized by hyperinsulinemia, where beta-cells respond to the mild hyperglycemia with the secretion of more insulin, despite its action being impaired by insulin resistance. At this stage, the progression to T2DM could be delayed or even reverted by changes in lifestyle, namely, increasing physical activity and through dietary changes, consequently controlling some of the risk factors (Nolan, Damm et al. 2011). When overt hyperglycemia is finally presented, the diagnosis of T2DM is established. Reaching this state implies a progressive beta-cells dysfunction and consequent impairment of insulin secretion. This progressive impairment is the result of numerous factors, such as, lipo- and glucotoxicity, age, genetics, insulin resistance, among others (DeFronzo 2004). In an initial stage, appropriate diet and metformin, a drug that acts in liver inhibiting glucose production and increasing insulin sensitivity, usually suffice in the control of hyperglycemia and are the standard treatment option. As the disease progresses, other agents for hyperglycemia control may be necessary, eventually reaching a stage where insulin therapy is required to counteract the complete beta-cell failure. However, a shift in treatment strategies towards the prevention and alteration of the usual course of the disease, as a way to improve the outcome and be more cost effective, has been proposed (Leahy 2005; Stumvoll, Goldstein et al. 2005; Nolan, Damm et al. 2011).

5. Physiological impact of diabetes mellitus

In a normal state, when blood glucose levels are high, beta-cells secrete insulin. Insulin then signals muscle cells and adipocytes to translocate GLUT4 transporters to the membrane, promoting the entry of glucose in the cells for posterior glycogenesis. In both these types of cells, as well as in hepatocytes, insulin also promotes the glycogen and fatty acid synthesis for energy storage (Figure 3). When blood glucose levels return to normal, insulin secretion is inhibited and these processes are slowed down. If glycemia levels lower below the normal threshold, glucagon secretion is increased and triggers the activation of the PKA cascade in liver resulting in increased glycogenolysis and gluconeogenesis and decreased glycolysis and glycogenesis, thus normalizing glycemia levels (Kahn and Saltiel 2005; Ruderman, Myers Jr. et al. 2005).

In T1DM there is a complete absence of insulin, therefore insulin-receptors are not triggered and muscle cells and adipocytes do not respond to high blood glucose levels. The lack of insulin signalling also promotes glucagon secretion, which induces hepatic glucose production. Likewise, in T2DM with the presence of insulin resistance, insulin-receptors in muscle cells and adipocytes are not triggered and these cells do not increase glucose uptake in response to hyperglycemia; additionally, hepatic glucose production is enhanced by glucagon (American Diabetes Association 2013). Hence, the overall physiological impact of insulin-dysfunctions depends on the integration of the metabolic changes observed in each insulin-sensitive cell type.

The intracellular signalling of insulin was already described in a previous section for muscle cells, adipocytes and hepatocytes. If the signalling pathway is blocked at its very beginning, all the downstream effects are also blocked. Consequently, in liver, there is no insulin-mediated transcriptional up-regulation of hexokinase and activation of glycogen synthase. The lower hexokinase levels limit the uptake of glucose by the hepatocyte, further reducing glycolysis and

glycogenesis. This effect, coupled to increased glucagon signalling, stimulates gluconeogenesis, powered by the ATP production from beta-oxidation of the increased fatty acids levels. Beta-oxidation increases the level of acetyl CoA, which inhibits pyruvate dehydrogenase and activates pyruvate carboxylase, further stimulating gluconeogenesis. Moreover, the excess of acetyl CoA is responsible for the formation of ketone bodies, whose accumulation in the bloodstream lowers the pH to a point where it may exceed the blood buffering ability and result in ketoacidosis. The increased free fatty acids are the result of impaired glucose uptake in adipocytes, as there is no insulin-mediated translocation of GLUT4-containing vesicles to the plasma membrane, which results in decreased synthesis of glycerol 3-phosphate, hence the impaired esterification of lipids and stimulation of lipolysis. In muscle cells, the translocation of GLUT4-containing vesicles is also blocked, so there is a shift towards glycogenolysis and energy production from beta-oxidation, which increases acetyl CoA levels, diverting glycolytic metabolites towards alanine and lactate synthesis that have a gluconeogenic effect in the liver (Basu and Jensen 2005; Collins, Ahima et al. 2005; Granner and Scott 2005; Jozsi and Goodyear 2005; Stump and Nair 2005; Fritsche, Weigert et al. 2008).

6. Cellular basis for complications of long-term hyperglycemia

The immediate complication of hyperglycemia is the development of ketoacidosis from the metabolic shift towards energy production from lipids, which increases the synthesis of ketone bodies in the liver. However, the available therapies allow patients to control hyperglycemia either with insulin replacement or insulin-sensitizing agents. Nonetheless, in the long-term, the ability to naturally regulate glycemia levels has systemic implications, even with a good therapeutic control.

Diabetic patients are known to have increased risk to develop cardiovascular disease (CVD), peripheral arterial disease (PAD), stroke,

nephropathy, retinopathy, neuropathy, skin infections and oral problems. Interestingly, the majority of such complications are related to the cardiovascular system, including both macrovascular and microvascular pathologies, with which endothelial dysfunction is closely related.

A healthy endothelium is responsible for actively decreasing vascular tone, maintaining vascular permeability within narrow bounds, inhibit platelet adhesion and aggregation, limit the activation of the coagulation system and stimulate fibrinolysis. Endothelial dysfunction is present when these functions are compromised in a way that turns impossible the preservation of organ function (Schram and Stehouwer 2005; Schmieder 2006). Considering that the endothelium is a specialized simple squamous epithelium that lines blood vessels, it is not surprising that significant alterations in blood, such as hyperglycemia, may have repercussions in endothelial cells. Additionally, some organs have a highly adapted endothelium, like the tightly packed blood-brain barrier or the fenestrated glomeruli, contributing to a diverse response to stress in different organs. These cells express mostly the GLUT1 transporter, so the uptake of glucose is not as dependent of insulin as in adipocytes or muscle cells, and most of it is meant to be delivered to the underlying tissues through GLUT1-mediated translocation, especially in the blood-brain barrier where there are no loose interendothelial junctions (Bakker, Eringa et al. 2009). However, insulin has to cross the endothelium to reach the insulin-sensitive tissues. In liver, the fenestrated endothelium allows the passage through interendothelial junctions but, in muscle and adipose tissue, insulin crosses the endothelial barrier via an insulin-receptor-mediated binding and exchange mechanism. Insulin may also regulate vasodilation through the release of endothelin-1 (ET-1) and stimulation of endothelial NO synthase (eNOS), both insulin-dependent mechanisms. Thus, the exposure of insulin-sensitive tissues may be regulated at the endothelial level. In hyperglycaemic patients, endothelial dysfunction ranges from structural changes in the endothelial barrier or matrix to the impairment of vasodilator response and increased

inflammatory activation. The ability to repair endothelial damages and regulate angiogenesis is also severely compromised. Antagonic effects are observed regarding angiogenesis. The reduction of vascularization mechanisms significantly contribute to most of the vascular-related complications, however, in retinopathy, is the excessive neovascularization that causes the progressive loss of vision. These processes are regulated by growth factors such as the vascular endothelial growth factor (VEGF), and although some organs present increased expression of VEGF in hyperglycemia, a reduction of the expression of VEGF receptors may contribute to the impairment of angiogenesis. Furthermore, there is also the absence of insulin-induced stimulation of cell proliferation (Bakker, Eringa et al. 2009).

Another tissue expressing high levels of GLUT1 is the glandular epithelium of salivary glands (Jurysta, Nicaise et al. 2013). Interestingly, the oral problems observed in diabetic patients are often associated with impaired salivary gland secretion. Insulin signalling was shown to be present in salivary glands, being responsible for the increase in protein synthesis through the transcriptional regulation of Shc/ERK1/2, Jak-2/STAT, and Akt pathways (Saad, Carvalho et al. 1996; Chen, Sadowski et al. 1997; Rocha, de et al. 2000; Rocha, Hirata et al. 2002; Rocha, Carvalho et al. 2003). Acinar cells are responsible by the secretion of 85% of saliva proteins, despite a significant contribution of glandular duct cells, responsible for secretion of proteins with important biological functions such as growth factors, immunoglobulins and kallikreins (Vitorino, Lobo et al. 2004; Amado, Vitorino et al. 2005; Esser, Alvarez-Llamas et al. 2008; Castagnola, Cabras et al. 2011). However, the ductal epithelium of salivary glands has been shown to be severely affected by long-term hyperglycemia, long before acini start to show morphological changes (Anderson, Garrett et al. 1993). So, although not in direct contact with hyperglycaemic blood, salivary gland cells suffer the effects of the lack of insulin and consequent hyperglycemia.

7. Epidemiology of diabetes mellitus

According to the World Health Statistics 2012, published by the WHO, diabetes mellitus (DM) is on the Top 5 worldwide causes of death by non-communicable diseases (NCD's) (World Health Organization. 2012). However, the WHO dully acknowledges that hyperglycemia is the cause of 22% of coronary heart disease and 16% of stroke deaths, and so, DM is also tightly related to the major death cause – cardiovascular diseases (World Health Organization. 2012).

This close relation would be sufficient to justify the study of diabetes in its several aspects, but the dramatic increase in the incidence of DM in developed countries in the last two decades, reinforces the importance of its study. The number of patients worldwide is estimated to be around 371 million by the International Diabetes Federation (IDF), while China, India and the USA lead in number of cases with over 179 million, altogether (Figure 4). This figure means that around 4.8 million people may have died, in 2012, from diabetes related complications (International Diabetes Federation 2012a; International Diabetes Federation 2012b).

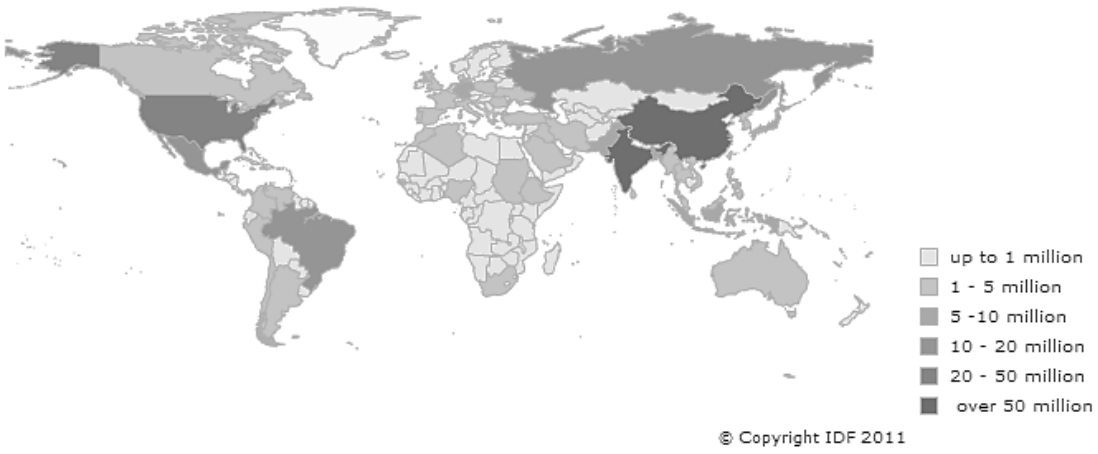

Figure 4 – World distribution of people with diabetes.
Adapted from the IDF Diabetes Atlas – Fifth Edition with the IDF estimations for 2012.

The annual number of deaths attributed to diabetes in Portugal has increased more than 50% in the period 1994-2010. A tendency also

verified, though not so dramatically, in the 27 countries that form the European Union, despite a relatively stable resident population (Figure 5) (Pordata 2012).

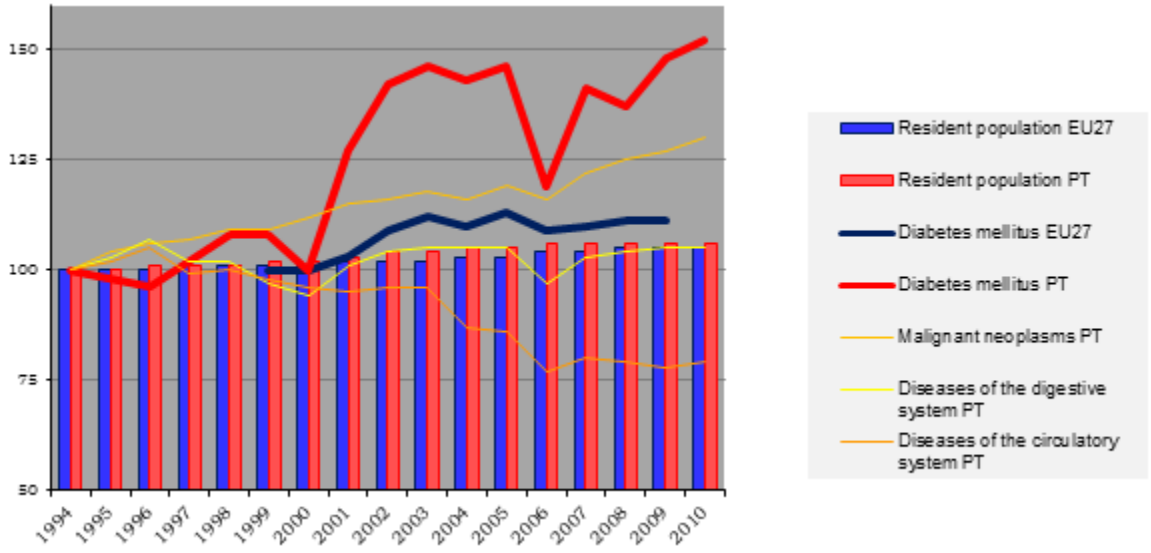

Figure 5 – Evolution of deaths by certain causes related to the total number of deaths (lines) and evolution of the resident population (columns) from 1994 to 2010.
Data were obtained from PORDATA referring to Portugal (PT) and the European Union (EU27) and are presented as an index (1st year with data available = index 100).

Whilst type 2 diabetes mellitus represents over 90% of the cases , in a 2009 study, covering the years 1989-2003, Patterson and colleagues predicted that the number of diabetic children (<15 years old) in Europe would roughly double in the period 2005-2020, to reach over 160,000 children (Patterson, Dahlquist et al. 2009). These numbers make type 1 diabetes mellitus the most common metabolic disease in children (Maahs, West et al. 2010; Gan, Albanese-O'Neill et al. 2012).

For all of these reasons, it is an imperative to conduct studies, such as the present one, that contribute to the full comprehension of this epidemic disease in its several aspects.

8. Aims of the thesis

So, considering the increased incidence of diabetes over the last years, it is proposed to analyse the response to hyperglycemia over time of two epithelial tissues strongly affected in diabetic patients: the endothelium and salivary glands. Additionally, it is proposed to discover potential biomarkers of T1DM in human saliva.

To accomplish this, specific aims were established and organized in 4 chapters, as follows:

Chapter II:

- Select the appropriate animal model to study these tissues
- Determine the adequate time points to carry a study of short- and long-term hyperglycemia

Chapter III:

- Isolate endothelial cells from the aorta
- Analyse the expression of proteins involved in cell proliferation and cell function impairment
- Evaluate damage and repair capacity of the endothelium
- Evaluate the activation of the complement system by abnormal glycation of endothelial cell proteins

Chapter IV:

- Evaluate the changes in protein expression in granule-enriched fractions of the submandibular gland exposed to hyperglycemia
- Correlate protein expression changes with the morphological alterations described in literature

Chapter V:

- analyse the post-translational modifications of the major family of proteins in human saliva – proline-rich proteins
- correlate the frequency of these modifications in T1DM patients with control individuals and cancer patients
- select potential biomarkers

9. References

Amado, F. M., R. M. Vitorino, P. M. Domingues, M. J. Lobo and J. A. Duarte (2005). "Analysis of the human saliva proteome." Expert Rev Proteomics **2**(4): 521-539.

American Diabetes Association (2013). "Diagnosis and classification of diabetes mellitus." Diabetes Care **36 Suppl 1**: S67-74.

Anderson, L. C., J. R. Garrett, A. H. Suleiman, G. B. Proctor, K. M. Chan and R. Hartley (1993). "In vivo secretory responses of submandibular glands in streptozotocin-diabetic rats to sympathetic and parasympathetic nerve stimulation." Cell Tissue Res **274**(3): 559-566.

Andralojc, K. M., A. Mercalli, K. W. Nowak, L. Albarello, R. Calcagno, L. Luzi, E. Bonifacio, C. Doglioni and L. Piemonti (2009). "Ghrelin-producing epsilon cells in the developing and adult human pancreas." Diabetologia **52**(3): 486-493.

Aronoff, S. L., K. Berkowitz, B. Shreiner and L. Want (2004). "Glucose Metabolism and Regulation: Beyond Insulin and Glucagon." Diabetes Spectrum **17**(3): 183-190.

Bakker, W., E. C. Eringa, P. Sipkema and V. W. van Hinsbergh (2009). "Endothelial dysfunction and diabetes: roles of hyperglycemia, impaired insulin signaling and obesity." Cell Tissue Res **335**(1): 165-189.

Basu, A. and M. D. Jensen (2005). Fat Metabolism in Diabetes. Joslin's diabetes mellitus. E. P. Joslin and C. R. Kahn. Philadelphia, Pa., Lippincott Williams & Willkins**:** 264-273.

Bays, H., L. Mandarino and R. A. DeFronzo (2004). "Role of the adipocyte, free fatty acids, and ectopic fat in pathogenesis of type 2 diabetes mellitus: peroxisomal proliferator-activated receptor agonists provide a rational therapeutic approach." J Clin Endocrinol Metab **89**(2): 463-478.

Belfiore, A., F. Frasca, G. Pandini, L. Sciacca and R. Vigneri (2009). "Insulin receptor isoforms and insulin receptor/insulin-like growth factor receptor hybrids in physiology and disease." Endocr Rev **30**(6): 586-623.

Bell, G. I., T. Kayano, J. B. Buse, C. F. Burant, J. Takeda, D. Lin, H. Fukumoto and S. Seino (1990). "Molecular biology of mammalian glucose transporters." Diabetes Care **13**(3): 198-208.

Bensellam, M., D. R. Laybutt and J. C. Jonas (2012). "The molecular mechanisms of pancreatic beta-cell glucotoxicity: recent findings and future research directions." Mol Cell Endocrinol **364**(1-2): 1-27.

Castagnola, M., T. Cabras, A. Vitali, M. T. Sanna and I. Messana (2011). "Biotechnological implications of the salivary proteome." Trends Biotechnol **29**(8): 409-418.

Chen, J., H. B. Sadowski, R. A. Kohanski and L. H. Wang (1997). "Stat5 is a physiological substrate of the insulin receptor." Proc Natl Acad Sci U S A **94**(6): 2295-2300.

Clark, A., C. A. Wells, I. D. Buley, J. K. Cruickshank, R. I. Vanhegan, D. R. Matthews, G. J. Cooper, R. R. Holman and R. C. Turner (1988). "Islet amyloid, increased A-cells, reduced B-cells and exocrine fibrosis: quantitative changes in the pancreas in type 2 diabetes." Diabetes Res **9**(4): 151-159.

Collins, S., R. S. Ahima and B. B. Kahn (2005). Biology of Adipose Tissue. Joslin's diabetes mellitus. E. P. Joslin and C. R. Kahn. Philadelphia, Pa., Lippincott Williams & Willkins**:** 207-227.

Dang, M., J. Rockell, R. Wagner, J. M. Wenzlau, L. Yu, J. C. Hutton, P. A. Gottlieb and H. W. Davidson (2011). "Human type 1 diabetes is associated with T cell autoimmunity to zinc transporter 8." J Immunol **186**(10): 6056-6063.

DeFronzo, R. A. (2004). "Pathogenesis of type 2 diabetes mellitus." Med Clin North Am **88**(4): 787-835, ix.

Deshpande, A. D., M. Harris-Hayes and M. Schootman (2008). "Epidemiology of diabetes and diabetes-related complications." Phys Ther **88**(11): 1254-1264.

Esser, D., G. Alvarez-Llamas, M. P. de Vries, D. Weening, R. J. Vonk and H. Roelofsen (2008). "Sample Stability and Protein Composition of Saliva: Implications for Its Use as a Diagnostic Fluid." Biomark Insights **3**: 25-27.

Fritsche, L., C. Weigert, H. U. Haring and R. Lehmann (2008). "How insulin receptor substrate proteins regulate the metabolic capacity of the liver--implications for health and disease." Curr Med Chem **15**(13): 1316-1329.

Gardner, D. G., D. M. Shoback and F. S. Greenspan (2011). Greenspan's basic & clinical endocrinology. New York, McGraw-Hill Medical.

Goldstein, D. E., R. R. Little, R. A. Lorenz, J. I. Malone, D. M. Nathan, C. M. Peterson and A. American Diabetes (2003). "Tests of glycemia in diabetes." Diabetes Care **26 Suppl 1**: S106-108.

Gould, G. W. and G. D. Holman (1993). "The glucose transporter family: structure, function and tissue-specific expression." Biochem J **295 (Pt 2)**: 329-341.

Granner, D. K. and D. K. Scott (2005). Regulation of Hepatic Glucose Metabolism. Joslin's diabetes mellitus. E. P. Joslin and C. R. Kahn. Philadelphia, Pa., Lippincott Williams & Willkins**:** 242-263.

Henquin, J. C. (2000). "Triggering and amplifying pathways of regulation of insulin secretion by glucose." Diabetes **49**(11): 1751-1760.

Henquin, J. C., M. Anello and Y. Sato (2000). "[ATP-dependent potassium channels and insulin secretion: essential but not sufficient role]." Journ Annu Diabetol Hotel Dieu: 13-24.

Henquin, J. C., M. A. Ravier, M. Nenquin, J. C. Jonas and P. Gilon (2003). "Hierarchy of the beta-cell signals controlling insulin secretion." Eur J Clin Invest **33**(9): 742-750.

International Diabetes Federation. (2012a). "Global diabetes out of control (Press release)." from http://www.idf.org/sites/default/files/Global%20press%20release%20for%20World%20Diabetes%20Day%202012.pdf.

International Diabetes Federation. (2012b). "IDF Diabetes Atlas - Fifth edition." from http://www.idf.org/atlasmap/atlasmap.

International Expert Committee (2009). "International Expert Committee report on the role of the A1C assay in the diagnosis of diabetes." Diabetes Care **32**(7): 1327-1334.

Jiang, G. and B. B. Zhang (2003). "Glucagon and regulation of glucose metabolism." Am J Physiol Endocrinol Metab **284**(4): E671-678.

Joost, H. G. and B. Thorens (2001). "The extended GLUT-family of sugar/polyol transport facilitators: nomenclature, sequence characteristics, and potential function of its novel members (review)." Mol Membr Biol **18**(4): 247-256.

Jozsi, A. C. and L. J. Goodyear (2005). Biology of Skeletal Muscle. Joslin's diabetes mellitus. E. P. Joslin and C. R. Kahn. Philadelphia, Pa., Lippincott Williams & Willkins**:** 228-241.

Jurysta, C., C. Nicaise, M. H. Giroix, S. Cetik, W. J. Malaisse and A. Sener (2013). "Comparison of GLUT1, GLUT2, GLUT4 and SGLT1 mRNA Expression in the Salivary Glands and Six Other Organs of Control, Streptozotocin-Induced and Goto-Kakizaki Diabetic Rats." Cell Physiol Biochem **31**(1): 37-43.

Kahn, C. R. and A. R. Saltiel (2005). The Molecular Mechanism of Insulin Action and the Regulation of Glucose and Lipid Metabolism. Joslin's diabetes mellitus. E. P. Joslin and C. R. Kahn. Philadelphia, Pa., Lippincott Williams & Willkins**:** 145-168.

Kaplan, S. A. (1984). "The insulin receptor." J Pediatr **104**(3): 327-336.

Leahy, J. L. (2005). "Pathogenesis of type 2 diabetes mellitus." Arch Med Res **36**(3): 197-209.

Nolan, C. J., P. Damm and M. Prentki (2011). "Type 2 diabetes across generations: from pathophysiology to prevention and management." Lancet **378**(9786): 169-181.

Novak, I. (2008). "Purinergic receptors in the endocrine and exocrine pancreas." Purinergic Signal **4**(3): 237-253.

Orban, T., J. M. Sosenko, D. Cuthbertson, J. P. Krischer, J. S. Skyler, R. Jackson, L. Yu, J. P. Palmer, D. Schatz, G. Eisenbarth and G. Diabetes Prevention Trial-Type 1

Study (2009). "Pancreatic islet autoantibodies as predictors of type 1 diabetes in the Diabetes Prevention Trial-Type 1." Diabetes Care **32**(12): 2269-2274.

Patterson, C. C., G. G. Dahlquist, E. Gyurus, A. Green, G. Soltesz and E. S. Group (2009). "Incidence trends for childhood type 1 diabetes in Europe during 1989-2003 and predicted new cases 2005-20: a multicentre prospective registration study." Lancet **373**(9680): 2027-2033.

Pordata (2012). Pordata - Base de dados Portugal contemporâneo. Lisboa, Portugal, Fundação Francisco Manuel dos Santos.

Rocha, E. M., C. R. Carvalho, M. J. Saad and L. A. Velloso (2003). "The influence of ageing on the insulin signalling system in rat lacrimal and salivary glands." Acta Ophthalmol Scand **81**(6): 639-645.

Rocha, E. M., M. L. M. H. de, C. R. Carvalho, M. J. Saad and L. A. Velloso (2000). "Characterization of the insulin-signaling pathway in lacrimal and salivary glands of rats." Curr Eye Res **21**(5): 833-842.

Rocha, E. M., A. E. Hirata, E. M. Carneiro, M. J. Saad and L. A. Velloso (2002). "Impact of gender on insulin signaling pathway in lacrimal and salivary glands of rats." Endocrine **18**(2): 191-199.

Ruderman, N. B., M. G. Myers Jr., S. R. Chipkin and K. Tornheim (2005). Hormone-Fuel Interrelationships: Fed State, Starvation, and Diabetes Mellitus. Joslin's diabetes mellitus. E. P. Joslin and C. R. Kahn. Philadelphia, Pa., Lippincott Williams & Willkins**:** 127-144.

Saad, M. J., C. R. Carvalho, A. C. Thirone and L. A. Velloso (1996). "Insulin induces tyrosine phosphorylation of JAK2 in insulin-sensitive tissues of the intact rat." J Biol Chem **271**(36): 22100-22104.

Schmieder, R. E. (2006). "Endothelial dysfunction: how can one intervene at the beginning of the cardiovascular continuum?" J Hypertens Suppl **24**(2): S31-35.

Schram, M. T. and C. D. Stehouwer (2005). "Endothelial dysfunction, cellular adhesion molecules and the metabolic syndrome." Horm Metab Res **37 Suppl 1**: 49-55.

Siddle, K. (2011). "Signalling by insulin and IGF receptors: supporting acts and new players." J Mol Endocrinol **47**(1): R1-10.

Sorensen, J. S., F. Vaziri-Sani, M. Maziarz, K. Kristensen, A. Ellerman, N. Breslow, A. Lernmark, F. Pociot, C. Brorsson, N. H. Birkebaek and D. Danish Study Group for Childhood (2012). "Islet autoantibodies and residual beta cell function in type 1 diabetes children followed for 3-6 years." Diabetes Res Clin Pract **96**(2): 204-210.

Stump, C. S. and S. Nair (2005). Alterations in Protein Metabolism in Diabetes Mellitus. Joslin's diabetes mellitus. E. P. Joslin and C. R. Kahn. Philadelphia, Pa., Lippincott Williams & Willkins**:** 274-290.

Stumvoll, M., B. J. Goldstein and T. W. van Haeften (2005). "Type 2 diabetes: principles of pathogenesis and therapy." Lancet **365**(9467): 1333-1346.

Tsirogianni, A., E. Pipi and K. Soufleros (2009). "Specificity of islet cell autoantibodies and coexistence with other organ specific autoantibodies in type 1 diabetes mellitus." Autoimmun Rev **8**(8): 687-691.

Uldry, M. and B. Thorens (2004). "The SLC2 family of facilitated hexose and polyol transporters." Pflugers Arch **447**(5): 480-489.

Vitorino, R., M. J. Lobo, A. J. Ferrer-Correira, J. R. Dubin, K. B. Tomer, P. M. Domingues and F. M. Amado (2004). "Identification of human whole saliva protein components using proteomics." Proteomics **4**(4): 1109-1115.

Walker, J. N., R. Ramracheya, Q. Zhang, P. R. Johnson, M. Braun and P. Rorsman (2011). "Regulation of glucagon secretion by glucose: paracrine, intrinsic or both?" Diabetes Obes Metab **13 Suppl 1**: 95-105.

Wang, Q., X. Liang and S. Wang (2012). "Intra-islet glucagon secretion and action in the regulation of glucose homeostasis." Front Physiol **3**: 485.

Wieczorek, G., A. Pospischil and E. Perentes (1998). "A comparative immunohistochemical study of pancreatic islets in laboratory animals (rats, dogs, minipigs, nonhuman primates)." Exp Toxicol Pathol **50**(3): 151-172.

Wilkin, T., P. J. Hoskins, M. Armitage, M. Rodier, C. Casey, J. L. Diaz, D. A. Pyke and R. D. Leslie (1985). "Value of insulin autoantibodies as serum markers for insulin-dependent diabetes mellitus." Lancet **1**(8427): 480-481.

World Health Organization. (2006). Definition and diagnosis of diabetes mellitus and intermediate hyperglycemia: report of a WHO/IDF consultation. Geneva, Switzerland, World Health Organization.

World Health Organization. (2012). World health statistics 2012. Geneva, Switzerland, World Health Organization.

Zimmet, P., K. G. Alberti and J. Shaw (2001). "Global and societal implications of the diabetes epidemic." Nature **414**(6865): 782-787.

II. SELECTING AN APPROPRIATE MODEL TO STUDY THE IMPACT OF HYPERGLYCEMIA IN EPITHELIAL-DERIVED TISSUES

1. Theoretical background

1.1. Introduction

The use of animals in scientific research is not exempt of ethical, moral and legal issues. Nonetheless, most of our present knowledge concerning human physiology, and a plethora of other related disciplines, has been achieved through animal experimentation. Biomedical research involving animals is still a necessary cost for the advancement of medical and biological sciences, among others. One of the guiding principles established throughout the years has been to use the "lowest" possible animal, making the use rodent models preferred to dogs, cats or primates, the exception being when these cannot properly reflect the human situation intended to study. Additionally, the less invasive procedures are generally preferred, making non-surgical methods favoured over surgical methods (Hau 2003). A perfect animal model does not exist. Its usefulness does not depend on how well it mimics the human disease, but instead on how well it answers the questions driven by the hypothesis in study. Hence, selecting the best model is a task that must consider the experimental hypothesis and specific aims of the study, but also more practical aspects such as the experimental facilities and the project staff (Hau 2003).

The use of animal experimentation to study DM goes back to the 1880's and the experiments of von Mering and Minkowsky in dogs. They noticed that by removing the pancreas, animals would present polyuria and polydipsia and developed hyperglycemia, being diagnosed with DM. It thus became evident that one of the easiest ways to induce DM, and reproduce the effects of hyperglycemia from the absence of insulin, would be the total or partial removal of the pancreas (Rees and Alcolado 2005; Chatzigeorgiou, Halapas et al. 2009).

Over the years several non-surgical rodent models were also developed to study the effects of DM or hyperglycemia; some are spontaneous models and others are induced models.

Spontaneous models are the result of the selection for hyperglycemia over generations of inbred strains in laboratories. This results in strains enriched in many genes and phenotypes, although not all may be relevant for the disease. Induced models, on the other hand, make use of substances known to have a diabetogenic effect, either by direct injection or other way of administration, but given the still diffuse knowledge on the aetiology of DM, they may not replicate the exact mechanisms responsible for the onset of the disease (Buschard and Thon 2003; Hau 2003). A brief description of the most common rodent models in the study of hyperglycemia and DM, followed by a discussion of pros and cons for each, will be presented.

1.2. The NOD mouse

The non-obese diabetic (NOD) mouse was developed in Japan by S. Makino while selecting for dominant cataract associated with microphthalmia (Makino, Kunimoto et al. 1980). He has noticed that some animals presented a phenotype where they did not present cataracts but exhibited high fasting glucose levels. He then tried to selectively breed this phenotype and, at the same time, breed a euglycemic control with the animals from the same generation that did not present high fasting glucose levels. Surprisingly, at the 20th generation, a female from the euglycemic control spontaneously developed T1DM with heavy leucocytic infiltrations in pancreas – insulitis – and thus became the “mother” of the new NOD strain, while the line selected to high fasting glycemia never progressed to overt diabetes and was later named as nonobese nondiabetic (NON) (Ikegami and Makino 2005; Mathews and Leiter 2005).

One of the advantages of the NOD mice model is the relatively high frequency of spontaneously developing T1DM. If maintained in a specific pathogen-free (SPF) environment, approximately 90% of females and 50-60% of males, progress into fully overt T1DM. The SPF facilities are required because the strain is easily prone to protective immunomodulation when stimulated by a wide number of pathogens. The

NOD strain develops autoantibodies to insulin, GAD and IA-2, most like in human T1DM. Likewise, the usual clinical manifestations of DM are also present, such as hyperglycemia, polyuria, polydipsia and glycosuria (Chatzigeorgiou, Halapas et al. 2009). Yet, other autoimmune manifestations may develop, like leucocytic infiltrations in salivary and lacrimal glands or the thyroid gland. The infiltration in salivary glands, mostly by T lymphocytes, does not imply the loss of acini in the same progression and extension as in the islets of Langerhans and occurs after the insulitis. However, the salivary flow rates and protein content is severely affected, resulting in xerostomia, which is a common symptom of T1DM and Sjögren's syndrome, although the destruction of the gland integrity is not as severe as in the human form of Sjögren's syndrome (Mathews and Leiter 2005). Unlike humans, NOD mice seem resistant to ketoacidosis, in a way that they can survive several weeks without insulin treatment, even with glycemia >500 mg/dl. If diabetes is left untreated, animals will eventually die from dehydration and not from ketoacidosis (Rees and Alcolado 2005; Chatzigeorgiou, Halapas et al. 2009).

1.3. The BB rat

The diabetes-prone BB rat was discovered in the 1970's at the Bio Breeding Laboratories (Ottawa, Canada) (Nakhooda, Like et al. 1977). Scientists noticed some weanling rats died with no apparent cause, other than severe cachexia, in an outbred Wistar-derived colony. They began to regularly weight all the animals to identify the affected animals and, eventually, were able to isolate a sufficient number for further studies. They have observed that the bedding of these animals was excessively wet and the water intake was 3 times the mean values of normal animals. The urine test revealed the presence of sugar and ketone values above normal, so fasting plasma glucose was measured to reveal values ranging between 500-700 mg/dl. The treatment with insulin was initiated and the symptoms were markedly reduced. Histological analysis of the pancreas showed fibrosis and an absence of beta-cells in the islets. Thus a program

was initiated for selective breeding and this new strain was named BB after the initials of the laboratory (Chappel and Chappel 1983). Nowadays, two main substrains exist, developed at the University of Massachusetts Medical School: the diabetes-prone BB (BB-DP) rat and the diabetes-resistant BB rat (BB-DR). The major genetic difference between these substrains is a recessive mutation in chromosome 4 of the BB-DP rat, rendering a phenotype with T-cell lymphopenia in circulating blood. As such, the BB-DP rat is immunocompromised and requires a higher degree of microbiological quality - specific and opportunistic pathogens free (SOPF). On the other hand, the BB-DR may be used as an induced-model of T1DM as the infection with the Kilham rat virus may trigger T1DM in this substrain (Mathews and Leiter 2005; Mordes, Bortell et al. 2005).

Like the NOD mouse, the BB rat presents as a model for autoimmune diabetes with heavy leucocyte infiltrations in pancreas and the presence of autoantibodies to insulin, GAD and IA-2 (Chatzigeorgiou, Halapas et al. 2009). However, rather than a NOD-like peri-insulitis, the insulitis is more similar to the human phenomenon and starts 2-3 weeks before the clinical onset of the disease (Mathews and Leiter 2005; Chatzigeorgiou, Halapas et al. 2009). The age of diagnosis is around 12 weeks, which is analogous to the one observed in humans (juvenile and adolescent populations) (Mordes, Bortell et al. 2005). Also, unlike the NOD mouse and more like the human T1DM, the BB rat is highly susceptible to ketoacidosis, dying within 2 weeks if insulin treatment is not initiated. This strain also has the advantage over the NOD mouse of a sex-independent high incidence of diabetes (80%) (Mathews and Leiter 2005). Like the NOD mouse, the BB rat exhibits salivary gland abnormalities, namely an enrichment of macrophages and T lymphocytes (Cohen, Talarico et al. 1997).

1.4. Leptin-signalling deficient rodents

A common model for mimicking T2DM is the use of obese animals with deficiencies in either the leptin gene (*ob/ob* "obese" mice) or in the leptin receptor gene (*db/db* "diabetic" mice and Zucker *fa/fa* "diabetic fatty" rats). Nowadays, the mice strains are known as Lep^{ob} and $Lepr^{db}$, while the rat strain may be referred to as $Lepr^{fa}$, to reflect the discovery of the genes involved in such genotypes (Herberg and Leiter 2005). Leptin is a hormone expressed in adipose tissue whose secretion is regulated by insulin and acts on the hypothalamus regulating appetite and energy intake.

The discovery of the Lep^{ob} mutation in chromosome 6 dates back to 1950, at The Jackson Laboratory (Ingalls, Dickie et al. 1950). The marked obesity and hyperphagia were the most immediate characteristics observed in homozygous animals. The mutation was then transferred into a B6 inbred strain where it developed juvenile onset obesity, hyperinsulinemia and insulin resistance. The increased proliferation of pancreatic beta-cells, in response to obesity and insulin resistance, led to a mild hyperglycemia eventually remitting to a normoglycemic state (Herberg and Leiter 2005).

The $Lepr^{db}$ mutation was discovered a few years later, in 1966 (Hummel, Dickie et al. 1966). It was identified in chromosome 4 of a BKS inbred strain and, unlike the Lep^{ob} mutation, the obesity and diabetes were permanent, hence the name "diabetic". In this new strain, there was a severe hyperglycemia and necrosis of beta-cells with concomitant atrophy of islets (Herberg and Leiter 2005). Within a few months they develop ketosis and their lifespan does not go further than 8-10 months (Chatzigeorgiou, Halapas et al. 2009).

The Zucker fatty rat (ZFR) was discovered by Zucker and Zucker (1961). It bears a mutation in the leptin receptor gene (*fa* mutation), in chromosome 5, that renders a shortened protein that does not interact with leptin. As a result of this deficiency, the animals have hyperphagia

and become obese within 4 weeks. Other characteristics are a mild hyperglycemia and insulin resistance (Peterson 2005). A substrain of this model was generated with selective inbred of ZFR for hyperglycemia. This substrain was named Zucker diabetic fatty rat (ZDF) because, unlike the ZFR, they develop diabetes as a result of the inability to compensate hyperglycemia and insulin resistance with an over-secretion of insulin. In fact, the pancreatic beta-cells rapidly succumb to apoptosis from the exacerbated stimuli to secrete more insulin (Peterson 2005; Chatzigeorgiou, Halapas et al. 2009).

1.5. The non-obese Goto Kakizaki rat

The Goto Kakizaki (GK) model was developed by Goto and co-workers in Japan in the 1970's, by selecting animals mildly intolerant to glucose, with glycemia levels near the upper limit of the normal range in an OGTT, from a Wistar colony. It eventually rendered a strain presenting glucose intolerance and impaired insulin secretion (Goto, Kakizaki et al. 1976; Östenson 2005).

Unlike the previously described models for T2DM, the GK model is not obese. Pancreas islets, however, are less numbered since birth and sustain morphological changes, losing the smooth round shape into a starfish-like shape, and have an age-progressing lower number of beta-cells. Also unlike the leptin-deficiency models, the diabetes exhibited by the GK rat is of polygenic nature with a markedly maternal inheritance, which puts it closer to what is believed to be the nature of human T2DM (Rees and Alcolado 2005).

Impaired glucose tolerance starts at 2 months and postprandial hyperglycemia rises in the first 6 months, progressing as a typical impaired insulin secretion/insulin resistance of T2DM. Despite an initial stage of general good health, in late stages, the animals develop vascular related complications such as retinopathy, neuropathy and nephropathy (Östenson 2005; Rees and Alcolado 2005).

1.6. Genetically engineered rodent models

The late developments in science allowed the targeting of specific genes to better understand their specific role in DM. The most common method is the production of knockout strains where a specific gene has been disrupted or deleted. Some of the models already produced bear the knockout of the genes for insulin receptor, insulin-receptor substrate 1 and 2 or glucokinase (Chang, Benecke et al. 1994; Tamemoto, Kadowaki et al. 1994; Grupe, Hultgren et al. 1995; Joshi, Lamothe et al. 1996; Withers, Gutierrez et al. 1998; Kubota, Tobe et al. 2000). Genetic engineering has even allowed the production of tissue-specific knockouts by using bacteriophage recombinase enzymes inserted next to a tissue-specific promoter. However, it is equally possible to add more copies of a given gene, and thus study the effects of its over-expression (Rees and Alcolado 2005).

Genetic modification techniques were more evolved in mice than in rats until recently; hence the availability of genetically modified mice is far superior to rats (Abbott 2004). However, the successful production of a genetically modified model is not as straightforward as it may seem in theory. Some homozygous deletions may be lethal and prevent embryos from further developing, while others may induce changes in the expression of non-targeted genes through compensatory mechanisms and result in a limited model (Rees and Alcolado 2005). For these reasons the cost of producing such models is extremely high.

1.7. STZ-induced hyperglycemia

Streptozotocin (2-deoxy-2-([methylnitrosoamino)carbonyl]amino)-D-glucopyranose) is a glucosamine derivative with antimicrobial properties, produced by *Streptomyces acromogenes*. It is recognized by GLUT2 transporters and, because the expression of GLUT2 is mainly observed in pancreatic beta-cells, liver and kidney (to a lesser extent) (Jurysta, Nicaise et al. 2013), the uptake is almost restricted to these cells. Once inside the cell, the nitrosourea moiety of STZ acts as a DNA alkylating agent, transferring a methyl group from STZ to DNA, especially at the O6

position of guanine, resulting in DNA fragmentation. Another mechanism thought to be present in STZ-mediated beta-cell toxicity is the overstimulation of poly(ADP-ribose) polymerase (PARP) in the attempt to repair the damages to the DNA molecule. This overstimulation leads to an increased consumption of NAD to a critical point that forces the cell to cease its cellular functions and ultimately induces cell necrosis. STZ is also capable of alkylating proteins. If along with DNA alkylation, STZ induces damages in glycolytic or mitochondrial enzyme, ATP production is impaired, as well as the resynthesis of NAD, already over-consumed by PARP (Lenzen 2008).

An interestingly feature of STZ-induced models is that both T1DM and T2DM may be mimicked according to the dose injected. A single high dose of STZ induces the destruction of all beta-cells. Without beta-cells, the organism does not produce insulin and is incapable to regulate glycemia, consequently presenting a clinical diagnosis of T1DM. However, multiple low doses of STZ do not have such a drastic effect, reducing the number of beta-cells but keeping some residual insulin secretion, and, when coupled with a high-fat diet, leads to the progressive development of insulin resistance, resembling the pathogenesis of T2DM (Mathews and Leiter 2005; Srinivasan, Viswanad et al. 2005).

1.8. Alloxan-induced hyperglycemia

Alloxan (2,4,5,6-pyrimidinetetrone) is a pyrimidine derivative whose molecular structure is also analogue to glucose. Like STZ, alloxan enters beta-cells through the GLUT2 transporter, although its mechanism of beta-cell toxicity is different. It presents two distinct levels of action, the first level is by inhibiting glucokinase, preventing glucose phosphorylation upon cellular uptake and its entry in glycolysis and thus blocking the ATP signal that triggers insulin secretion; the other level is by generating reactive oxygen species (ROS). Alloxan initially reacts with glutathione, or other thiols, generating the alloxan radical and dialuric acid, which generate the superoxide radical and hydrogen peroxide. The amount of

ROS generated eventually surpasses the antioxidant defence capacity of the cell, accumulating and damaging the cell components, inducing necrosis. It is this mechanism that explains the low toxicity observed in liver, which also expresses GLUT2 transporters, but whose antioxidant defence pool, namely of catalase, is much more abundant (Lenzen 2008).

Like in the STZ-induced model, hyperglycemia is achieved with the destruction of beta-cells and inability to secrete insulin.

1.9. Discussion

Considering the available options, a careful analysis of the pros and cons had to be done for each, in order to select the best model for the aims proposed. Some of the most important characteristics for each one of the models previously described are summarized in Table 3. As previously mentioned, both the aims of the study and more practical aspects, like the facilities available, should be considered in the selection of an adequate model. To carry on the present study, it was aimed to isolate aortic endothelial cells, so the animal chosen should have the largest vessels possible, not exceeding the animal facilities capacity that only houses rodents. Moreover, it was aimed to conduct a proteomic study on the response of submandibular glands, but leucocytic infiltrations are common in glandular tissue of animal models of DM, so a model that is not prone to such feature should be preferred. Additionally, many of the analysis are based in immunodetection of specific proteins; therefore the availability of antibodies for the species chosen is also an important issue.

Table 3 – Summary of the characteristics of each animal model. M: *Mus musculus*; R: *Rattus norvegicus*; SPF: Specific Pathogens Free; SOPF: Specific and Opportunistic Pathogens Free; C: Conventional, Sp: Spontaneous; Ind: Induced; +: High; –: Low; n.a.: not applicable

	NOD	Lep^{ob}	$Lepr^{db}$	ZDF	BB	GK	Genetically engineered	STZ	Alloxan
Species	M	M	R	R	R	R	M/R	M/R	M/R
Type of DM mimicked	1	2	2	2	1	2	1/2	1/2	1/2
Housing microbiological control	SPF	C	C	C	SOPF	C	variable	C	C
Spontaneous/ Induced	Sp	Sp	Sp	Sp	Sp	Sp	n.a.	Ind	Ind
Insulin: secretion (long-term) /resistance /treatment	–/–/–	+/+/–	–/+/–	–/+/–	–/+/+	–/+/–	variable	–/–/–	–/–/–
Ketoacidosis	–				+		variable	–	–
Lipidemia	–	+	+	+	–	–	variable	–	–
Saliva secretion	–				–		variable	–	–
Salivary glands histology	Leucocytic infiltrations			Increased extracellular fatty droplets (Mozaffari, Abdelsayed et al. 2011)	Leucocytic infiltrations		variable	Loss of ductal cells (long-term) (Anderson, Suleiman et al. 1994)	Increased acinar cell size (Reuterving, Hagg et al. 1987)
Vascular complications	+				+		variable	+	+
Antibody availability	+	+	–	–	–	–	+ (M) – (R)	+ (M) – (R)	+ (M) – (R)
Price	EUR 22[a]	EUR 68[b]	EUR 72[b]	EUR 108[b]	USD 277[c]	USD 126[d]	USD 156(M) 184(R)[d]	EUR 15[a,e] 15[b,f]	EUR 15[a,e] 15[b,f]

[a] Taconic Catalog Europe 2013; [b] Harlan Catalog Spain 2012; [c] Biomere email inquire 2009; [d] Charles River Catalog USA 2013; [e] B6 mice; [f] Wistar rats.

To study the impact of hyperglycemia in the long term, one has to exclude the Lep^{ob} model because hyperglycemia is usually transient and compensated by the increase of islets and insulin secretion. On the other hand, one should avoid the presence of other variables that could interfere in cellular metabolism and tissue morphology. The use of obese models, such as $Lepr^{db}$ mice or ZDF rats, should be avoided as the increase in

adipose tissue and hyperlipidemia usually induces morphological changes in tissue with the inclusion of lipid droplets and metabolic changes, despite being one of the causes of insulin resistance and consequent hyperglycemia (Mozaffari, Abdelsayed et al. 2011). For the same reasons, the spontaneous T1DM models of NOD mice and BB rats should be excluded because the heavy leucocytic infiltrations in salivary glands would interfere in the proteomic analysis of those organs. Moreover, these models are severely immunocompromised and require special housing conditions, not available at the moment of the beginning of the experimental protocol and would increase the costs involved (Ikegami and Makino 2005; Mordes, Bortell et al. 2005). The economic criteria could also be a reason to exclude genetically modified models, however, it should not stay above the scientific criteria and it is a fact that studies with genetically modified animals are scarcer than with STZ- or alloxan-induced hyperglycemia, which could limit the impact of the study and severely limit the comparison of the data obtained with the literature available. Choosing the STZ- or alloxan-induced models gives us the advantage of using either mice or rats. The choice of the species brings the need to look at other, more practical, criteria. Mouse models are generally chosen because they are considered to be easy to handle, faster in reproduction and require less space; also the gene manipulation technology is highly advanced for mice, making it a widespread model for various diseases (Abbott 2004; Iannaccone and Jacob 2009). Another advantage is that the availability of antibodies specific for mice proteins is far superior. However, rats present some important advantages. For starter, its physiology is in many cases more like the human than mice (Nature Methods Editorial 2010). But also, its larger size allows the potential recover of more material using fewer animals and a larger animal was one of the features identified as preferable for this study.

The choice would now rest on the drug used to induce hyperglycemia. Both drugs lack reports of leucocytic infiltrations that could interfere in proteomic analysis of salivary glands (Reuterving, Hagg

et al. 1987; Anderson, Suleiman et al. 1994). However, STZ has an important practical advantage; it is stable in physiological conditions (pH 7.4, 37ºC) for up to 1 hour, while alloxan has a half-life of approximately 90 seconds in the same conditions (Lenzen 2008). The use of any of these drugs, however, has a disadvantage: because the uptake is mediated by GLUT2 transporters, both enter hepatocytes and may induce liver damage. Nonetheless, several studies have demonstrated that the deleterious effects in hepatic function are recoverable within a few weeks (Carnovale and Rodriguez Garay 1984; Evelson, Susemihl et al. 2005). As this study aims for the long-term effects of hyperglycemia, when the drug has obviously cleared the system and its remaining effect is only the irreversible destruction of beta-cells, the STZ-induced hyperglycaemic rat would be the best model.

It becomes clear that the STZ-induced hyperglycemia in rat is the more advantageous model to conduct the proposed study because it is a widely used model, and thus comparable to a wide range of published works (over 800 entries in PubMed for “rat streptozotocin”); it presents the chronic complications in study, vascular and salivary secretion impairments without significant morphological changes in the organs in study, other than the ones caused by hyperglycemia; and it is an economic and easy to maintain model, not requiring insulin treatment for survival over long periods or specific housing conditions.

2. Experimental design

2.1. Outline

The study of long term effects in animal models needs to take into account that the rat's lifespan and development is much faster than human's, which is actually a major advantage of using animal models. As such, one must draw a parallel correspondence between rat years and human years. According to Quinn, a human year is roughly equivalent to 16.7 rat days in average, although the correspondence is not linear throughout the rat lifespan (Quinn 2005). The literature on the effects of hyperglycemia has a wide range in the duration of experimental diabetes, according to the effect studied or if one is aiming for acute or chronic consequences. Renal function has been evaluated with only 8 days of STZ-induced hyperglycemia (Carney, Wong et al. 1979), to over 10 weeks without insulin therapy or 11 months with insulin therapy (Zatz, Meyer et al. 1985); while neuropathy and axonemal transport has been evaluated over a 4 weeks period (Marini, Vitadello et al. 1986) and cataract formation over a 9 weeks to 5 months period (Fukushi, Merola et al. 1980). In the case of endothelial and salivary gland effects of hyperglycemia, which are the target tissues of this study, a work of Bucciarelli and co-workers (2009) has observed a progressive impairment of mice arterial and venal endothelial cells over a period of 3 and 7 months, namely through the increased expression of inflammatory proteins mRNA; whereas a work of Anderson and co-workers (1994) has shown that the submandibular glands start to show morphological changes in ducts after 3 months of uncontrolled hyperglycemia, progressing to acini after 6 months (Anderson, Suleiman et al. 1994; Bucciarelli, Pollreisz et al. 2009). The present study aims to study the effect of hyperglycemia in the endothelium and the submandibular glands. To study the endothelium, it was proposed to isolate endothelial cells from rat aorta to perform a direct analysis without in vitro proliferation steps, and evaluate endothelial damage and repair by flow cytometry analysis of

circulating endothelial cells. To study salivary glands, it was proposed to conduct a quantitative proteomic analysis of submandibular glands. To optimize procedures and evaluate the feasibility of the analysis of endothelial cells, a preliminary study was conducted with 13 rats, during 1 month, before defining the time-points for an experimental animal protocol.

2.2. Material and methods

2.2.1. Preliminary study

Eight male Wistar rats were injected with streptozotocin (S0130, Sigma-Aldrich) (60 mg/kg) in citrate buffer (pH 4.5), and 5 others were injected with citrate buffer alone. Hyperglycemia was observed 3 days post-injection of STZ and was retained during 1 month. Upon sacrifice, blood was collected from the inferior vena cava into EDTA tubes (Vacutainer® Blood Collection Tubes, BD Biosciences, USA) and a portion of aorta was collected for endothelial cell isolation. A detailed description of the flow cytometry and endothelial cell isolation is provided in Chapter III. Glycemia and HbA1c values were also determined as described ahead.

2.2.2. Animals

Forty 6-week-old male Wistar rats were randomly divided into 2 groups. Animals were housed at constant temperature (21°-24°C) with a 12-hour period of light vs. dark and provided with food and water ad libitum. One group (Diabetic) received an intraperitoneal injection of streptozotocin (S0130, Sigma-Aldrich) (60 mg/kg) in citrate buffer (pH 4.5), while the other group (Control) received an injection with citrate buffer alone. After 72 hours, the animals were subjected to glycemic control. During the first month, weekly measurements of glycemia and weight were performed. Animals were considered hyperglycemic if the glycemia levels were consistently above 200 mg/dl. Following the experimental design previously established (Figure 8), after two-months

half the animals from the control group and half from the diabetic group were euthanized. After four-months the remaining animals were euthanized.

Blood was collected with a syringe from the inferior vena cava and immediately aliquoted into EDTA, citrate and serum tubes (Vacutainer® Blood Collection Tubes, BD Biosciences, USA) and stored on ice for no more than 3 hours before further processing. Salivary glands were excised and stored on ice in phosphate-buffered saline (pH 7.35) until further processing. A portion of aorta with approximately 5 cm was excised for endothelial cell isolation and stored on ice in PBS until further processing. Tissue samples were collected for microscopic evaluation in 4% para-formaldehyde in PBS.

2.2.3. Glycemic control

Glycemia was measured using a Glucocard™ G meter (A. Menarini Diagnosis, Portugal) with Glucocard™ G sensor test strips. This device allows an accurate measurement of glycemia levels up to 600 mg/dl with a small drop of capillary blood obtained with a puncture in the tail extremity. The tail was briefly disinfected with a cotton ball embedded in 70% ethanol and once it dried out, a lancing device was triggered puncturing the tail. The small drop of blood obtained was loaded on the test strip and the reading was registered. No pain manifestation was ever observed in the animals.

2.2.4. Measurement of HbA1c

Glycated haemoglobin was determined with a Hemoglobin A1C chromatographic kit (Biosystems, Spain). Blood collected in EDTA tubes (50 µl) was mixed with Reagent 1 (200 µl) and kept at room temperature for 15 min. Then 50 µl of the hemolysate was applied on the upper filter of the column and allowed to drain, eventually adding 200 µl of Reagent 2 to ensure no residues of the hemolysate would remain above the filter. Afterwards, 2 ml of Reagent 2 were added and allowed to drain, thus

washing HbA1a+b. To elute the HbA1c bound to the resin, 4 ml were added to the column and the eluate was collected in a test tube. The OD 415nm was measured against distilled water. The total haemoglobin OD 415nm was measured from a hemolysate prepared by mixing 6ml of Reagent 3 with 25 µl of blood. Glycated haemoglobin was expressed as a percentage of total haemoglobin by applying the formula:

$$\frac{OD_{HbA1c} \times V_{HbA1c}}{OD_{HbTOTAL} \times V_{HbTOTAL}} = \%HbA1c$$

Where V_{HbA1c} and $V_{HbTOTAL}$ are 4 ml and 6 ml, respectively.

2.2.5. Statistical analysis

All statistical tests were performed using GraphPad Prism v5.00 (GraphPad Software, Inc., USA). Data were analysed using a two-way ANOVA with Bonferroni's post hoc tests to compare groups. A p-value <0.05 was considered significant.

2.3. Results and Discussion

The use of STZ-induced hyperglycemia model in the study of DM has been widely spread. Given that one of the objectives of the present work was to study the effects of DM in the proteome of salivary glands, but these glands suffer from leucocyte infiltrations in the case of real DM and general spontaneous animal models (Mathews and Leiter 2005), a method to induce hyperglycemia, without such alterations, was chosen. Moreover, to optimize procedures and decide the appropriate time points to use in the main study, a preliminary study was conducted with 13 animals.

Hyperglycemia was successfully induced with STZ in 7 animals (Figure 6A). Consistently with the effect of prolonged hyperglycemia, the % HbA1c was slightly elevated in hyperglycaemic rats (Figure 6B). Flow cytometry analysis of circulating endothelial cells (CEC) and endothelial progenitor cells (EPC) revealed that with only a month of hyperglycemia

there were significant changes in the number of these cells in circulation (Figure 6C-D).

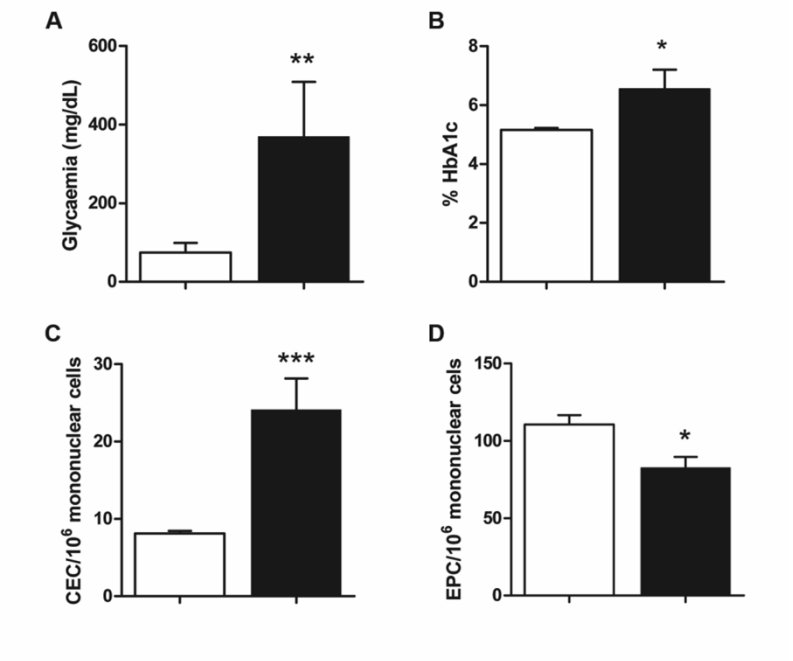

Figure 6 – Results of the preliminary study.
White bars represent control animals, filled bars represent hyperglycemic animals. A - glycemia; B - % HbA1c; C - Circulating endothelial cells (CD45-, CD146+, CD133-); D - Endothelial progenitor cells (CD45-, CD146+, CD133+). * $p<0.05$; ** $p<0.01$; *** $p<0.001$

Moreover, the isolation of endothelial cells appeared successful when observing the magnetic beads suspension under the microscope (Figure 7).

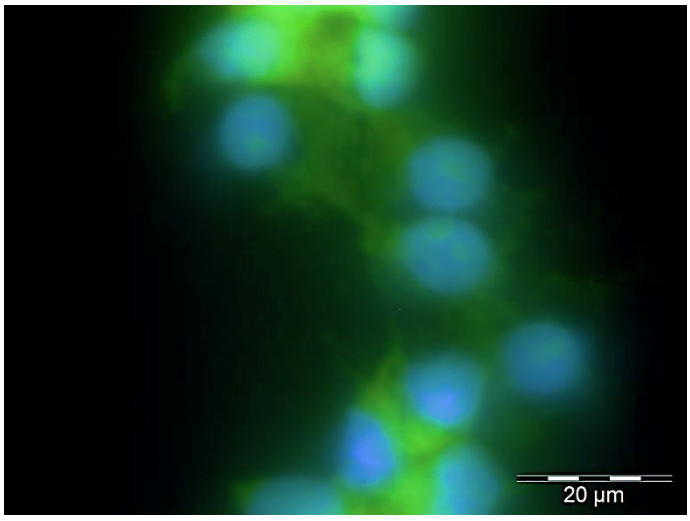

Figure 7 – Suspension of endothelial cells isolated with anti-CD146-coated magnetic beads.
CD146 positive cells were labelled with Alexa Fluor 488 (green), nuclei were stained with Hoechst.

So, considering the results in the preliminary study, vascular impairment is already started within 1 month of permanent hyperglycemia. However, salivary glands only seem to show morphological changes within 3 months of hyperglycemia (Anderson, Suleiman et al. 1994). Because is likely that morphological changes are preceded by protein changes in the cells, it was decided to establish a first time point at 2 months of hyperglycemia and a second point at 4 months of hyperglycemia, resulting in the experimental protocol schematized in Figure 8.

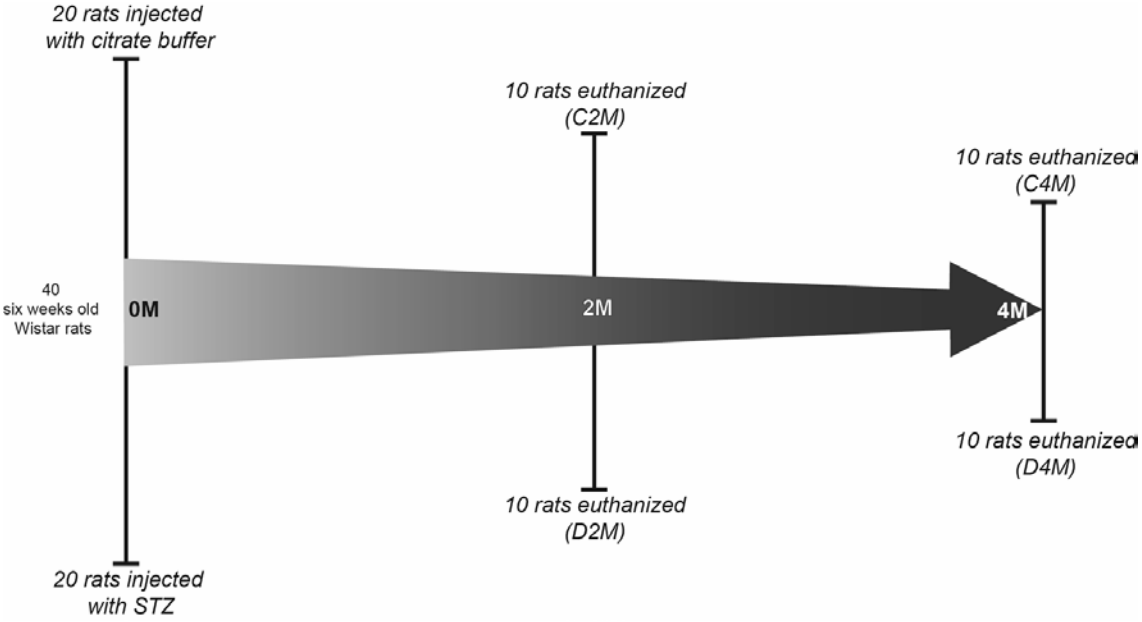

Figure 8 - Experimental design of the animal protocol.

At the time of injection, the animals presented an average weight of 250.5±10.5 grams. After 72 hours, all but one of the animals treated with STZ, presented hyperglycemia. This one was once again injected with a new dose of 60 mg/kg of STZ in citrate buffer, but, since it did not present hyperglycemia after the two treatments, it was excluded from the experiment. The remaining animals were weekly monitored for glycemia and weight during the first two-months. After 2-weeks, the treated animals presented hyperglycemia with consistent values above the upper limit of detection of the equipment used (>600 mg/dl), while untreated

animals presented values <100 mg/dl. It was observed that treated animals did not gain weight during the following weeks, while untreated animals rapidly increased in size and weight (Figure 9). During all the experimental period, other effects of hyperglycemia were observed in treated animals, namely, polydipsia, polyuria and, reaching the 4-months of the trial, loss of sight. None of the animals died during the experimental period and none present behavioural changes that could indicate suffering.

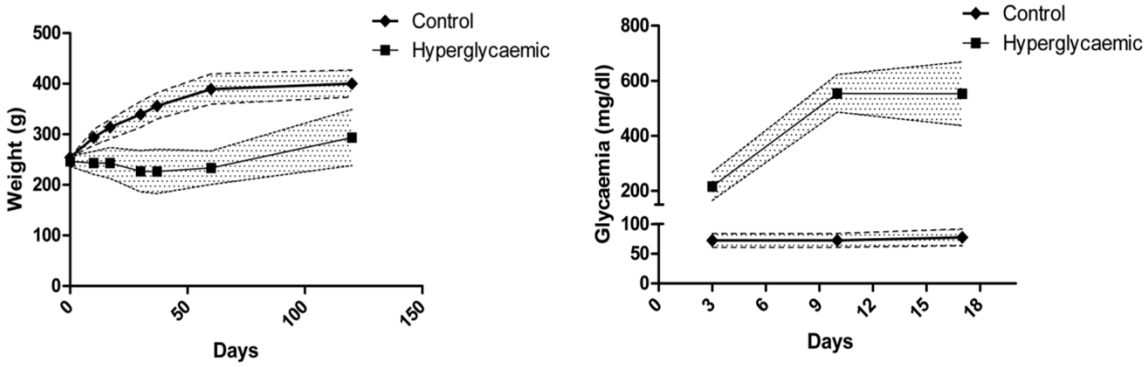

Figure 9- Evolution of weight and glycemia in the first days post STZ injection.
Data are presented as mean±SD.

Half of the animals of each group were euthanized 2-months after the injection with STZ or vehicle alone, rendering the first two groups: Control 2-months (C2M) and Diabetic 2-months (D2M), with n=10 and n=9, respectively. The remaining animals were euthanized after 4-months of being injected, rendering the last two groups: Control 4-months (C4M) and Diabetic 4-months (D4M), with n=10, each. At the time of sacrifice, there were highly significant ($p<0.001$) differences in weight, glycemia and HbA1c between control and treated animals (Figure 10).

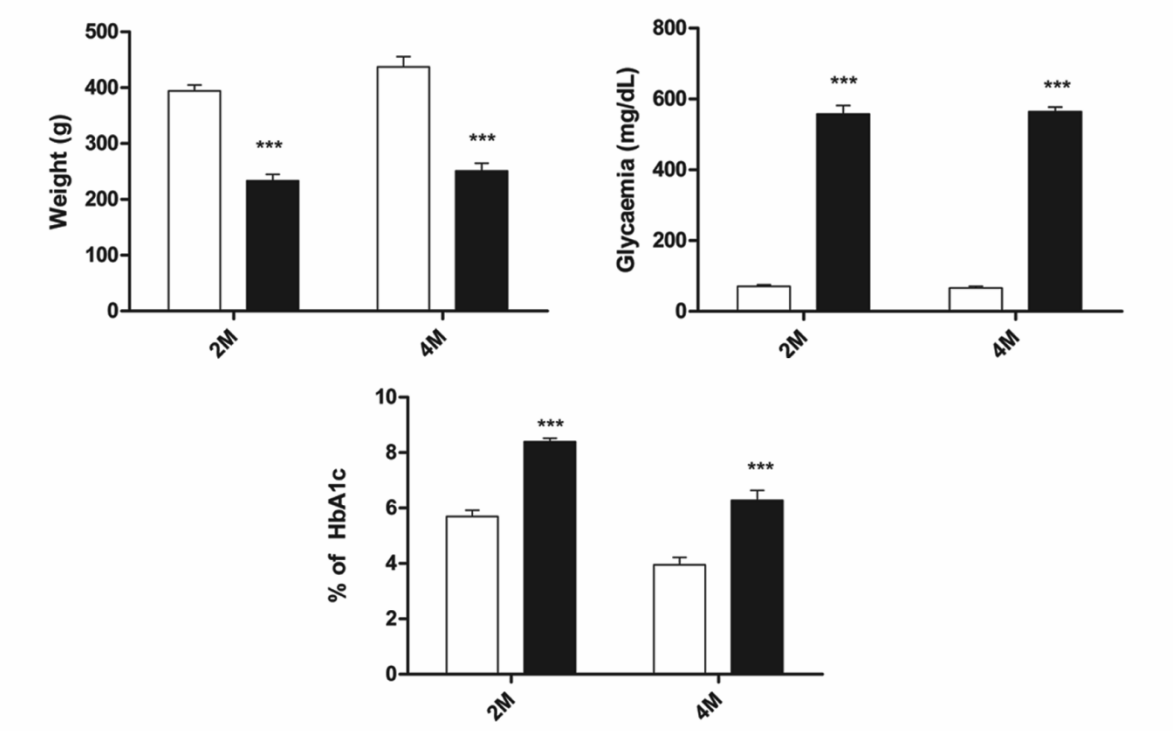

Figure 10 – Differences in weight, glycemia and % of Hb1Ac at the time of sacrifice.
White bars: control; filled bars: hyperglycaemic. Data are presented as mean±SD. *** p<0,001 vs. control

The macroscopic observation of the internal organs revealed only a higher level of visceral fat in control animals. Because STZ could damage the liver (Lenzen 2008), special attention was given to this organ but no macroscopic damages were observed either at 2 or 4 months.

3. Conclusion

Given the results obtained, it is possible to conclude that the STZ-induced hyperglycemia model presents as an economic, yet reliable and effective animal model to study the hyperglycemia-derived complications in the endothelium and salivary glands present in DM.

4. References

Abbott, A. (2004). "Laboratory animals: the Renaissance rat." Nature **428**(6982): 464-466.

Anderson, L. C., A. H. Suleiman and J. R. Garrett (1994). "Morphological effects of diabetes on the granular ducts and acini of the rat submandibular gland." Microsc Res Tech **27**(1): 61-70.

Bucciarelli, L. G., A. Pollreisz, M. Kebschull, A. Ganda, A. Z. Kalea, B. I. Hudson, Y. S. Zou, E. Lalla, R. Ramasamy, P. C. Colombo, A. M. Schmidt and S. F. Yan (2009). "Inflammatory stress in primary venous and aortic endothelial cells of type 1 diabetic mice." Diab Vasc Dis Res **6**(4): 249-261.

Buschard, K. and R. Thon (2003). Diabetic animal models. Handbook of laboratory animal science. J. Hau and G. L. Van Hoosier. Boca Raton, Fla., CRC Press. **2:** 153-182.

Carney, S. L., N. L. Wong and J. H. Dirks (1979). "Acute effects of streptozotocin diabetes on rat renal function." J Lab Clin Med **93**(6): 950-961.

Carnovale, C. E. and E. A. Rodriguez Garay (1984). "Reversible impairment of hepatobiliary function induced by streptozotocin in the rat." Experientia **40**(3): 248-250.

Chang, P. Y., H. Benecke, Y. Le Marchand-Brustel, J. Lawitts and D. E. Moller (1994). "Expression of a dominant-negative mutant human insulin receptor in the muscle of transgenic mice." J Biol Chem **269**(23): 16034-16040.

Chappel, C. I. and W. R. Chappel (1983). "The discovery and development of the BB rat colony: an animal model of spontaneous diabetes mellitus." Metabolism **32**(7 Suppl 1): 8-10.

Chatzigeorgiou, A., A. Halapas, K. Kalafatakis and E. Kamper (2009). "The use of animal models in the study of diabetes mellitus." In Vivo **23**(2): 245-258.

Cohen, R. E., G. Talarico and B. Noble (1997). "Phenotypic characterization of mononuclear inflammatory cells in salivary glands of bio-breeding rats." Arch Oral Biol **42**(9): 649-655.

Evelson, P., C. Susemihl, I. Villarreal, S. Llesuy, R. Rodriguez, H. Peredo, A. Lemberg, J. Perazzo and E. Filinger (2005). "Hepatic morphological changes and oxidative stress in chronic streptozotocin-diabetic rats." Ann Hepatol **4**(2): 115-120.

Fukushi, S., L. O. Merola and J. H. Kinoshita (1980). "Altering the course of cataracts in diabetic rats." Invest Ophthalmol Vis Sci **19**(3): 313-315.

Goto, Y., M. Kakizaki and N. Masaki (1976). "Production of spontaneous diabetic rats by repetition of selective breeding." Tohoku J Exp Med **119**(1): 85-90.

Grupe, A., B. Hultgren, A. Ryan, Y. H. Ma, M. Bauer and T. A. Stewart (1995). "Transgenic knockouts reveal a critical requirement for pancreatic beta cell glucokinase in maintaining glucose homeostasis." Cell **83**(1): 69-78.

Hau, J. (2003). Animal models. Handbook of laboratory animal science. J. Hau and G. L. Van Hoosier. Boca Raton, Fla., CRC Press. **2:** 1-9.

Herberg, L. and E. H. Leiter (2005). Obesity/Diabetes in mice with mutations in the Leptin or leptin receptor genes. Animal Models of Diabetes: A Primer. A. A. F. Sima and E. Shafir. Amsterdam, The Netherlands, Harwood Academic**:** 56-94.

Hummel, K. P., M. M. Dickie and D. L. Coleman (1966). "Diabetes, a new mutation in the mouse." Science **153**(3740): 1127-1128.

Iannaccone, P. M. and H. J. Jacob (2009). "Rats!" Dis Model Mech **2**(5-6): 206-210.

Ikegami, H. and S. Makino (2005). The NOD mouse and its related strains. Animal Models of Diabetes: A Primer. A. A. F. Sima and E. Shafir. Amsterdam, The Netherlands, Harwood Academic**:** 38-55.

Ingalls, A. M., M. M. Dickie and G. D. Snell (1950). "Obese, a new mutation in the house mouse." J Hered **41**(12): 317-318.

Joshi, R. L., B. Lamothe, N. Cordonnier, K. Mesbah, E. Monthioux, J. Jami and D. Bucchini (1996). "Targeted disruption of the insulin receptor gene in the mouse results in neonatal lethality." EMBO J **15**(7): 1542-1547.

Jurysta, C., C. Nicaise, M. H. Giroix, S. Cetik, W. J. Malaisse and A. Sener (2013). "Comparison of GLUT1, GLUT2, GLUT4 and SGLT1 mRNA Expression in the Salivary Glands and Six Other Organs of Control, Streptozotocin-Induced and Goto-Kakizaki Diabetic Rats." Cell Physiol Biochem **31**(1): 37-43.

Kubota, N., K. Tobe, Y. Terauchi, K. Eto, T. Yamauchi, R. Suzuki, Y. Tsubamoto, K. Komeda, R. Nakano, H. Miki, S. Satoh, H. Sekihara, S. Sciacchitano, M. Lesniak, S. Aizawa, R. Nagai, S. Kimura, Y. Akanuma, S. I. Taylor and T. Kadowaki (2000). "Disruption of insulin receptor substrate 2 causes type 2 diabetes because of liver insulin resistance and lack of compensatory beta-cell hyperplasia." Diabetes **49**(11): 1880-1889.

Lenzen, S. (2008). "The mechanisms of alloxan- and streptozotocin-induced diabetes." Diabetologia **51**(2): 216-226.

Makino, S., K. Kunimoto, Y. Muraoka, Y. Mizushima, K. Katagiri and Y. Tochino (1980). "Breeding of a non-obese, diabetic strain of mice." Jikken Dobutsu **29**(1): 1-13.

Marini, P., M. Vitadello, R. Bianchi, C. Triban and A. Gorio (1986). "Impaired axonal transport of acetylcholinesterase in the sciatic nerve of alloxan-diabetic rats: effect of ganglioside treatment." Diabetologia **29**(4): 254-258.

Mathews, C. E. and E. H. Leiter (2005). Rodent Models for the Study of Diabetes. Joslin's diabetes mellitus. E. P. Joslin and C. R. Kahn. Philadelphia, Pa., Lippincott Williams & Willkins**:** 291-327.

Mordes, J. P., R. Bortell, H. Groen, D. Guberski, A. A. Rossini and D. L. Greiner (2005). Autoimmune diabetes mellitus in the BB rat. Animal Models of Diabetes: A Primer. A. A. F. Sima and E. Shafir. Amsterdam, The Netherlands, Harwood Academic**:** 1-37.

Mozaffari, M. S., R. Abdelsayed, I. Zakhary, M. El-Salanty, J. Y. Liu, H. Wimborne and A. El-Marakby (2011). "Submandibular gland and caries susceptibility in the obese Zucker rat." J Oral Pathol Med **40**(2): 194-200.

Nakhooda, A. F., A. A. Like, C. I. Chappel, F. T. Murray and E. B. Marliss (1977). "The spontaneously diabetic Wistar rat. Metabolic and morphologic studies." Diabetes **26**(2): 100-112.

Nature Methods Editorial (2010). "Rats!" Nat Methods **7**(6): 413-413.

Östenson, C.-G. (2005). The Goto-Kakizaki rat. Animal Models of Diabetes: A Primer. A. A. F. Sima and E. Shafir. Amsterdam, The Netherlands, Harwood Academic**:** 174-187.

Peterson, R. G. (2005). The Zucker Diabetic Fatty (ZDF) rat. Animal Models of Diabetes: A Primer. A. A. F. Sima and E. Shafir. Amsterdam, The Netherlands, Harwood Academic**:** 95-112.

Quinn, R. (2005). "Comparing rat's to human's age: How old is my rat in people years?" Nutrition **21**(6): 775-777.

Rees, D. A. and J. C. Alcolado (2005). "Animal models of diabetes mellitus." Diabet Med **22**(4): 359-370.

Reuterving, C. O., E. Hagg, R. Henriksson and J. Holm (1987). "Salivary glands in long-term alloxan-diabetic rats. A quantitative light and electron-microscopic study." Acta Pathol Microbiol Immunol Scand A **95**(3): 131-136.

Srinivasan, K., B. Viswanad, L. Asrat, C. L. Kaul and P. Ramarao (2005). "Combination of high-fat diet-fed and low-dose streptozotocin-treated rat: a model for type 2 diabetes and pharmacological screening." Pharmacol Res **52**(4): 313-320.

Tamemoto, H., T. Kadowaki, K. Tobe, T. Yagi, H. Sakura, T. Hayakawa, Y. Terauchi, K. Ueki, Y. Kaburagi, S. Satoh and et al. (1994). "Insulin resistance and growth retardation in mice lacking insulin receptor substrate-1." Nature **372**(6502): 182-186.

Withers, D. J., J. S. Gutierrez, H. Towery, D. J. Burks, J. M. Ren, S. Previs, Y. Zhang, D. Bernal, S. Pons, G. I. Shulman, S. Bonner-Weir and M. F. White (1998). "Disruption of IRS-2 causes type 2 diabetes in mice." Nature **391**(6670): 900-904.

Zatz, R., T. W. Meyer, H. G. Rennke and B. M. Brenner (1985). "Predominance of hemodynamic rather than metabolic factors in the pathogenesis of diabetic glomerulopathy." Proc Natl Acad Sci U S A **82**(17): 5963-5967.

Zucker, L. M. and T. F. Zucker (1961). "Fatty, a new mutation in the rat." Journal of Heredity **52**(6): 275-278.

III. PROGRESSIVE RESPONSE OF THE ENDOTHELIUM TO CHRONIC HYPERGLYCEMIA

1. Introduction

Almost all long-term complications of diabetes mellitus are strongly related to damages in blood vessels. Vascular complications may be separated into macrovascular, if affecting larger vessels as in the case of peripheral/coronary artery disease or stroke, or microvascular complications, if affecting capillaries like in retinopathy, neuropathy or nephropathy (Fowler 2008). Lining the inner surface of the vascular system is a thin single cell layer: the endothelium. Considering that the endothelium is in permanent contact with the bloodstream, it is not surprising that variations in blood composition will have an effect in endothelial cells. Hence it is important to understand the mechanisms underlying the endothelial response to hyperglycemia.

1.1. Embryonic origin and development of the endothelium

The endothelium is the innermost layer of cells in the circulatory system. Depending on the organ, one may consider the vascular endothelium, in blood vessels; the endocardium, in the heart cavities; or the lymphatic endothelium, in lymphatic vessels. The average human adult endothelium weights approximately 1 Kg and may have surface area up to 7000 m^2 (Aird 2005).

The endothelium has its embryonic origin in the mesoderm as loose aggregations of cells expressing early endothelial markers, which give origin to angioblasts in a process not fully understood. The existence of a pluripotent intermediate hemangioblast precursor, which could differentiate into endothelial and hematopoietic precursors, has been postulated but it has been shown that mesoderm cells could differentiate directly into angioblasts without the need of an intermediate hemangioblast (Pardanaud and Dieterlen-Lievre 1993; Choi, Kennedy et al. 1998; Ferguson, Kelley et al. 2005; Patterson 2007). The angioblast formation appears to involve members of fibroblast growth factor (FGF)

and bone morphogenetic protein (BMP) families, as well as an endoderm-mesoderm interaction (Vokes and Krieg 2002; Patterson 2007).

Vasculogenesis, the formation of blood vessels from the in situ differentiation of angioblasts into endothelial cells, in contrast to angiogenesis that results from the extension or remodelling of existing vessels, starts in the para-arotic region of mesoderm and originates the dorsal aorta and cardinal veins in a primary vascular network. Simultaneously, the endocardium originates from angioblasts that migrate from other region of mesoderm (Ferguson, Kelley et al. 2005; Patterson 2007). Further development of the vascular system occurs mostly by angiogenesis until the full development of a mature network (Figure 11).

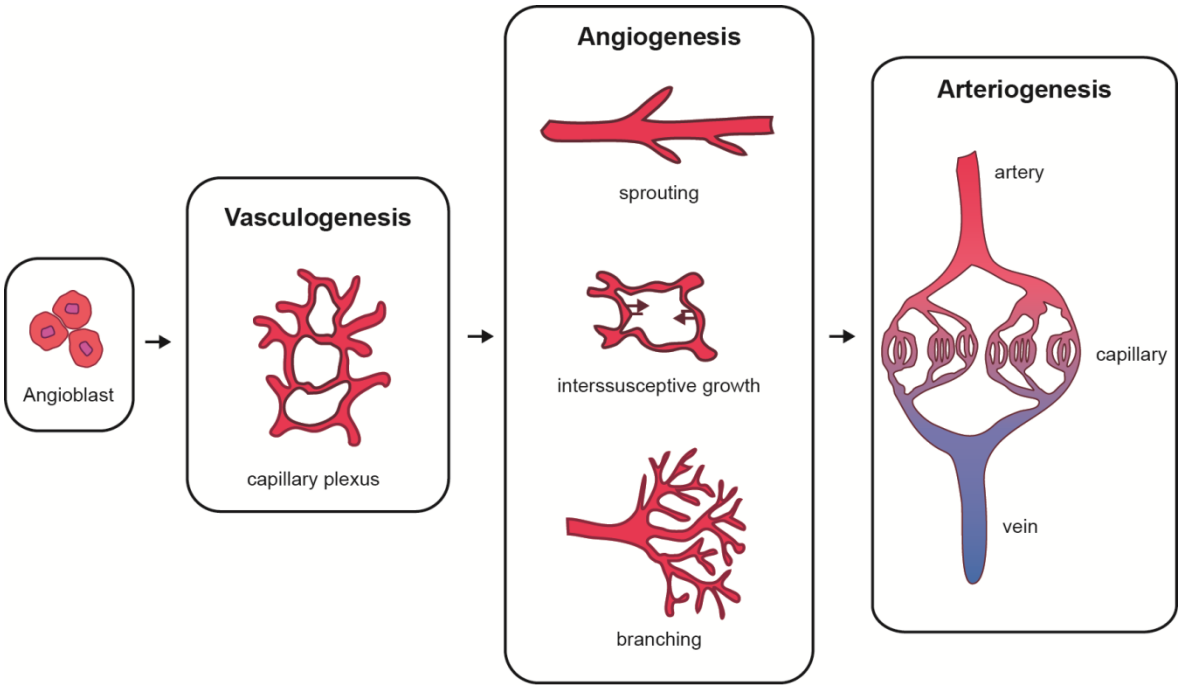

Figure 11 – Process of blood vessel formation during embryonic development.
Adapted from Carmeliet and Collen (2000)

The processes of vessel formation are coordinated by the vascular endothelial growth factor (VEGF) and its receptors (VEGFR1 and VEGFR2) and neuropilin co-receptors (NP1 and NP2). To be able to respond to VEGF, cells need to firstly express its receptors. VEGFR2 is expressed very early in embryonic development and it has been reported that BMP stimulated VEGFR2 transcription (Eichmann, Corbel et al. 1997; Wu,

Moser et al. 2003). VEGF is secreted not only by endothelial cells, but also by other cells in endothelial vicinity and its expression is regulated by hypoxia-inducible factor 1 (HIF-1) (Carmeliet and Collen 2000). The binding of VEGF to its receptors activates intracellular cascades that induce cell proliferation and which will be discussed further ahead.

1.2. The endothelium as a specific type of epithelial tissue

The classification of the endothelium as an epithelial tissue is not consensual. The term endothelium was coined by Wilhelm His, in 1865, to distinguish this tissue from the traditional epithelium. His considered three major differences between endothelium and "true" epithelium: the embryonic origin was different, the endothelium had a clearly recognizable structure and the endothelium did not present physiological secretion; hence he considered it should be identified by its own name: endothelium (Laubichler, Aird et al. 2007). Indeed, the evolution of scientific knowledge since His introduced the term, allowed the discovery of several structural and physiological properties, some unique, others common to epithelial tissues. For instance, it is now known that endothelial cells have an active secretory function of remarkable importance in the development and proliferation of blood vessels and in the regulation of vasodilation, coagulation and inflammation (Esper, Nordaby et al. 2006). On the other hand, endothelial cells have intermediate filaments of vimentin, while epithelial cells have filaments of cytokeratin. Moreover, endothelial cells possess a unique type of intercellular junctions with vascular endothelial (VE)-cadherin, which are not found in other tissues, as well as specific receptors involved in cross-talk between endothelial and vascular smooth muscle layers (Munoz-Chapuli, Carmona et al. 2005). Despite these differences, classic reference books of histology still classify tissues into four basic types: epithelial, connective, muscular and nervous. Although recognizing the existence of specificities to the mesodermal-derived lining tissues, such as the endothelium or the mesothelium, it is considered that such differences have a low practical value by both morphological and

functional criteria. Hence, the endothelium is considered a simple squamous epithelium (Henrikson 1997; Young 2006; Mescher 2009).

1.3. Endothelial heterogeneity as an organ-dependant specialization

Despite being always a single layer of cells, the vascular endothelium has a heterogeneous morphology. Capillary may have a continuous non-fenestrated endothelium, with cells densely juxtaposed connected by tight-junctions that block any interendothelial transport; a continuous fenestrated endothelium, where cells have fenestrae covered with a non-membranous diaphragm, which increase permeability but retain some filtering properties from the diaphragm; or a discontinuous endothelium with large gaps (fenestrae lacking diaphragm), allowing the free passage of larger molecules (Figure 12). Arteries have a continuous non-fenestrated endothelium, formed by long and narrow cells with numerous tight junctions and aligned with the blood flow. Venous endothelium is also continuous and non-fenestrated, but cells are not aligned, are wider and possess valves (Aird 2003; Aird 2007b; Aird 2007a; Stan 2007).

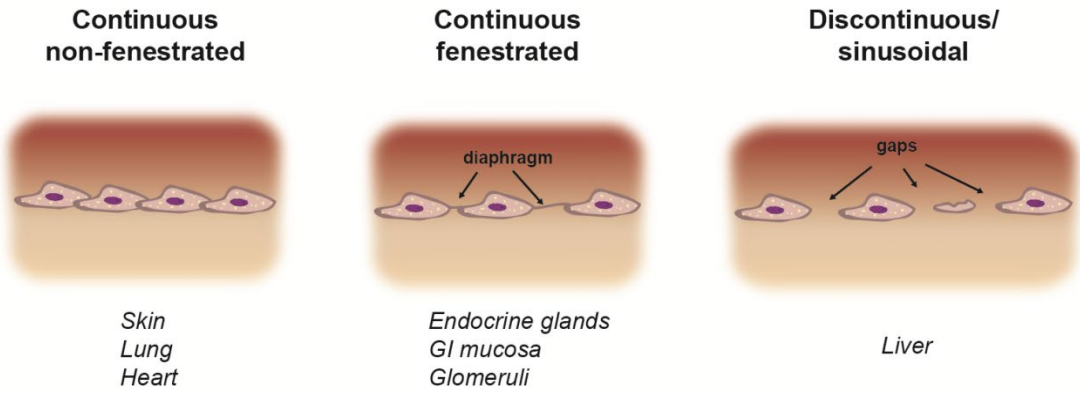

Figure 12 – Schematic representation of the types of capillary endothelium.

The morphology of the endothelium is tightly connected to the specific functions it may have in specific organs/tissues. In brain, skin, heart muscle and lung, capillary form a tissue-blood barrier to prevent the

entry or the leakage of unwanted molecules and cells from blood; hence it is of a continuous non-fenestrated type. In the gastrointestinal tract, there is a need to rapidly allow the passage of nutrients from the intestinal lumen to the bloodstream, so the endothelium has numerous fenestrae with diaphragms. Similarly, kidney glomeruli also have continuous fenestrated endothelium to facilitate blood filtration (Aird 2007b). Liver needs to permanently exchange numerous molecules with blood, namely lipid particles, serum proteins, blood toxins and bilirubin; to facilitate this exchange, the liver endothelium is discontinuous and has a large number of fenestrae without diaphragm. Within the same organ, it is also possible to observe heterogeneous endothelium. Pancreas is simultaneously an endocrine and an exocrine gland; exocrine pancreas, secretes digestive enzymes and electrolytes into ducts and has a continuous endothelium with some fenestrae; endocrine pancreas, on the other hand, secretes hormones directly into the bloodstream and needs to act rapidly to regulate glycemia, consequently, the endothelium is continuous but highly fenestrated (Stevens, Rosenberg et al. 2001; Aird 2003; Aird 2007a; Lammert 2007).

1.4. Endothelial dysfunction and repair

As previously mentioned, the endothelium is more than a simple lining tissue or barrier. Several physiological functions were already shown to have a strong involvement of the endothelium, making it a dynamic organ. The endothelium regulates vasodilator tone in response to shear stress, temperature changes, bradykinin and acetylcholine. This is achieved with the secretion of molecules, such as, nitric oxide (NO), prostacyclin, endothelium-derived hyperpolarizing factors (EDHF), carbon monoxide and endothelin, which act on the vascular smooth muscle. Moreover, endothelium also regulates coagulation, platelet aggregation, adhesion of inflammatory cells and its own repair and regeneration (Ozkor, Murrow et al. 2010). Lining the luminal surface of endothelial cells is a carbohydrate-rich layer – the glycocalyx – that has critical roles in the

regulation of vascular permeability, reduction of blood cell-vessel wall interactions, mediation of shear stress sensing, balancing signalling and has a general vasculoprotective role (Reitsma, Slaaf et al. 2007). Endothelial dysfunction is defined as the loss of any of these proper physiological functions (Schram and Stehouwer 2005; Schmieder 2006; Avogaro, Albiero et al. 2011).

The vascular endothelium is permanently subject to chemical and physical stress as a consequence of alterations in blood composition and the pressure of the blood flow, respectively. As such, the integrity of this single-cell layer is kept by its highly effective repair mechanisms. As previously mentioned, the growth of endothelial tissue occurs either by vasculogenesis – the differentiation of angioblasts into new endothelial cells – or by angiogenesis – the proliferation of existent endothelial cells. It was thought that vasculogenesis was restricted to the embryonic stage; however, the discovery of bone marrow-derived circulating endothelial progenitor cells (EPC) has challenged this concept. It has been demonstrated the capacity of mobilization of EPC from the bone marrow to neoangiogenic sites and participation in the formation of new blood vessels (Asahara, Takahashi et al. 1999; Takahashi, Kalka et al. 1999; Lyden, Hattori et al. 2001; Costa 2011). Vascular injury may result in endothelial cell apoptosis or detachment of endothelial cells from the basal lamina, leaving naked areas. Cell detachment may result from mechanical injury, alteration of cell adhesion molecules or defective binding to anchoring matrix proteins, and cells are released in the blood stream, originating a population of circulating endothelial cells (CEC). These cells are correlated with severe endothelial damage and their increase is often associated to endothelial dysfunction and inflammatory markers (Goon, Lip et al. 2006).

Endothelial proliferation is regulated by VEGF. An increase of serum levels of VEGF is correlated to endothelial damage. Upon recognition by the VEGF receptors on the surface of endothelial plasma membrane, the pro-survival Akt cascade is activated, inducing gene transcription and

proliferation. VEGF was also shown to promote the recruitment of EPC from bone marrow to injury sites. Thus, the repair of injury may be conducted by proliferation of adjacent endothelial cells and/or by the recruitment of EPC (Figure 13). Other molecules have a similar role in the activation of the Akt cascade and inhibiting apoptosis. It was shown that angiopoietin 1, insulin and IGF-1, sphingosine-1-phosphate, HGF, leptin, adiponectin and fluid shear stress, also activate PI3K-Akt signalling (Shiojima and Walsh 2002).

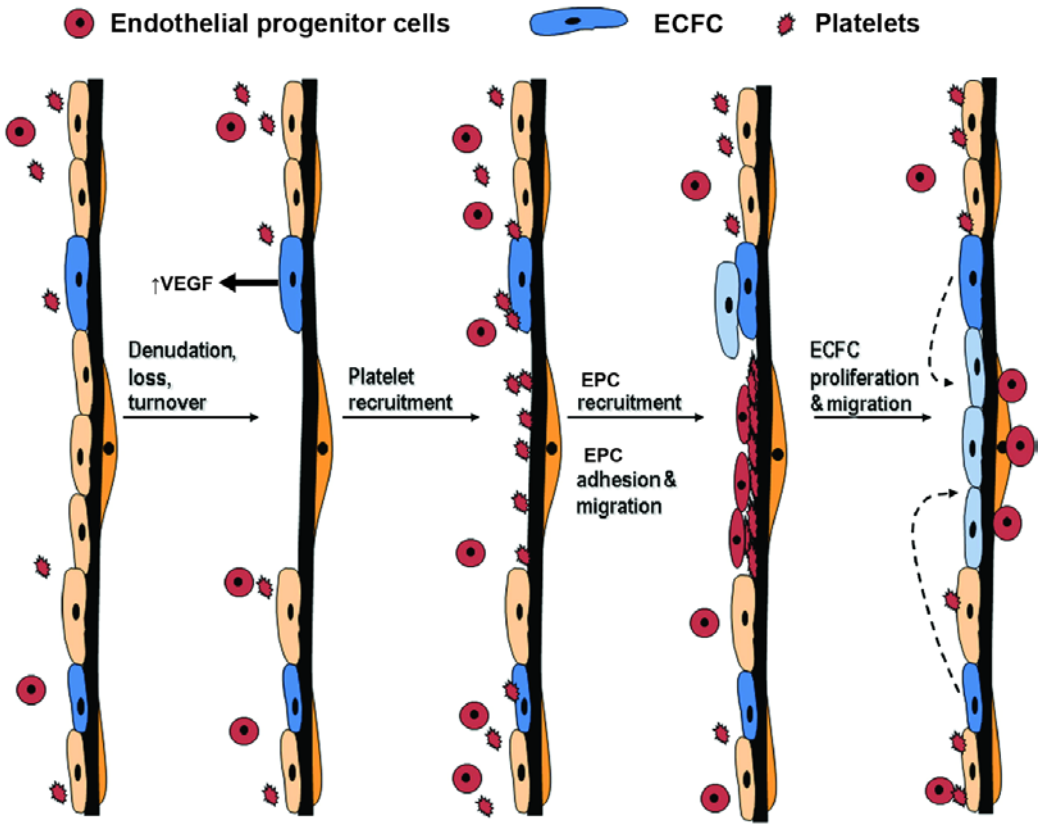

Figure 13 – Mechanisms of endothelial repair by proliferation of existing endothelial cells and recruitment of progenitor cells.
Upon the detachment of endothelial cells, there is an increase of VEGF secretion and other proliferation and mobilization stimuli. These stimuli recruits endothelial progenitor cells (EPC) to the injury site. These differentiate into mature endothelial cells to repair the injury. Simultaneously, mature endothelial cells with proliferative potential (ECFC) adjacent to the injury site, may also proliferate and repair the injury. Adapted from Richardson and Yoder (2011) with permission from Elsevier.

1.5. Endothelium, inflammation and immunity

The endothelium releases several important physiological and pathophysiological inflammatory mediators. The changes that occur in the

endothelium, allowing it to participate in the inflammatory response, are called endothelial activation (Hunt and Jurd 1998; Hartge, Unger et al. 2007). When any stimulus induces the release of proinflammatory cytokines IL-1beta and TNF-alpha by macrophages, these activate the expression of leucocyte adhesion molecules (ELAMs), altering the protein composition of the glycocalyx. Activated endothelial cells also secrete chemokines and in conjunction with the ELAMs E-selectin, intercellular adhesion molecule-1 (ICAM-1) and vascular cell adhesion molecule-1 (VCAM-1), interact with receptors on the surface of leucocytes and guide them to intercellular junctions where they cross into tissue space, resulting in inflammation. The endothelial response may be modulated by T-cell-derived cytokines; IFN-gamma prolongs the expression of E-selectin, whereas IL-4 suppresses it and promotes VCAM-1 expression. Such modulation favours the recruitment of T-helper-1 leucocytes by IFN-gamma or the T-helper-2 leucocytes by IL-4 (Pober 2002).

Proinflammatory cytokines also have an effect in the innate immunity system. The endothelial expression of a membrane protein named decay-accelerating factor (DAF) is highly responsive to TNF-alpha and IFN-gamma cytokines, as well as to growth factors (FGF, VEGF) and thrombin. This protein is an important regulator of the complement system and, together with the other complement regulators CD46 and CD59, is also highly expressed in the presence of C-reactive protein. Inflammatory agonists were also shown to induce the synthesis of complement proteins in endothelial cells (Augustin 2007).

The complement system is a set of more than 30 plasma soluble proteins, cell receptors and control proteins that act in a cascade-like manner to protect against bacteria, viruses, parasites and tumour-cells (Rus, Cudrici et al. 2005). It has three independent activation pathways: the classical pathway, the alternative pathway and the lectin pathway. Each one of these pathways is activated through the recognition of specific molecules or complexes. Antigen-antibody complexes are recognized by the C1-complex and activate the classical pathway; the spontaneous

activation of C3 and certain molecules on the surface of pathogens, such as lipopolysaccharides, activate the alternative pathway; some sugars, such as mannose, fructosamine or glucose, when in the terminal end of glycoproteins on the surface of pathogens, are recognized by the lectins ficollin of mannose-binding lectin (MBL) and activate the lectin pathway (Fortpied, Vertommen et al. 2010). All of these pathways converge in the activation of C3 convertase, which continues a proteolytic cascade throughout sever of the complement functions are activated. The deposition of C5b peptide on the surface of cells, initiates the formation of the membrane attack complex (MAC), opening pores on foreign cells and inducing cell lysis; C3a and C5a promote the degranulation of mast cells and enhance vascular permeability; C3b acts as an opsonin, enhancing phagocytosis (Figure 14) (Janeway, Travers et al. 2001; Rus, Cudrici et al. 2005).

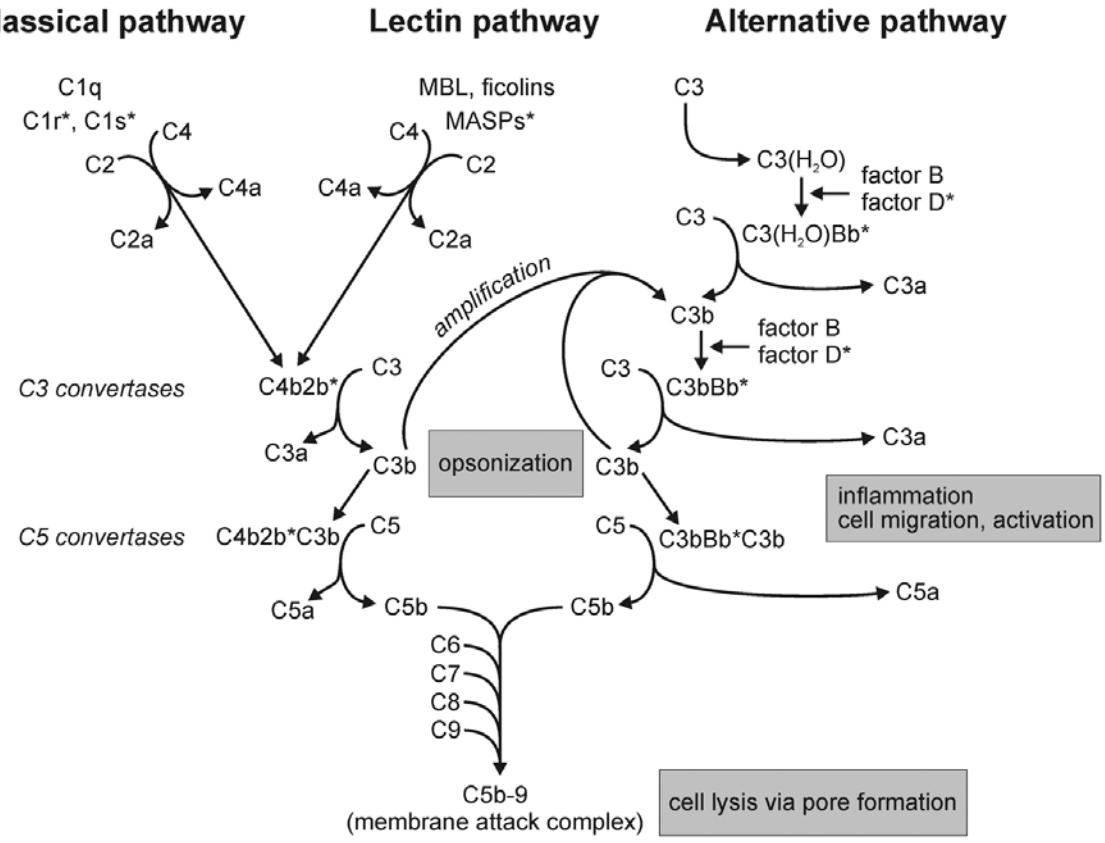

Figure 14 – Activation pathways for the complement system and respective proteolytic cascade.
Published in Józsi (2011)

Endothelial cells express G-protein-coupled receptors for C3a and C5a proteins, and both activate the expression of IL-1beta and IL-8. C5a also induces the release of von Willebrand factor and the expression of P-selectin and E-selectin, increasing endothelial adhesiveness for neutrophils. C5b-9 induces vesiculation in endothelial cells, which become sites for clothing factor Va binding, thus having a procoagulant activity in conjunction with endothelial cells (Augustin 2007).

1.6. Endothelial dysfunction in hyperglycemia

Poorly controlled glycemia levels mean that blood vessels, in particular the endothelium, are in a permanent contact with high concentrations of glucose. Thus, it is not surprising that hyperglycemia is correlated to endothelial dysfunction (Schram and Stehouwer 2005; Bakker, Eringa et al. 2009; Avogaro, Albiero et al. 2011). The mechanisms relating both events are not fully disclosed.

It has been reported a progressive increase of inflammatory markers in endothelial cells with the duration of hyperglycemia (Bucciarelli, Pollreisz et al. 2009). Insulin signalling is present in endothelial cells and, in diabetes, the impairment of this signalling pathways has consequences in cell proliferation and vascular tone regulation (Abebe and Mozaffari 2010).

The formation of advanced glycation endproducts (AGEs) and oxidative stress have also been implied in vascular damage and have been extensively studied (Tan, Chow et al. 2002; Basta, Schmidt et al. 2004; Potenza, Gagliardi et al. 2009; Alkhalaf, Kleefstra et al. 2012). Despite the low reactivity of glucose with amines when compared to other sugars, it is possible that such reactions occur (Bunn and Higgins 1981; Negre-Salvayre, Salvayre et al. 2009). Moreover, ROS may also be generated by mitochondrial dysfunction as a consequence of increased free fatty acids (Abebe and Mozaffari 2010).

Due to the presence of glycation events, the complement activation by the lectin pathway has been proposed to play an important role in

endothelial dysfunction (Hansen, Tarnow et al. 2004; Ostergaard, Hansen et al. 2005; Saraheimo, Forsblom et al. 2005; Ostergaard, Thiel et al. 2007; Ostergaard, Bjerre et al. 2013). MBL recognizes and binds mannose, N-acetylglucosamine and fructosamine residues (Fortpied, Vertommen et al. 2010), this triggers the complement proteolytic cascade starting on the MBL-associated serine protease-1 and -2 (MASP-1/-2).

Because of the relation of the endothelium, inflammation, the complement system and the increased glycation observed in hyperglycemia, we proposed the hypothesis that glycation of membrane proteins of endothelial cells could generate carbohydrate moieties that would be recognized by the mannose-binding lectin and thus activate the complement system against the endothelium and promoting an inflammatory state. We have tried to analyse endothelial cells isolated from the aorta, as well as markers of endothelial damage and repair, linking these to the activity of the MBL activity in control and hyperglycemic rats.

2. Methods

2.1. Aortic endothelial cells isolation

Aortic endothelial cells were isolated from portions with magnetic beads coated with a specific antibody for endothelial cells. First, Dynabeads® M-270 Epoxy (14301, Invitrogen, UK) were coated with anti-CD146 antibody, according to the manufacturer's instructions. In brief, 300 µl of beads suspension were washed with 0.1 M sodium phosphate buffer, pH 7.4, to remove the storage buffer. Afterwards, beads were ressuspended in PBS for 2 minutes and 10 µl of anti-Rabbit IgG HRP-conjugated (RPN2124, GE Healthcare, UK) were added. After an overnight incubation at 37°C with agitation, the beads were washed twice with PBS supplemented with 0.1% (m/v) of BSA (A7906, Sigma, USA) and once more with 0.2 M Tris, pH 8.5, supplemented with 0.1% BSA, to block the remaining free epoxy groups, and once again with PBS/BSA. Next, the

beads were ressuspended in PBS/BSA and 10 µl of Anti-CD146 antibody (ab75769, Abcam, UK) were added and incubated overnight at 4ºC with agitation. Coated beads were then washed 4 times with PBS/BSA, 5 minutes at 4ºC with agitation, to block any unspecific binding sites and stored at 4ºC in PBS/BSA.

On the days of animal sacrifices, pieces with approximately 5 cm of aorta were collected and kept in PBS, on ice, for no longer than 3 hours until the start of the isolation procedure (Figure 15). Cell collection from the aortic pieces was performed according to Jaffe, Nachman et al. (1973). The aortic piece lumen was washed with PBS using a syringe and needle, to remove any traces of blood. One of the extremities was then clamped and the blood vessel was filled with a solution of 0.1% type I collagenase (17100-017, Gibco, Invitrogen, UK) in PBS was injected through the open extremity. The open extremity was also clamped and the blood vessel was submersed in PBS at 37ºC for 20 minutes for the collagenase to act, releasing the interior layers of cells. The cell suspension was collected in a test tube and an approximately equal volume of PBS was injected again in the blood vessel to increase cell recovery. The cell suspension was then centrifuged at 250x *g*, 10 minutes at room temperature, the supernatant was discarded and the pellet was ressuspended in PBS to wash collagenase traces. After another centrifugation, the cell pellet was ressuspended in 300 µl of buffer A (PBS supplemented with 2 mM of EDTA and 5% (m/v) BSA) for endothelial cells isolation. Endothelial cells isolation was performed with the previously prepared anti-CD146-coated magnetic beads, adapted from Neurauter, Bonyhadi et al. (2007). Magnetic beads were ressuspended in 700 µl of buffer A and added to the cell suspension. Following an overnight incubation with agitation, at 4ºC, the beads were washed three times with buffer A, 15 minutes at 4ºC with agitation. To release the cells from the magnetic beads, 1ml of trypsin-EDTA solution was added and allowed to incubate for 5 minutes at 37ºC with agitation. The supernatant containing the cell suspension was then

centrifuged at 300x *g* for 3 minutes, at room temperature and the pellet was ressuspended in 150 µl of PBS.

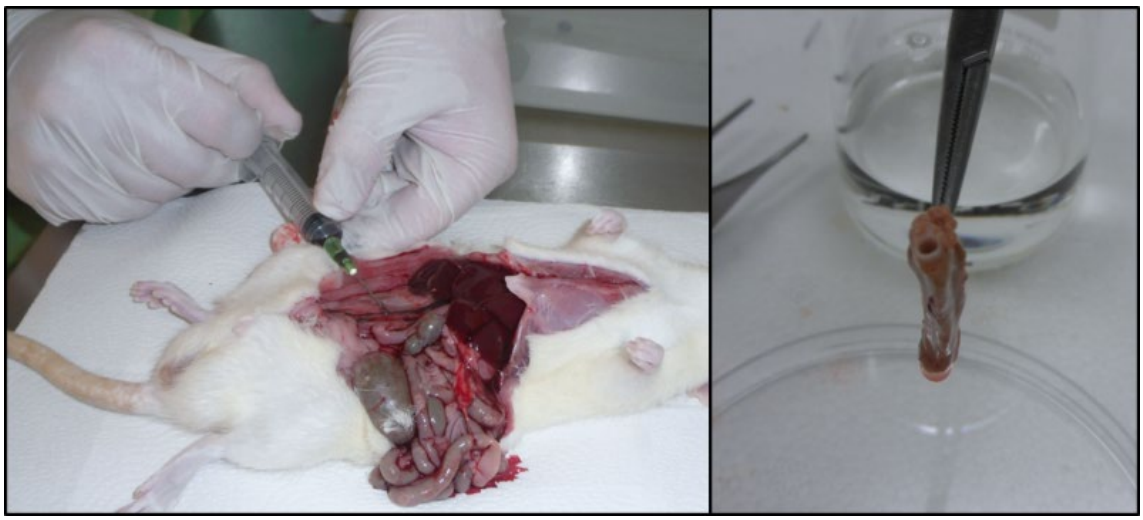

Figure 15 – Collection of blood from the inferior vena cava (left) and aorta pieces used in endothelial cells isolation (right).

2.2. Circulating endothelial cells and endothelial progenitor cells labelling

Blood collected into EDTA tubes was kept on ice and no more than 3 hours passed between collection and analysis (Figure 15). Red blood cells (RBC) were lysed by adding 1 ml of blood to 14 ml of lysis buffer freshly prepared from a 10x stock solution (0.15 M NH_4Cl, 10 mM $KHCO_3$, 0.1 mM EDTA, pH 7.3). RBC were allowed to lyse for 3-5 minutes and then centrifuged at 300x *g* for 5 min, at room temperature. The supernatant was discarded and the cell pellet was washed, ressuspending it in 5 ml of ice-cold phosphate-buffered saline (PBS) and centrifuging once more at 300x *g*, for 5 minutes. The washed cell pellet was then ressuspended in 1ml of ice-cold PBS and white blood cells were blocked with 100 µg of rat IgG (I4131, Sigma,USA), for 15 minutes, at room temperature. Cells were then incubated with 5 µl of the unlabelled primary anti-CD133 antibody (ab19898, Abcam, UK), followed by the incubation with labelled antibodies: 20 µl of PE-anti-CD146 (FAB3250P, R&D Systems, USA), 10 µl of PE/Cy5-anti-CD45 (559135,

BD Pharmingen, USA) and 2 µl FITC-anti-rabbit IgG (F9887, Sigma-Aldrich, USA). All antibody incubations were conducted at room temperature, for 20 minutes. Excess antibody was removed by washing once with PBS supplemented with 1% BSA and 0.05% NaN_3, and the labelled cells were pelleted at 500x *g* for 5 min and ressuspended in 1 ml of PBS/BSA/NaN_3.

2.3. Flow cytometry analysis

Each sample was analysed in a 3-colour FACScalibur flow cytometer (BD Biosciences, USA). Non-labelled samples were firstly analysed to establish selection gates and to serve as negative control (Figure 16). Samples were analysed for a minimum of 500,000 mononuclear cellular events. Cells were initially plotted according to forward- and side-scatter profiles and a gate was established to select only mononuclear cell events (Figure 18). A second gate was set to exclude CD45 positive cells, but not $CD45^{dim}$, as these may include endothelial progenitor cells. Cells doubly positive for CD146 and CD133 were considered endothelial progenitor cells (EPC), while cells only positive for CD146 were considered circulating endothelial cells (CEC).

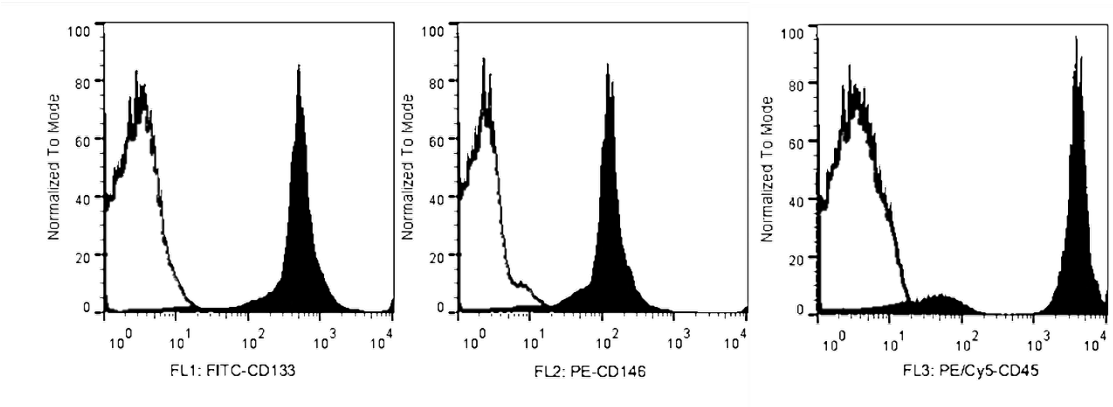

Figure 16 – Flow cytometry histograms of labelled (black) and non-labelled (white) samples for each of the fluorescence channels.

2.4. In vivo labelling with 5-bromo-2'-deoxyuridine

Two hyperglycemic animals and one control animal from the groups of long-term exposure to hyperglycemia (4 months) were injected intraperitoneally with a single dose (100 mg/kg) of 5-bromo-2'-deoxyuridine (BrdU) 72 hours prior to sacrifice. Upon sacrifice, pieces of aorta were collected and processed through paraffin embedding for light microscopy. Tissue sections were stained with anti-BrdU primary antibody (ab1893, Abcam, UK) followed by horseradish-conjugated anti-Goat IgG secondary antibody (ab7125, Abcam, UK) and detected with Fast Dab Tablets (D0426, Sigma, USA).

2.5. Western blot

Approximately 20 μg of serum protein were electrophoresed in a 12.5% SDS-PAGE, according to Laemmli (1970) and blotted onto a nitrocellulose membrane. Non-specific protein binding sites were blocked with 5% dry non-fat milk in TBS supplemented with 0.05% Tween-20 (TBS-T), followed by a 3-hour incubation, at room temperature, with mouse anti-VEGF antibody (ab1316, Abcam, UK) diluted 1:1000 in blocking solution, three 15-minute washes with TBS-T and a 45-minute incubation with horseradish peroxidase-conjugated anti-mouse IgG antibody (A9917, Sigma, USA), at room temperature. Immunoreactive bands were detected with home-made chemiluminesce substrate on X-ray films (Hyperfilm ECL, GE Healthcare, UK) and digital images were acquired on a Molecular Imager Gel Doc XR system (Bio-Rad, USA) and analysed with QuantityOne software (v4.6.3, Bio-Rad, USA). Results are presented as mean±SD for each experimental group of at least three independent experiments with n=5.

2.6. MBL-pathway complement activation

MBL complex activity was determined as described by Petersen and colleagues (2001). Microtiter wells (cat. no. 456537, Maxisorp®, Nunc, Germany) were coated with 1 μg of mannan (M7504, Sigma, USA) in

100 µl of coating buffer (15 mM Na_2CO_3, 35 mM $NaHCO_3$, 1.5 mM NaN_3, pH 9.6). After an overnight incubation at room temperature, the wells were blocked for 1 hour with 200 µl of 0.1% (w/v) rat serum albumin (RSA) (A6414, Sigma, USA) in TBS (10 mM Tris-HCl, 140 mM NaCl, 1.5 mM NaN_3, pH 7.4). Wells were incubated overnight, at 4ºC, with 100 µl of rat serum diluted 1:50 in MBL-binding buffer (20 mM Tris, 10 mM $CaCl_2$, 1 M NaCl, 0,05% Tween-20, 0,1% RSA, pH 7.4), in duplicates. Then, 100 µl of a solution of C4 protein (1 ng/µl) (ab98983, Abcam, UK) in barbital buffer (4 mM barbital, 145 mM NaCl, 2 mM $CaCl_2$, 1 mM $MgCl_2$, 3.8 mM NaN_3, pH 7.5) were added and the plate was incubated for 90 minutes at 37ºC. Negative controls were also conducted for each sample with barbital buffer without C4 protein. Next, 100 µl of sheep anti-C4 antibody (ab8786, Abcam, UK), diluted 1:1000 in washing solution (TBS supplemented with 0.05% of Tween-20 and 5 mM $CaCl_2$), were added and incubated 90 min at room temperature, followed by an 1-hour incubation, at room temperature, with 100 µl of Rabbit anti-Sheep IgG H&L (AP) secondary antibody (ab6748, Abcam, UK), diluted 1:1000 in washing solution. Then, 100 µl of substrate solution (1 mg/ml p-nitrophenyl phosphate in 1 M dietanolamine, 1 mM $MgCl_2$, 3 mM NaN_3, pH 9.6) were added and allowed to react at 37ºC with mild shaking for 5 minutes before reading optical density at 450nm. The values obtained for the negative controls were subtracted to their respective counterparts and the resulting values were used to evaluate MBL-complex activity in serum. Between each of the incubation steps, excess reagent from the previous incubation was washed twice with washing solution.

2.7. Statistical analysis

All statistical tests were performed using GraphPad Prism v5.00 (GraphPad Software, Inc., USA). Data were analysed using a two-way ANOVA with Bonferroni's post hoc tests to compare groups. A p value <0.05 was considered significant.

3. Results

3.1. Analysis of aortic endothelial cells

The use of magnetic beads for the isolation of endothelial cells was successful in the preliminary study, as could be observed under the microscope (Figure 7). However, the western blot analysis of specific endothelial proteins, such as VEGF or eNOS, was not possible (Figure 17). Further attempts to enrich the samples in protein content and load more protein in the gel were made using acetone precipitation and ultrafiltration approaches, but were also unsuccessful.

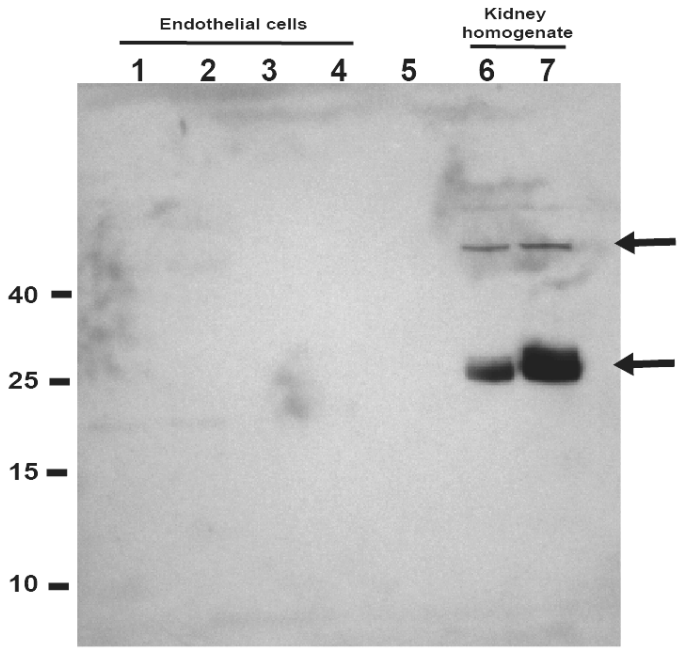

Figure 17 – Representative western blot of endothelial cell suspension for VEGF.
Endothelial cell suspensions were loaded in lanes 1-4; a positive control for control (lane 6) and hyperglycemic (lane 7) animals made from kidney homogenate in PBS was used. Anti-VEGF antibody recognizes a specific and intense band of approximately 24kDa and may recognize dimeric forms of VEGF at 43 kDa (arrows). In endothelial cell suspensions, no bands were detected.

3.2. Evaluation of endothelial damage and repair

Flow cytometry was successfully applied in the quantification of both circulating endothelial cells (CEC) and endothelial progenitor cells (EPC) (Figure 18). It was observed a highly significant increase of CEC in hyperglycemic animals, which is also progressively accentuated with the

duration of hyperglycemia. On the other hand, despite a significant reduction of circulating EPC over time, long-term hyperglycemia induced a significant reduction of EPC in peripheral blood (Figure 19).

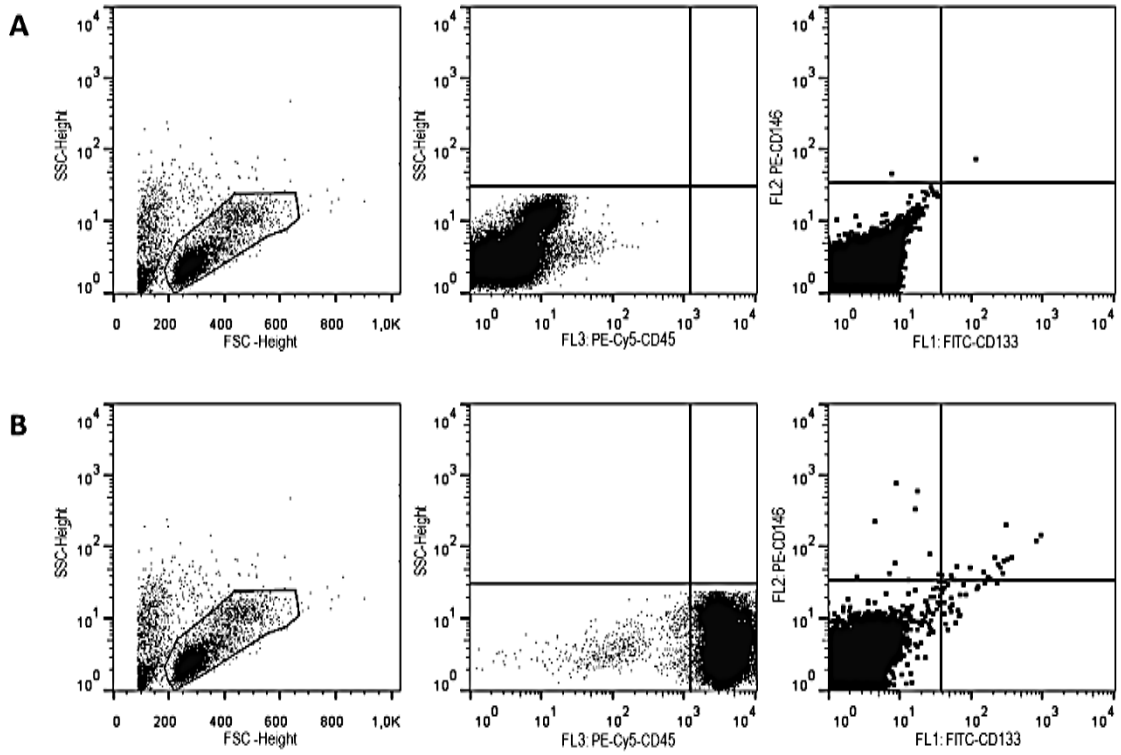

Figure 18 – Representative flow cytometry dotplots of a non-labelled (panel A) and labelled (panel B) sample with the gating strategy.
Left plot exhibits front- vs side-scatter distribution of the whole sample and the selection gate for mononuclear cells; middle plot exhibits the CD45 (FL3 channel) vs. side-scatter distribution of mononuclear cells where a selecting gate was established in the lower-left quadrant; right plot exhibits the CD133 (FL1 channel) vs. CD146 (FL2 channel) distribution of cells selected in the middle plot, where the upper-left quadrant contains CEC and the upper-right quadrant contains EPC (dot size was enhanced to allow a better visualization).

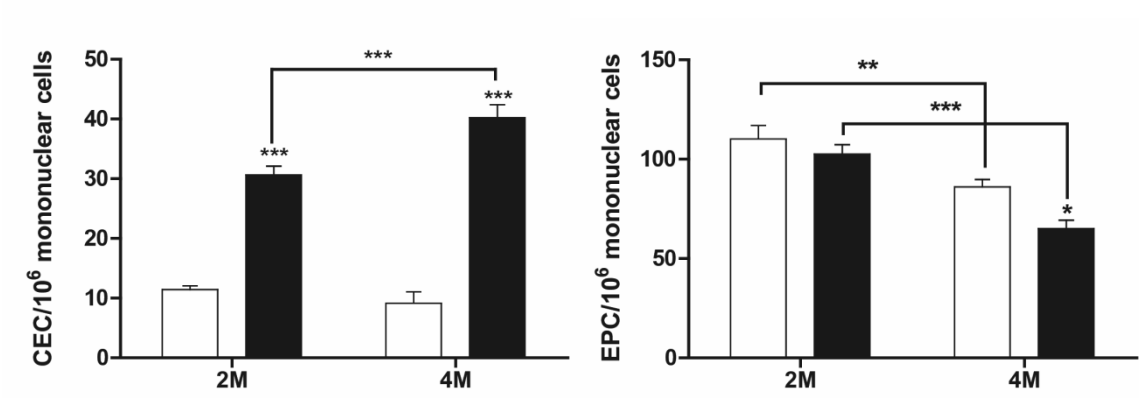

Figure 19 – Variations in the number of CEC and circulating EPC with short- and long-time exposure to hyperglycemia.
The number of cells was determined by flow cytometry; CEC were defined as mononuclear events with a CD45-/CD146+/CD133- phenotype, EPC were defined as mononuclear events with a CD45-/CD146+/CD133+ phenotype. White columns represent control and black columns represent hyperglycemic animals; data are presented as mean±SD of the number of cells per million of mononuclear events. * p<0.05, ** p<0.01, *** p<0.001.

Given that the increase of CEC is a signal of endothelial damage, an analysis of circulating VEGF was conducted to determine if the organism was responding to endothelial damage by stimulating endothelial cell proliferation. It was observable a progressive increase of serum VEGF over time. However, hyperglycemia induced a very significant increase of serum VEGF levels versus the control after 2 months, which was attenuated at 4 months, though still significantly higher than controls (Figure 20).

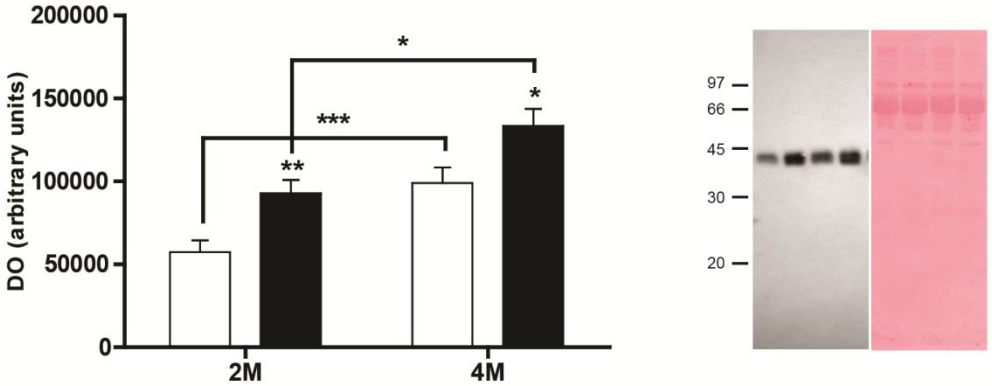

Figure 20 – Variation of the levels of serum VEGF with short- and long-term hyperglycemia.
On the left is the quantitative data obtained with western blot, white columns represent control and black columns represent hyperglycemic animals. On the right is a representative western blot and respective nitrocellulose membrane stained with Ponceau S, as a control of the protein loaded. Data are presented as mean±SD of the optical density, in arbitrary units, of the immunoreactive band at 43kDa. * p<0.05, **p<0.01, ***p<0.001

The increase in serum VEGF after just two-months of exposure to hyperglycemia suggested that proliferation of endothelial cells could be increased. So, it was decided to evaluate if there were qualitative differences in endothelial proliferation, after four-months of exposure to hyperglycemia, through a BrdU incorporation assay. It was observed a higher number of labelled nuclei in endothelial cells from the aorta of hyperglycemic animals, suggesting a higher turnover rate (Figure 21).

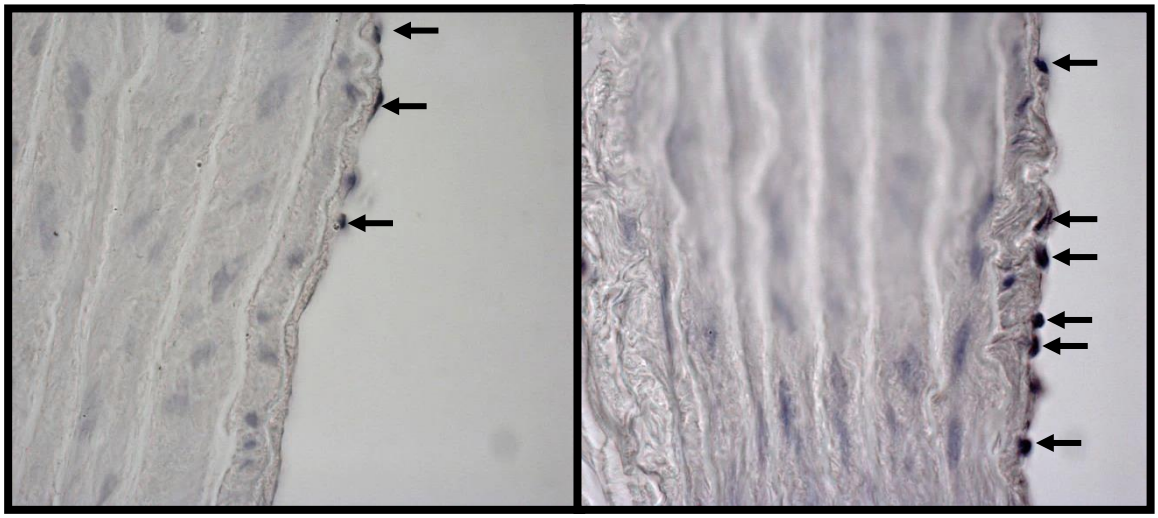

Figure 21 - BrdU incorporation in aortic endothelium of control (left) and long-term (right) hyperglycemic animals.
Nuclei immunoreactive to anti-BrdU antibody are indicated by the arrows.

3.3. MBL-pathway activity in hyperglycemia

Considering the role of endothelial cells in the complement system and that the activation of the complement cascade may be initiated through the recognition of some specific carbohydrate moieties on the cell surface, an assay was conducted to determine if the activity of the MBL/MASP complex presented differences in a hyperglycemic state. It was observed a significant increase of the C4b peptide deposition, originated from the specific activation of the complement cascade by the MBL pathway, with the serum from hyperglycemic animals, thus suggesting an increased activity of the MBL/MASP complex, regardless of the duration of hyperglycemia (Figure 22).

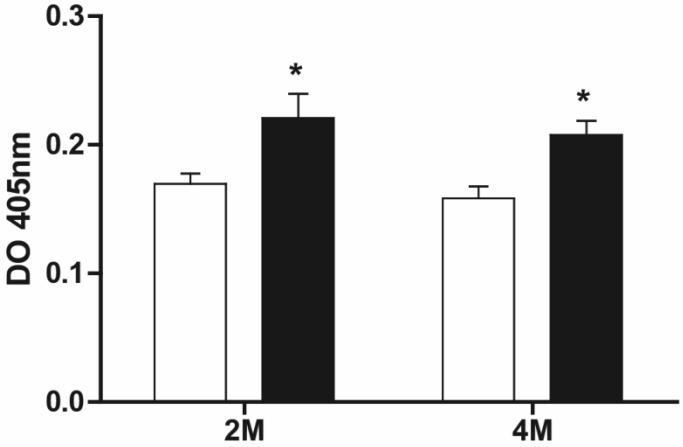

Figure 22 – Variation of C4b deposition with short- and long-term hyperglycemia.
White columns represent control and black columns represent hyperglycemic animals; data are presented as mean±SD of the optical density at 405nm in a specific MBL-pathway activity assay. * $p<0.05$.

4. Discussion

The physiological response to hyperglycemia is not specific of an organ or tissue, but rather a multifactorial systemic response. Hence, in vitro studies have a strong limitation in the integrated analysis of mechanisms modulated by variations in glycemia levels. Such limitation is even more evident in the study of vascular endothelium. As blood circulates throughout the whole organism, it is an important carrier of signalling molecules to and from the various organs. Using endothelial cell culture, either with cell lines or primary cultures, limits the comprehension of the endothelium response to hyperglycemia because it is not possible to mimic, in vitro, the various stimuli carried out by the blood stream, and it is usually limited to the study of cellular response in high-glucose media or in the presence of cytokines (Chavakis, Bierhaus et al. 2004; Schalkwijk and Stehouwer 2005; Son 2007; Packard and Libby 2008; Maugeri, Rovere-Querini et al. 2009). Moreover, the origin of the cells may have influence on their response (Balconi, Pietra et al. 1983). To overcome these limitations, indirect forms of analysing the endothelium have been used, such as the analysis of circulating endothelial cells. However, there is still the perception that a direct analysis of endothelial

cells could drastically improve the knowledge about the underlying mechanisms of endothelial dysfunction (Onat, Brillon et al. 2011). Thus, it is important to carry out direct analyses to endothelial cells obtained from in vivo models, in order to keep the integrated systemic perspective.

This study would have been an important milestone, as proteomic studies of the endothelial response to hyperglycemia are, to the best of our knowledge, limited to cell culture approaches. However, a critical step in the analysis of endothelial cells is the purification of a large enough number of cells, suitable for proteomic analysis. Two major strategies have been used: fluorescence-activated cell sorting (FACS) and immunomagnetic isolation (Scott and Bicknell 1993; Laurens and Hinsbergh 2004; van Beijnum, Rousch et al. 2008; Sobczak, Dargatz et al. 2010). It was chosen the immunomagnetic approach for its simplicity and lower requirements of specialized equipment and also because of the successful isolation carried out in the preliminary study observed by fluorescence microscopy (Chapter II). Unfortunately, it was not possible to perform a protein analysis of the isolated cell suspensions because no protein was detected by western blot, despite the high levels of protein concentration in the samples (Figure 17). The result of the preliminary study proved the feasibility of such approach for the isolation of endothelial cells with the chosen method; however, the evaluation of the success was limited to microscopy and protein concentration. Microscopy was only applied for verifying the presence of positive cells to an endothelial specific marker (CD146), without any quantification concerns, and protein concentration was probably overestimated because the buffers used in cell isolation had BSA and cells were released from the magnetic beads with trypsin. Moreover, considering an average circumference of 6 mm, the aorta pieces have an average internal area of 300 mm^2, which, together with an average cell surface area of 300 μm^2, would fit only 10^3 cells. So, it is conceivable that despite a successful isolation of endothelial cells, the number of recovered cells was not enough to allow a proteomic analysis. In the future, the focus should be on the recovery of a higher

number of cells by applying a different approach, either by using FACS or by isolating cells from a larger cell pool, such as the aorta of a larger animal or from a highly vascularized tissue like the lung.

The application of the number of circulating mature endothelial cells (CEC) as a marker of endothelial damage has been proposed by various studies, and there is a correlation of diabetes with vascular complications and the increase of CEC (Jessani, Lane et al. 2009; Asicioglu, Gogas Yavuz et al. 2010; El Amine, Sohawon et al. 2010; Orrico, Pasquinelli et al. 2010; Kotb, Gaber et al. 2012; Lanuti, Santilli et al. 2012). Similarly, the reduction of endothelial progenitor cells (EPC) has also been linked to diabetes and vascular complications through a reduction of endothelial repair ability (Lev, Singer et al. 2013; Oh, Oh et al. 2013; Westerweel, Teraa et al. 2013; Zhang and Yan 2013). The results presented herein, corroborate these linkages. The particular subset of EPC analysed in this study, has a special relevance because it expresses both a marker for mature endothelial cells (CD146) and a marker of stem cells (CD133), which means this subset of cells has already suffered some maturation stimuli and reinforces the conclusion that there is an impairment of reendothelization from the EPC recruitment mechanism. Interestingly, the incorporation of BrdU assay demonstrated that the turnover rate of endothelial cells in hyperglycemic animals was increased. Endothelial cells have a very slow turnover rate, measured in months or years (Hobson and Denekamp 1984; Cines, Pollak et al. 1998; Goon, Lip et al. 2006); the incorporation of BrdU in so many cells in just 72 hours, indicates a very pronounced turnover rate, which is in accordance with the increased stimulus observed by the higher levels of serum VEGF. Nonetheless, the increased proliferation should not be sufficient to overcome the damages, as the animals presented clear signs of renal function impairment and loss of sight.

The initial hypothesis was that hyperglycemia could result in aberrant glycation of endothelial membrane proteins and be recognized by MBL as a pathogen, activating the complement cascade to destroy the

"invader". Indeed, the relationship between MBL levels and diabetes have been the target of numerous studies (Hansen, Tarnow et al. 2004; Hovind, Hansen et al. 2005; Ostergaard, Hansen et al. 2005; Saraheimo, Forsblom et al. 2005; Ostergaard, Thiel et al. 2007; Elawa, AoudAllah et al. 2011; Ostergaard, Bjerre et al. 2012; Pavlov, La Bonte et al. 2012; Ostergaard, Bjerre et al. 2013) but, to the best of our knowledge, no study has successfully shown the binding of MBL to the endothelium or identified the carbohydrate moieties recognized by MBL on endothelial cell surface. It was expected to find such connection with the isolation of endothelial cells. Nonetheless, it was shown that hyperglycemic animals present increased activity of MBL and its associated proteases, which strongly suggests the involvement of this complement pathway in the pathophysiology of hyperglycemia complications.

In conclusion, it was shown a progressive effect of hyperglycemia on vascular endothelium. Despite the increase of endothelial damage, there is still a physiological response to promote cell proliferation after 4-months of chronic hyperglycemia, although it is mainly by angiogenesis. Additionally, there is strong evidence of complement involvement in endothelial damage.

5. References

Abebe, W. and M. Mozaffari (2010). "Endothelial dysfunction in diabetes: potential application of circulating markers as advanced diagnostic and prognostic tools." EPMA J **1**(1): 32-45.

Aird, W. C. (2003). "Endothelial cell heterogeneity." Crit Care Med **31**(4 Suppl): S221-230.

Aird, W. C. (2005). The endothelium as an organ. Endothelial cells in health and disease. W. C. Aird, Taylor & Francis**:** 1-37.

Aird, W. C. (2007a). "Phenotypic heterogeneity of the endothelium: I. Structure, function, and mechanisms." Circ Res **100**(2): 158-173.

Aird, W. C. (2007b). "Phenotypic heterogeneity of the endothelium: II. Representative vascular beds." Circ Res **100**(2): 174-190.

Alkhalaf, A., N. Kleefstra, K. H. Groenier, H. J. G. Bilo, R. O. B. Gans, P. Heeringa, J. L. Scheijen, C. G. Schalkwijk, G. J. Navis and S. J. L. Bakker (2012). "Effect of Benfotiamine on Advanced Glycation Endproducts and Markers of Endothelial Dysfunction and Inflammation in Diabetic Nephropathy." PLoS One **7**(7): e40427.

Asahara, T., T. Takahashi, H. Masuda, C. Kalka, D. Chen, H. Iwaguro, Y. Inai, M. Silver and J. M. Isner (1999). "VEGF contributes to postnatal neovascularization by mobilizing bone marrow-derived endothelial progenitor cells." EMBO J **18**(14): 3964-3972.

Asicioglu, E., D. Gogas Yavuz, M. Koc, B. Ozben, D. Yazici, O. Deyneli and S. Akalin (2010). "Circulating endothelial cells are elevated in patients with type 1 diabetes mellitus." Eur J Endocrinol **162**(4): 711-717.

Augustin, H. G. (2007). Endothelial Cell Input Endothelial Biomedicine. W. Aird, Cambridge University Press**:** 225-229.

Avogaro, A., M. Albiero, L. Menegazzo, S. de Kreutzenberg and G. P. Fadini (2011). "Endothelial dysfunction in diabetes: the role of reparatory mechanisms." Diabetes Care **34 Suppl 2**: S285-290.

Bakker, W., E. C. Eringa, P. Sipkema and V. W. van Hinsbergh (2009). "Endothelial dysfunction and diabetes: roles of hyperglycemia, impaired insulin signaling and obesity." Cell Tissue Res **335**(1): 165-189.

Balconi, G., A. Pietra, M. Busacca, G. de Gaetano and E. Dejana (1983). "Success rate of primary human endothelial cell culture from umbilical cords is influenced by maternal and fetal factors and interval from delivery." In Vitro **19**(11): 807-810.

Basta, G., A. M. Schmidt and R. De Caterina (2004). "Advanced glycation end products and vascular inflammation: implications for accelerated atherosclerosis in diabetes." Cardiovasc Res **63**(4): 582-592.

Bucciarelli, L. G., A. Pollreisz, M. Kebschull, A. Ganda, A. Z. Kalea, B. I. Hudson, Y. S. Zou, E. Lalla, R. Ramasamy, P. C. Colombo, A. M. Schmidt and S. F. Yan (2009). "Inflammatory stress in primary venous and aortic endothelial cells of type 1 diabetic mice." Diab Vasc Dis Res **6**(4): 249-261.

Bunn, H. F. and P. J. Higgins (1981). "Reaction of monosaccharides with proteins: possible evolutionary significance." Science **213**(4504): 222-224.

Carmeliet, P. and D. Collen (2000). "Transgenic mouse models in angiogenesis and cardiovascular disease." J Pathol **190**(3): 387-405.

Chavakis, T., A. Bierhaus and P. P. Nawroth (2004). "RAGE (receptor for advanced glycation end products): a central player in the inflammatory response." Microbes Infect **6**(13): 1219-1225.

Choi, K., M. Kennedy, A. Kazarov, J. C. Papadimitriou and G. Keller (1998). "A common precursor for hematopoietic and endothelial cells." Development **125**(4): 725-732.

Cines, D. B., E. S. Pollak, C. A. Buck, J. Loscalzo, G. A. Zimmerman, R. P. McEver, J. S. Pober, T. M. Wick, B. A. Konkle, B. S. Schwartz, E. S. Barnathan, K. R. McCrae, B. A. Hug, A.-M. Schmidt and D. M. Stern (1998). "Endothelial Cells in Physiology and in the Pathophysiology of Vascular Disorders." Blood **91**(10): 3527-3561.

Costa, C. (2011). Vasculogenesis in Diabetes-Associated Diseases: Unraveling the Diabetic Paradox. Vasculogenesis and Angiogenesis - from Embryonic Development to Regenerative Medicine. D. Simionescu, InTech**:** 107-130.

Eichmann, A., C. Corbel, V. Nataf, P. Vaigot, C. Breant and N. M. Le Douarin (1997). "Ligand-dependent development of the endothelial and hemopoietic lineages from embryonic mesodermal cells expressing vascular endothelial growth factor receptor 2." Proc Natl Acad Sci U S A **94**(10): 5141-5146.

El Amine, M., S. Sohawon, L. Lagneau, N. Gaham and S. Noordally (2010). "Plasma levels of ICAM-1 and circulating endothelial cells are elevated in unstable types 1 and 2 diabetes." Endocr Regul **44**(1): 17-24.

Elawa, G., A. M. AoudAllah, A. E. Hasaneen and A. M. El-Hammady (2011). "The predictive value of serum mannan-binding lectin levels for diabetic control and renal complications in type 2 diabetic patients." Saudi Med J **32**(8): 784-790.

Esper, R. J., R. A. Nordaby, J. O. Vilarino, A. Paragano, J. L. Cacharron and R. A. Machado (2006). "Endothelial dysfunction: a comprehensive appraisal." Cardiovasc Diabetol **5**: 4.

Ferguson, J. E., 3rd, R. W. Kelley and C. Patterson (2005). "Mechanisms of endothelial differentiation in embryonic vasculogenesis." Arterioscler Thromb Vasc Biol **25**(11): 2246-2254.

Fortpied, J., D. Vertommen and E. Van Schaftingen (2010). "Binding of mannose-binding lectin to fructosamines: a potential link between hyperglycaemia and complement activation in diabetes." Diabetes Metab Res Rev **26**(4): 254-260.

Fowler, M. J. (2008). "Microvascular and Macrovascular Complications of Diabetes." Clinical Diabetes **26**(2): 77-82.

Goon, P. K., G. Y. Lip, C. J. Boos, P. S. Stonelake and A. D. Blann (2006). "Circulating endothelial cells, endothelial progenitor cells, and endothelial microparticles in cancer." Neoplasia **8**(2): 79-88.

Hansen, T. K., L. Tarnow, S. Thiel, R. Steffensen, C. D. Stehouwer, C. G. Schalkwijk, H. H. Parving and A. Flyvbjerg (2004). "Association between mannose-binding lectin and vascular complications in type 1 diabetes." Diabetes **53**(6): 1570-1576.

Hartge, M. M., T. Unger and U. Kintscher (2007). "The endothelium and vascular inflammation in diabetes." Diabetes and Vascular Disease Research **4**(2): 84-88.

Henrikson, R. C. (1997). Histology. Baltimore, Williams & Wilkins.

Hobson, B. and J. Denekamp (1984). "Endothelial proliferation in tumours and normal tissues: continuous labelling studies." Br J Cancer **49**(4): 405-413.

Hovind, P., T. K. Hansen, L. Tarnow, S. Thiel, R. Steffensen, A. Flyvbjerg and H. H. Parving (2005). "Mannose-binding lectin as a predictor of microalbuminuria in type 1 diabetes: an inception cohort study." Diabetes **54**(5): 1523-1527.

Hunt, B. J. and K. M. Jurd (1998). "Endothelial cell activation." BMJ **316**(7141): 1328.

Jaffe, E. A., R. L. Nachman, C. G. Becker and C. R. Minick (1973). "Culture of human endothelial cells derived from umbilical veins. Identification by morphologic and immunologic criteria." J Clin Invest **52**(11): 2745-2756.

Janeway, C. A., P. Travers, M. Walport and M. J. Shlomchik (2001). "The complement system and innate immunity."

Jessani, S. S., D. A. Lane, E. Shantsila, T. Watson, T. A. Millane and G. Y. Lip (2009). "Impaired glucose tolerance and endothelial damage, as assessed by levels of von Willebrand factor and circulating endothelial cells, following acute myocardial infarction." Ann Med **41**(8): 608-618.

Józsi, M. (2011). Anti-Complement Autoantibodies in Membranoproliferative Glomerulonephritis and Dense Deposit Disease.

Kotb, N. A., R. Gaber, W. Salah and A. Elhendy (2012). "Relations among glycemic control, circulating endothelial cells, nitric oxide, and flow mediated dilation in patients with type 2 diabetes mellitus." Exp Clin Endocrinol Diabetes **120**(8): 460-465.

Laemmli, U. K. (1970). "Cleavage of structural proteins during the assembly of the head of bacteriophage T4." Nature **227**(5259): 680-685.

Lammert, E. (2007). Pancreas and Liver: Mutual Signaling during Vascularized Tissue Formation Endothelial Biomedicine, Cambridge University Press**:** 173-180.

Lanuti, P., F. Santilli, M. Marchisio, L. Pierdomenico, E. Vitacolonna, E. Santavenere, A. Iacone, G. Davi, M. Romano and S. Miscia (2012). "A novel flow cytometric approach to distinguish circulating endothelial cells from endothelial microparticles: relevance for the evaluation of endothelial dysfunction." J Immunol Methods **380**(1-2): 16-22.

Laubichler, M. D., W. C. Aird and J. Maienschein (2007). The Endothelium in History. Endothelial Biomedicine. W. C. Aird, Cambridge University Press**:** 3-20.

Laurens, N. and V. M. Hinsbergh (2004). Isolation,Purification and Culture of Human Micro- and Macrovascular Endothelial Cells. Methods in Endothelial Cell Biology. H. Augustin, Springer Berlin Heidelberg**:** 3-13.

Lev, E. I., J. Singer, D. Leshem-Lev, M. Rigler, O. Dadush, M. Vaduganathan, A. Battler and R. Kornowski (2013). "Effect of intensive glycaemic control on endothelial progenitor cells in patients with long-standing uncontrolled type 2 diabetes." Eur J Prev Cardiol.

Lyden, D., K. Hattori, S. Dias, C. Costa, P. Blaikie, L. Butros, A. Chadburn, B. Heissig, W. Marks, L. Witte, Y. Wu, D. Hicklin, Z. Zhu, N. R. Hackett, R. G. Crystal, M. A. Moore, K. A. Hajjar, K. Manova, R. Benezra and S. Rafii (2001). "Impaired recruitment of bone-marrow-derived endothelial and hematopoietic precursor cells blocks tumor angiogenesis and growth." Nat Med **7**(11): 1194-1201.

Maugeri, N., P. Rovere-Querini, M. Baldini, M. G. Sabbadini and A. A. Manfredi (2009). "Translational mini-review series on immunology of vascular disease: mechanisms of vascular inflammation and remodelling in systemic vasculitis." Clin Exp Immunol **156**(3): 395-404.

Mescher, A. (2009). Junqueira's Basic Histology, 12th Edition, McGraw-Hill Education.

Munoz-Chapuli, R., R. Carmona, J. A. Guadix, D. Macias and J. M. Perez-Pomares (2005). "The origin of the endothelial cells: an evo-devo approach for the invertebrate/vertebrate transition of the circulatory system." Evol Dev **7**(4): 351-358.

Negre-Salvayre, A., R. Salvayre, N. Auge, R. Pamplona and M. Portero-Otin (2009). "Hyperglycemia and glycation in diabetic complications." Antioxid Redox Signal **11**(12): 3071-3109.

Neurauter, A. A., M. Bonyhadi, E. Lien, L. Nokleby, E. Ruud, S. Camacho and T. Aarvak (2007). "Cell isolation and expansion using Dynabeads." Adv Biochem Eng Biotechnol **106**: 41-73.

Oh, B. J., S. H. Oh, S. M. Jin, S. Suh, J. C. Bae, C. G. Park, M. S. Lee, M. K. Lee, J. H. Kim and K. W. Kim (2013). "Co-Transplantation of Bone Marrow-Derived Endothelial Progenitor Cells Improves Revascularization and Organization in Islet Grafts." Am J Transplant.

Onat, D., D. Brillon, P. C. Colombo and A. M. Schmidt (2011). "Human vascular endothelial cells: a model system for studying vascular inflammation in diabetes and atherosclerosis." Curr Diab Rep **11**(3): 193-202.

Orrico, C., G. Pasquinelli, L. Foroni, D. Muscara, P. L. Tazzari, F. Ricci, M. Buzzi, E. Baldi, N. Muccini, M. Gargiulo and A. Stella (2010). "Dysfunctional vasa vasorum in diabetic peripheral artery obstructive disease with critical lower limb ischaemia." Eur J Vasc Endovasc Surg **40**(3): 365-374.

Ostergaard, J., T. K. Hansen, S. Thiel and A. Flyvbjerg (2005). "Complement activation and diabetic vascular complications." Clin Chim Acta **361**(1-2): 10-19.

Ostergaard, J., S. Thiel, M. Gadjeva, T. K. Hansen, R. Rasch and A. Flyvbjerg (2007). "Mannose-binding lectin deficiency attenuates renal changes in a streptozotocin-induced model of type 1 diabetes in mice." Diabetologia **50**(7): 1541-1549.

Ostergaard, J. A., M. Bjerre, F. Dagnaes-Hansen, T. K. Hansen, S. Thiel and A. Flyvbjerg (2013). "Diabetes-induced changes in mannan-binding lectin levels and complement activation in a mouse model of type 1 diabetes." Scand J Immunol **77**(3): 187-194.

Ostergaard, J. A., M. Bjerre, S. P. RamachandraRao, K. Sharma, J. R. Nyengaard, T. K. Hansen, S. Thiel and A. Flyvbjerg (2012). "Mannan-binding lectin in diabetic kidney disease: the impact of mouse genetics in a type 1 diabetes model." Exp Diabetes Res **2012**: 678381.

Ozkor, M., J. Murrow and A. Quyyumi (2010). Endothelium: Dysfunction and Repair. Advances in Vascular Medicine. D. Abraham, H. Clive, M. Dashwood and G. Coghlan, Springer London**:** 187-210.

Packard, R. R. and P. Libby (2008). "Inflammation in atherosclerosis: from vascular biology to biomarker discovery and risk prediction." Clin Chem **54**(1): 24-38.

Pardanaud, L. and F. Dieterlen-Lievre (1993). "Emergence of endothelial and hemopoietic cells in the avian embryo." Anat Embryol (Berl) **187**(2): 107-114.

Patterson, C. (2007). Endothelial Cell Differentiation and Vascular Development in Mammals. Endothelial Biomedicine, Cambridge University Press**:** 161-166.

Pavlov, V. I., L. R. La Bonte, W. M. Baldwin, M. M. Markiewski, J. D. Lambris and G. L. Stahl (2012). "Absence of mannose-binding lectin prevents hyperglycemic cardiovascular complications." Am J Pathol **180**(1): 104-112.

Petersen, S. V., S. Thiel, L. Jensen, R. Steffensen and J. C. Jensenius (2001). "An assay for the mannan-binding lectin pathway of complement activation." J Immunol Methods **257**(1-2): 107-116.

Pober, J. (2002). "Endothelial activation: intracellular signaling pathways." Arthritis Res **4**(Suppl 3): S109 - S116.

Potenza, M. A., S. Gagliardi, C. Nacci, M. R. Carratu and M. Montagnani (2009). "Endothelial dysfunction in diabetes: from mechanisms to therapeutic targets." Curr Med Chem **16**(1): 94-112.

Reitsma, S., D. W. Slaaf, H. Vink, M. A. M. J. van Zandvoort and M. G. A. O. Egbrink (2007). "The endothelial glycocalyx: composition, functions, and visualization." Pflugers Archiv-European Journal of Physiology **454**(3): 345-359.

Richardson, M. R. and M. C. Yoder (2011). "Endothelial progenitor cells: Quo Vadis?" J Mol Cell Cardiol **50**(2): 266-272.

Rus, H., C. Cudrici and F. Niculescu (2005). "The role of the complement system in innate immunity." Immunologic Research **33**(2): 103-112.

Saraheimo, M., C. Forsblom, T. K. Hansen, A. M. Teppo, J. Fagerudd, K. Pettersson-Fernholm, S. Thiel, L. Tarnow, P. Ebeling, A. Flyvbjerg and P. H. Groop (2005). "Increased levels of mannan-binding lectin in type 1 diabetic patients with incipient and overt nephropathy." Diabetologia **48**(1): 198-202.

Schalkwijk, C. G. and C. D. Stehouwer (2005). "Vascular complications in diabetes mellitus: the role of endothelial dysfunction." Clin Sci (Lond) **109**(2): 143-159.

Schmieder, R. E. (2006). "Endothelial dysfunction: how can one intervene at the beginning of the cardiovascular continuum?" J Hypertens Suppl **24**(2): S31-35.

Schram, M. T. and C. D. Stehouwer (2005). "Endothelial dysfunction, cellular adhesion molecules and the metabolic syndrome." Horm Metab Res **37 Suppl 1**: 49-55.

Scott, P. A. E. and R. Bicknell (1993). "The isolation and culture of microvascular endothelium." J Cell Sci **105**(2): 269-273.

Shiojima, I. and K. Walsh (2002). "Role of Akt Signaling in Vascular Homeostasis and Angiogenesis." Circ Res **90**(12): 1243-1250.

Sobczak, M., J. Dargatz and M. Chrzanowska-Wodnicka (2010). "Isolation and culture of pulmonary endothelial cells from neonatal mice." J Vis Exp(46).

Son, S. M. (2007). "Role of vascular reactive oxygen species in development of vascular abnormalities in diabetes." Diabetes Res Clin Pract **77 Suppl 1**: S65-70.

Stan, R. V. (2007). "Endothelial stomatal and fenestral diaphragms in normal vessels and angiogenesis." J Cell Mol Med **11**(4): 621-643.

Stevens, T., R. Rosenberg, W. Aird, T. Quertermous, F. L. Johnson, J. G. Garcia, R. P. Hebbel, R. M. Tuder and S. Garfinkel (2001). "NHLBI workshop report: endothelial cell phenotypes in heart, lung, and blood diseases." Am J Physiol Cell Physiol **281**(5): C1422-1433.

Takahashi, T., C. Kalka, H. Masuda, D. Chen, M. Silver, M. Kearney, M. Magner, J. M. Isner and T. Asahara (1999). "Ischemia- and cytokine-induced mobilization of

bone marrow-derived endothelial progenitor cells for neovascularization." Nat Med **5**(4): 434-438.

Tan, K. C., W. S. Chow, V. H. Ai, C. Metz, R. Bucala and K. S. Lam (2002). "Advanced glycation end products and endothelial dysfunction in type 2 diabetes." Diabetes Care **25**(6): 1055-1059.

van Beijnum, J. R., M. Rousch, K. Castermans, E. van der Linden and A. W. Griffioen (2008). "Isolation of endothelial cells from fresh tissues." Nat Protoc **3**(6): 1085-1091.

Vokes, S. A. and P. A. Krieg (2002). "Endoderm is required for vascular endothelial tube formation, but not for angioblast specification." Development **129**(3): 775-785.

Westerweel, P. E., M. Teraa, S. Rafii, J. E. Jaspers, I. A. White, A. T. Hooper, P. A. Doevendans and M. C. Verhaar (2013). "Impaired endothelial progenitor cell mobilization and dysfunctional bone marrow stroma in diabetes mellitus." PLoS One **8**(3): e60357.

Wu, Y., M. Moser, V. L. Bautch and C. Patterson (2003). "HoxB5 is an upstream transcriptional switch for differentiation of the vascular endothelium from precursor cells." Mol Cell Biol **23**(16): 5680-5691.

Young, B. (2006). Wheater's functional histology : a text and colour atlas. Edinburgh, Churchill Livingstone/Elsevier.

Zhang, W. and H. Yan (2013). "Dysfunction of circulating endothelial progenitor cells in type 1 diabetic rats with diabetic retinopathy." Graefes Arch Clin Exp Ophthalmol **251**(4): 1123-1131.

IV. ADAPTIVE RESPONSE OF SUBMANDIBULAR GLANDS TO CHRONIC HYPERGLYCEMIA

1. Introduction

Salivary glands are a set of organs possessed by terrestrial animals, which secrete saliva into the oral cavity. Saliva is a watery fluid whose primary role is the maintenance of oral lubrication. Nonetheless, other physiological roles, namely protective and digestive, are performed by saliva. Consequently, any dysfunction in salivary secretion leads to increased susceptibility to infections, loss of taste and difficulties in eating and talking (Holsinger and Bui 2007; Miletich 2010). The decrease in salivary secretion, and consequent oral dryness, is called xerostomia and is a common complaint among diabetic patients. Moreover, diabetic patients also have increased incidence of dental caries, gingivitis, periodontitis, delayed healing and oral infections (Löe and Genco 1995; SHIP 2003), which reflect a possible impairment of the protective roles of salivary secretions. Thus, it is important to understand how hyperglycemia affects salivary glands.

1.1. Histological features of salivary glands

Salivary glands are branched organs that are composed of a parenchymatous region, which is surrounded by a stroma. The parenchyma is composed by epithelial tissue that is organized in secretory units called “endpieces” connected by an extensive network of duct eventually opening into the oral cavity, while the stroma is a layer of connective tissue surrounding the gland and dividing it in lobes (Miletich 2010).

Secretory endpieces may be classified into three types according to the type of cells and their secretions. Mucous endpieces secrete a viscous fluid rich in complex carbohydrates attached to mucin proteins, which have an essential role in lubrication; secretory cells are usually simple columnar cells gathered in tubular shaped acini. Serous endpieces secretions are more watery and very rich in proteins, though almost absent of glycoproteins; the secretory cells are pyramidal, forming

spheroidal acini. Seromucous endpieces have both types of cells, thus producing both types of secretions; usually mucous cells are arranged in a tubule caped by demilunes of serous cells (Holsinger and Bui 2007; Miletich 2010).

The ductal system is also heterogeneous. Acinar secretions are collected into the intercalated ducts, made up from squamous or low cuboidal epithelium, which drain into the striated ducts. The striated duct cells have basally located membrane invaginations, conferring them a striated aspect. The striated ducts empty in excretory ducts, which then empty into major ducts with specific names according to the gland. Excretory ducts start with simple cuboidal epithelium that becomes columnar as the ducts enlarge, eventually becoming stratified columnar or squamous epithelium towards the end portion. Although the acini are major contributors to salivary secretions, the ducts are not limited to the conduction of their secretions into the oral cavity. Some segments of the ducts also play a role in electrolyte modification and secretion of some proteins. In the intercalated duct, cells secrete bicarbonate ions, absorbing chloride ions. Striated ducts are involved in sodium reabsorption in exchange with potassium, hence the numerous mitochondria located in striations to produce energy for the active transport of these ions. They also secrete IgA, lysozyme and other proteases, as well as some growth factors. In rodents, however, these secretions come from a specialized part of ducts located between intercalated and striated ducts, called granular ducts, composed of cells with numerous granules (Holsinger and Bui 2007; Miletich 2010).

In close association with secretory and ductal cells, there is another type of cells, myoepithelial cells, which lie between the epithelial cells and the basal lamina and have the ability to contract, thus forcing secretion (Miletich 2010).

Salivary glands are also highly vascularized and enervated, which allow the rapid transfer of molecules from the bloodstream and the

conduction of sympathetic and parasympathetic stimuli for secretory regulation, respectively (Holsinger and Bui 2007; Miletich 2010).

1.2. Anatomy of salivary glands in humans and rodents

Salivary glands may be classified as major and minor salivary glands. Major salivary glands comprise the parotid glands, the submandibular glands and the sublingual glands, and are responsible for approximately 90% of salivary secretions; whereas minor salivary glands comprise numerous uncapsulated small secretory units scattered throughout the oral mucosa (Henrikson 1997; Chambers, Artopoulou et al. 2007; Holsinger and Bui 2007; Miletich 2010). Despite having the three major pairs of salivary gland, humans and rodents have significant differences in their relative size and morphology.

The parotid gland is the largest salivary gland in humans with a pyramidal shape and defined lobes, located in the back of the mouth between the mandible and the ear, while in rodents is a more diffuse organ extending from the submandibular gland to the base of the ear (Figure 23) (Henrikson 1997; Treuting and Dintzis 2012). Parotid glands are composed of serous acini which empty in the oral cavity through a long duct called Stensen's duct (Miletich 2010). It is responsible by roughly two-thirds of the saliva secreted under stimulation, falling to about one quarter of unstimulated saliva (Chambers, Artopoulou et al. 2007; Holsinger and Bui 2007).

The human submandibular gland is located in the floor of the mouth between muscle layers, in the digastric triangle, whereas the rodent gland is located in the ventral cervical subcutaneous region, closely associated to the sublingual gland, and is the largest rodent salivary gland (Figure 23) (Holsinger and Bui 2007; Treuting and Dintzis 2012). It is a lobular seromucous gland with a predominance of serous tubular acini and only 10% of mucous acini, arranged in demilunes. It connects to the oral cavity through the Wharton's duct, whose opening lies near the base of the lingual frenum (Miletich 2010). The submandibular secretions

represent over 70% of unstimulated saliva, hence being crucial to the maintenance of oral lubrication (Chambers, Artopoulou et al. 2007; Holsinger and Bui 2007).

The sublingual gland is the smallest of the major salivary glands, both in humans and rodents. It is located in the anterior part of the mouth floor, in humans, and in the ventral cervical subcutaneous region, closely associated with the submandibular gland, in rodents (Figure 23) (Miletich 2010; Treuting and Dintzis 2012). In humans, it is also a seromucous gland where there is predominance of mucous acini, while in rodents it has only mucous acini (Treuting and Dintzis 2012). It empties in the oral cavity through numerous small ducts, located on the mouth floor, and a major sublingual duct that opens into the Wharton's duct (Miletich 2010). The sublingual secretions represent only 5% of saliva (Holsinger and Bui 2007).

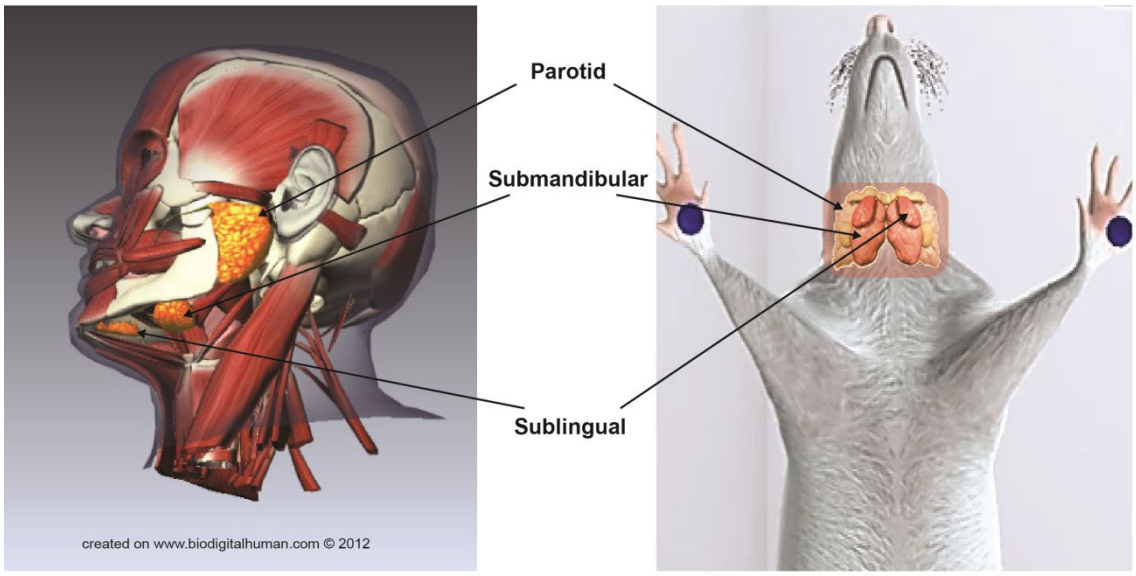

Figure 23 – Anatomical location of the major salivary glands in humans and rodents.

The minor salivary glands have a disperse location and are surrounded by connective tissue but not encapsulated like the major salivary glands. These glands represent about 10% of salivary secretions regardless of stimulation and may be of different natures: serous, mucous or seromucous (Miletich 2010; Treuting and Dintzis 2012).

1.3. Salivary glands embryonic origin and development

The origin of salivary glands is not consensual. It seems established that parotid glands originate from the ectodermal layer and minor salivary glands derive from the endodermal layer. However, the origin of sublingual and submandibular glands is still a matter of debate (Miletich 2010). Despite that, it is generally assumed that major salivary glands are ectodermal organs. The embryonic development of the mouse submandibular gland is usually regarded as a model to salivary gland development. It starts with a thickening of the epithelial layer on the mouth floor, which progresses into an invagination in the underlying mesenchyme, originating a stalk with a terminal bulb. Simultaneously, there is an arrangement of mesenchymal cells that condense around the epithelial protuberance, originating the stroma. The bulb then starts a branching process with multiple furcations in the distal ends resulting in a network of epithelial branches with terminal buds. Soon enough, the branches and buds start to hollow out and eventually form ducts and acini. The branching allows the expansion of the tissue surface area within the confinement of the organ (Denny, Ball et al. 1997; Jaskoll and Melnick 2006; Miletich 2010) (Figure 24).

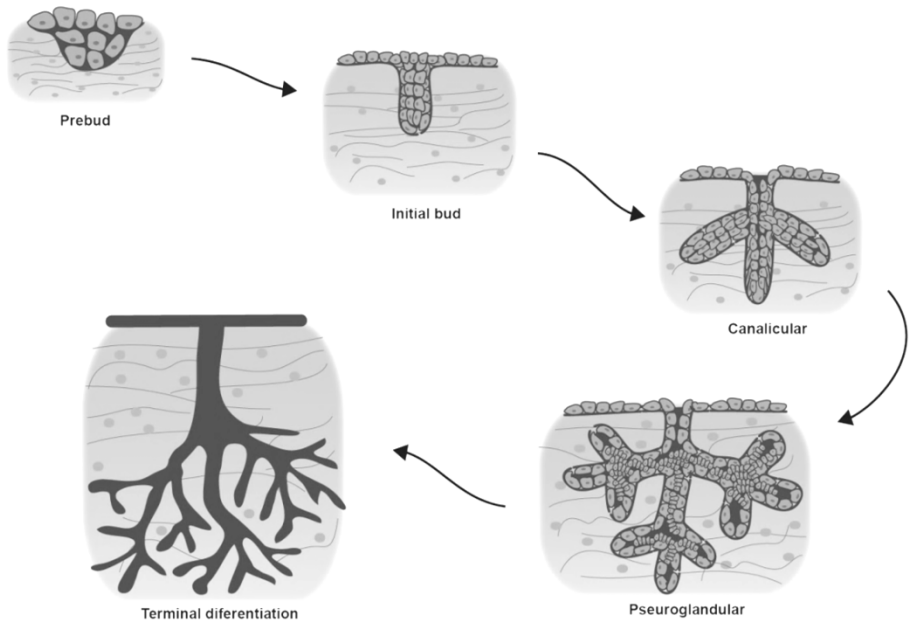

Figure 24 – Stages of glandular development. Adapted from Miletich (2010)

1.4. Proliferation and regeneration of salivary glands tissue

Salivary glands size is usually proportional to body size. The regulation of the gland's size is determined by a balance between cell proliferation and cell death (Carpenter and Cotroneo 2010). Despite the low levels of mitosis observed in adult glands, the regular stimulus of mastication through the parasympathetic nerves up-regulates mitosis, thus keeping a relatively stable gland size (Schneyer, Humphreys-Beher et al. 1993). The regeneration of salivary glands may occur either by proliferation from the existing acini and ducts or by an embryonic-like pathway through branching from ductal buds. Studies of regeneration following ductal ligation-induced atrophy have shown that, not only both processes occur, but they also allow the full restoration of tissue function (Takahashi and Wakita 1993; Cotroneo, Proctor et al. 2008).

Salivary glands secrete several growth factors, namely, fibroblast growth factor (FGF), epidermal growth factor (EGF), insulin and insulin-like growth factors 1 and 2 (IGF-1 and -2), transforming growth factors (TGF) alpha and beta, nerve growth factor (NGF) and hepatocyte growth factor (HGF) (Zelles, Purushotham et al. 1995; Mathison 2010). A bioinformatics analysis of the gene expression profile in ligation studies with different time-points revealed the activation of MAPK, Wnt and Notch pathways. Such pathways are mediated by growth factors and salivary glands express several receptors that may activate the proliferation pathways. It was shown that the fibroblast growth factor (FGF) receptors were up-regulated in regenerating glands, suggesting a possible link to the MAPK pathway activation (Carpenter and Cotroneo 2010). Epidermal growth factor receptors (EGFR) are also expressed in salivary glands and were shown to be involved in morphogenesis, proliferation and differentiation (Piludu, Lantini et al. 2003; Dang, Elliott et al. 2008; Häärä, Koivisto et al. 2009). Likewise, salivary glands express insulin receptors and insulin-like growth factor-1 receptors, which also are involved in the activation of these proliferation/differentiation pathways

(Chapter I) (Rocha, de et al. 2000; Rocha, Hirata et al. 2002; Rocha, Carvalho et al. 2003). The kinin receptor B2 is also abundant in salivary glands, stimulating DNA synthesis and cell proliferation, and salivary glands express high levels of several tissue kallikreins, namely in ductal cells, that release the kinin peptide from kininogen (Garrett, Smith et al. 1982; Yahiro and Miyoshi 1996; Mahabeer, Naidoo et al. 2000; Dlamini and Bhoola 2005). As previously mentioned, parasympathetic stimuli may also promote cellular proliferation, as acetylcholine signalling activates muscarinic M1 receptors of embryonic epithelium increasing morphogenesis and proliferation (Knox, Lombaert et al. 2010).

Thus, salivary glands are enriched in several mechanism of cell proliferation, which not only account for the healing properties of saliva but may also play a role in gland regeneration.

1.5. Salivary secretions and oral health

Salivary glands are responsible for the daily production of about 800 to 1500 ml of saliva (Ellis 1991; Aps and Martens 2005; Melvin, Yule et al. 2005; Moore, Dalley et al. 2010). Saliva is an essential fluid in the maintenance of oral health. Among the most abundant proteins secreted in saliva we can find immunoglobulins (IgG and IgA), proline-rich proteins, mucins, histatins, cystatins, statherin, complement proteins, and also a rich pool of growth factors (Zelles, Purushotham et al. 1995; Amado, Vitorino et al. 2005; Amado, Ferreira et al. 2012).

Although the precise functions of some proteins are not yet fully disclosed, there is a clear association of these to the maintenance of oral health. Mucins and proline-rich proteins are important in the lubrication of the oral mucosa, statherin is essential for the protection of teeth through the oversaturation of calcium and phosphate salts, histatins and lysozyme have an anti-microbial activity, cystatins protect the periodontium destruction by some cathepsin proteases and also contribute to the mineral balance for teeth protection, and immunoglobulins and complement proteins are elements of the immune

system (Zelles, Purushotham et al. 1995; Baron, DeCarlo et al. 1999; Vitorino, Calheiros-Lobo et al. 2006)

This unique composition allows a multitude of protective and healing properties to saliva.

1.6. Salivary gland impairment in chronic hyperglycemia

Poor glycemic control is strongly connected to oral complications, namely xerostomia, gingivitis, periodontitis, tooth decay and oral candidiasis (Sreebny, Yu et al. 1992; Ryan, Carnu et al. 2003; Lamster, Lalla et al. 2008; Yeh, Harris et al. 2012). Xerostomia is a subjective feeling of dry mouth, which may be the result of reduced secretion of saliva. Considering the already mentioned roles played by saliva in the maintenance of oral health, it is conceivable that the impairment of salivary gland secretion will increase the risk of all the aforementioned complications. Understanding the mechanism that leads to the reduction of salivary secretion is thus crucial for delaying the onset of such complications and developing therapies.

Salivary secretion is controlled by stimuli from the sympathetic and parasympathetic nerves, with water and electrolyte secretion controlled by muscarinic receptors and protein synthesis and secretion controlled by the beta-adrenergic receptors (Yeh, Harris et al. 2012). It has been described a decreased response to beta-adrenergic/cholinergic stimulation either by decreased receptor expression or loss of neurotransmitter responsiveness (Yamamoto, Sims et al. 1996; Yamamoto, Ishibashi et al. 1997). Also, the salivary composition in both T1DM and T2DM has been revealed to suffer dramatic changes in protein and electrolyte concentrations (Mata, Marques et al. 2004). Furthermore, morphological changes were also reported, namely alterations in secretory granule structure and content (Mednieks, Szczepanski et al. 2009) and progressive loss of ductal (Anderson, Suleiman et al. 1994) and acinar cells (Cutler, Pinney et al. 1979; Anderson, Suleiman et al. 1994). However, the molecular mechanisms underlying such events are poorly understood.

It is in this framework that the following article is presented as a first quantitative proteomic study of the progressive effects of hyperglycemia in salivary gland protein expression.

2. References

Amado, F. M., R. P. Ferreira and R. Vitorino (2012). "One decade of salivary proteomics: Current approaches and outstanding challenges." Clin Biochem.

Amado, F. M., R. M. Vitorino, P. M. Domingues, M. J. Lobo and J. A. Duarte (2005). "Analysis of the human saliva proteome." Expert Rev Proteomics **2**(4): 521-539.

Anderson, L. C., A. H. Suleiman and J. R. Garrett (1994). "Morphological effects of diabetes on the granular ducts and acini of the rat submandibular gland." Microsc Res Tech **27**(1): 61-70.

Aps, J. K. and L. C. Martens (2005). "Review: The physiology of saliva and transfer of drugs into saliva." Forensic Sci Int **150**(2-3): 119-131.

Baron, A., A. DeCarlo and J. Featherstone (1999). "Functional aspects of the human salivary cystatins in the oral environment." Oral Dis **5**(3): 234-240.

Carpenter, G. H. and E. Cotroneo (2010). "Salivary gland regeneration." Front Oral Biol **14**: 107-128.

Chambers, M., I.-I. Artopoulou and A. Garden (2007). Xerostomia. Salivary Gland Disorders. E. Myers and R. Ferris, Springer Berlin Heidelberg**:** 185-199.

Cotroneo, E., G. B. Proctor, K. L. Paterson and G. H. Carpenter (2008). "Early markers of regeneration following ductal ligation in rat submandibular gland." Cell Tissue Res **332**(2): 227-235.

Cutler, L. S., H. E. Pinney, C. Christian and S. B. Russotto (1979). "Ultrastructural studies of the rat submandibular gland in streptozotocin induced diabetes mellitus." Virchows Arch A Pathol Anat Histol **382**(3): 301-311.

Dang, H., J. J. Elliott, A. L. Lin, B. Zhu, M. S. Katz and C. K. Yeh (2008). "Mitogen-activated protein kinase up-regulation and activation during rat parotid gland atrophy and regeneration: role of epidermal growth factor and beta2-adrenergic receptors." Differentiation **76**(5): 546-557.

Denny, P., W. Ball and R. Redman (1997). "Salivary glands: a paradigm for diversity of gland development." Critical Reviews in Oral Biology & Medicine **8**(1): 51-75.

Dlamini, Z. and K. D. Bhoola (2005). "Upregulation of tissue kallikrein, kinin B1 receptor, and kinin B2 receptor in mast and giant cells infiltrating oesophageal squamous cell carcinoma." J Clin Pathol **58**(9): 915-922.

Ellis, A., Gnepp (1991). Surgical Pathology of the Salivary Glands. Philadelphia, W. B. Saunders Company.

Garrett, J. R., R. E. Smith, A. Kidd, K. Kyriacou and R. J. Grabske (1982). "Kallikrein-like activity in salivary glands using a new tripeptide substrate, including preliminary secretory studies and observations on mast cells." Histochem J **14**(6): 967-979.

Häärä, O., T. Koivisto and P. J. Miettinen (2009). "EGF-receptor regulates salivary gland branching morphogenesis by supporting proliferation and maturation of epithelial cells and survival of mesenchymal cells." Differentiation **77**(3): 298-306.

Henrikson, R. C. (1997). Histology. Baltimore, Williams & Wilkins.

Holsinger, F. C. and D. Bui (2007). Anatomy, Function, and Evaluation of the Salivary Glands. Salivary Gland Disorders. E. Myers and R. Ferris, Springer Berlin Heidelberg**:** 1-16.

Jaskoll, T. and M. Melnick (2006). Embryonic salivary gland branching morphogenesis. Branching Morphogenesis, Springer**:** 160-175.

Knox, S. M., I. M. Lombaert, X. Reed, L. Vitale-Cross, J. S. Gutkind and M. P. Hoffman (2010). "Parasympathetic innervation maintains epithelial progenitor cells during salivary organogenesis." Science **329**(5999): 1645-1647.

Lamster, I. B., E. Lalla, W. S. Borgnakke and G. W. Taylor (2008). "The relationship between oral health and diabetes mellitus." J Am Dent Assoc **139 Suppl**: 19S-24S.

Löe, H. and R. J. Genco (1995). Oral Complications in Diabetes. Diabetes in America. National Diabetes Data Group (U.S.), National Institute of Diabetes and Digestive and Kidney Diseases (U.S.) and National Institutes of Health (U.S.). Bethesda,

Md., National Institutes of Health, National Institute of Diabetes and Digestive and Kidney Diseases**:** 501-506.

Mahabeer, R., S. Naidoo and D. M. Raidoo (2000). "Detection of Tissue Kallikrein and Kinn B1 and B2 Receptor mRNAs in Human Brain by In Situ RT-PCR." Metabolic Brain Disease **15**(4): 325-335.

Mata, A. D., D. Marques, S. Rocha, H. Francisco, C. Santos, M. F. Mesquita and J. Singh (2004). "Effects of diabetes mellitus on salivary secretion and its composition in the human." Mol Cell Biochem **261**(1-2): 137-142.

Mathison, R. (2010). "Submandibular salivary gland endocrine secretions and systemic pathophysiological responses." Open Inflammation Journal **3**: 9-21.

Mednieks, M. I., A. Szczepanski, B. Clark and A. R. Hand (2009). "Protein expression in salivary glands of rats with streptozotocin diabetes." Int J Exp Pathol **90**(4): 412-422.

Melvin, J. E., D. Yule, T. Shuttleworth and T. Begenisich (2005). "Regulation of fluid and electrolyte secretion in salivary gland acinar cells." Annu Rev Physiol **67**: 445-469.

Miletich, I. (2010). "Introduction to salivary glands: structure, function and embryonic development." Front Oral Biol **14**: 1-20.

Moore, K. L., A. F. Dalley and A. M. R. Agur (2010). Clinically oriented anatomy. Philadelphia, Wolters Kluwer/Lippincott Williams & Wilkins.

Piludu, M., M. S. Lantini, M. Isola, R. Puxeddu and M. Cossu (2003). "Localisation of epidermal growth factor receptor in mucous cells of human salivary glands." Eur J Morphol **41**(2): 107-109.

Rocha, E. M., C. R. Carvalho, M. J. Saad and L. A. Velloso (2003). "The influence of ageing on the insulin signalling system in rat lacrimal and salivary glands." Acta Ophthalmol Scand **81**(6): 639-645.

Rocha, E. M., M. L. M. H. de, C. R. Carvalho, M. J. Saad and L. A. Velloso (2000). "Characterization of the insulin-signaling pathway in lacrimal and salivary glands of rats." Curr Eye Res **21**(5): 833-842.

Rocha, E. M., A. E. Hirata, E. M. Carneiro, M. J. Saad and L. A. Velloso (2002). "Impact of gender on insulin signaling pathway in lacrimal and salivary glands of rats." Endocrine **18**(2): 191-199.

Ryan, M. E., O. Carnu and A. Kamer (2003). "The influence of diabetes on the periodontal tissues." J Am Dent Assoc **134 Spec No**: 34S-40S.

Schneyer, C. A., M. G. Humphreys-Beher, H. D. Hall and D. Jirakulsomchok (1993). "Mitogenic activity of rat salivary glands after electrical stimulation of parasympathetic nerves." Am J Physiol **264**(5 Pt 1): G935-938.

SHIP, J. A. (2003). "Diabetes and oral health: An overview." The Journal of the American Dental Association **134**(suppl 1): 4S-10S.

Sreebny, L. M., A. Yu, A. Green and A. Valdini (1992). "Xerostomia in diabetes mellitus." Diabetes Care **15**(7): 900-904.

Takahashi, S. and M. Wakita (1993). "Regeneration of the intralobular duct and acinus in rat submandibular glands after YAG laser irradiation." Arch Histol Cytol **56**(2): 199-206.

Treuting, P. M. and S. M. Dintzis (2012). Salivary Glands. Comparative anatomy and histology : a mouse and human atlas. P. M. Treuting and S. M. Dintzis. Amsterdam Boston, Elsevier/Academic Press**:** 111-120.

Vitorino, R., M. J. Calheiros-Lobo, J. A. Duarte, P. Domingues and F. Amado (2006). "Salivary clinical data and dental caries susceptibility: is there a relationship?" Bull Group Int Rech Sci Stomatol Odontol **47**(1): 27-33.

Yahiro, J. and S. Miyoshi (1996). "Immunohistochemical localization of kallikrein in salivary glands of the Japanese monkey, Macaca fuscata." Arch Oral Biol **41**(2): 225-228.

Yamamoto, H., K. Ishibashi, Y. Nakagawa, N. Maeda, T. Zeng, C. P. Robinson, G. E. Oxford, N. Chegini and M. G. Humphreys-Beher (1997). "Detection of alterations in the levels of neuropeptides and salivary gland responses in the non-obese diabetic mouse model for autoimmune sialoadenitis." Scand J Immunol **45**(1): 55-61.

Yamamoto, H., N. E. Sims, S. P. Macauley, K. H. Nguyen, Y. Nakagawa and M. G. Humphreys-Beher (1996). "Alterations in the secretory response of non-obese diabetic (NOD) mice to muscarinic receptor stimulation." Clin Immunol Immunopathol **78**(3): 245-255.

Yeh, C. K., S. E. Harris, S. Mohan, D. Horn, R. Fajardo, Y. H. Chun, J. Jorgensen, M. Macdougall and S. Abboud-Werner (2012). "Hyperglycemia and xerostomia are key determinants of tooth decay in type 1 diabetic mice." Lab Invest **92**(6): 868-882.

Zelles, T., K. R. Purushotham, S. P. Macauley, G. E. Oxford and M. G. Humphreys-Beher (1995). "Saliva and growth factors: the fountain of youth resides in us all." J Dent Res **74**(12): 1826-1832.

3. Article "iTRAQ-based quantitative proteomic analysis of submandibular glands from rats with STZ-induced hyperglycemia"

Alves, Renato M. P; Vitorino, Rui; Padrão, Ana I; Moreira-Gonçalves, Daniel; Duarte, José A; Ferreira, Rita; Amado, Francisco. 2012. "*iTRAQ-based quantitative proteomic analysis of submandibular glands from rats with STZ-induced hyperglycemia*", Journal of Biochemistry 153, 2: 209 - 220. DOI: 10.1093/jb/mvs142, by permission of Oxford University Press

J. Biochem. 2013;153(2):209–220 doi:10.1093/jb/mvs142

JB THE JOURNAL OF BIOCHEMISTRY

iTRAQ-based quantitative proteomic analysis of submandibular glands from rats with STZ-induced hyperglycemia

Received July 26, 2012; accepted October 23, 2012; published online December 5, 2012

Renato M.P. Alves[1], Rui Vitorino[1], Ana I. Padrão[1], Daniel Moreira-Gonçalves[2], José A. Duarte[2], Rita M.P. Ferreira[1] and Francisco Amado[1,*]

[1]QOPNA, Department of Chemistry, University of Aveiro, 3810-193 Aveiro, Portugal; and [2]CIAFEL, Faculty of Sports, University of Porto, 4200-450 Porto, Portugal

*Francisco Amado, Escola Superior de Saúde da Universidade de Aveiro, Campus de Santiago, 3810-190 Aveiro, Portugal. Tel: +351-234-234-401-558, Fax: +351-234-401-597, email: famado@ua.pt

The impairment of salivary glands activity is often connected to the complaints of dry-mouth and subsequent degradation of the periodontium of diabetic patients. In this context, submandibular glands (SMGs) play a central role in saliva production and so the understanding of the molecular pathways affected is of paramount importance. Using a streptozotocin-induced hyperglycemia rat model and two different time points (2 and 4 months), we applied mass spectrometry-based proteomic techniques, validated with standard western blot analysis, to identify and quantify the effect of chronic hyperglycemia on the proteome of SMGs. We observed significant variations of proteins such as kallikreins, protein S100A6 or annexins. After 2 months of hyperglycemia, we observed an early phase response characterized by a significant increase of protein S100A6, linked to the inflammatory response, together with the impairment of metabolic and energy production processes. On the other hand, vesicular transport appeared to be favoured in such conditions. Interestingly, in a long-term response to hyperglycemia after 4 months of exposure, we observed a general attenuation of the variations. In conclusion, we present data that support the existence of an adaptation of the gland to long-term stress.

Keywords: diabetes mellitus/kallikrein/salivary glands/vesicular transport.

Abbreviations: iTRAQ, isobaric tags for relative and absolute quantitation; STZ, streptozotocin; SMG, submandibular gland.

Diabetes mellitus has assumed pandemic proportions in the developed and developing world. The World Health Organization projects that diabetes-related deaths will double within two decades, and the burdens of diabetes and diabetes-associated complications in the economy are reaching alarming levels (*1*, *2*). A better understanding of the pathophysiology of the disease, provided by the unravelling of the mechanisms involved, will provide an important aid in the prevention and treatment of diabetic patients, and subsequent relieve of the weight of this disease in health systems worldwide (*2*). It is now established a direct link between diabetes and oral pathologies, with diabetic patients exhibiting a higher prevalence of periodontal diseases (*3*). Xerostomia, associated with pathological thirst, is a common manifestation of diabetes. Its origin is often linked to impaired salivary gland activity, namely in the ability to synthesize and secrete saliva (*4*, *5*). Producing ~70% of unstimulated saliva, the submandibular glands (SMGs) play a major role in the maintenance of oral health and lubrication (*6*). Thus, knowing the mechanisms that lead to glandular impairment in diabetes mellitus is essential to try to attenuate this condition.

A common model to study the effect of Type 1 diabetes mellitus on salivary glands is the streptozotocin (STZ)-induced destruction of pancreatic beta-cells resulting in the loss of the ability to produce insulin and consequent hyperglycemia (*7*). Reports on the effects of STZ-induced diabetes have suggested ultrastructural changes in rat SMGs with less than 1 month exposure to hyperglycemia, namely the fusion of granules and the accumulation of lipid vacuoles, eventually leading to cellular degeneration and death (*8*). However, in an apparent contradiction, Anderson *et al.* (*9*) reported that glands retained relatively normal physiological responses with up to 6 months of exposure to hyperglycemia. The same group has later resolved this contradiction reporting that the structural changes were mainly confined to the granular ducts, whereas granular acini remained mostly unchanged after 3 months, and only started to show some profile changes at 6 months of exposure (*10*). Nonetheless, the biochemical events underlying such structural changes remain largely undisclosed and a proteomic analysis of salivary glands could help to explain the histological alterations reported and ultimately link them to the variations in saliva composition and oral health.

Despite the extensive reports on the salivary secretions proteome (*11*–*15*), to the best of our knowledge, the existing reports on protein analysis of salivary glands, in either control or disease situations, were focused on specific proteins such as antioxidant defense proteins (*16*, *17*), mucins (*18*), proline-rich proteins (*18*, *19*), epidermal growth factor (*20*) or kallikreins (*21*).

Thus, the purpose of our study was to disclose some of the biochemical pathways that are affected by chronic hyperglycemia in the SMG. Applying

proteomic techniques to identify and quantify the differences in the proteome of an organelle membranes-enriched fraction from SMGs, we were able to identify an early phase response after 2 months of hyperglycemia, with pronounced variations of kallikreins and proteins involved in vesicular transport, followed by some signs of tissue adaptation at 4 months of chronic hyperglycemia, as the variations were not so pronounced.

Materials and Methods

Chemicals

All reagents were supplied by Sigma-Aldrich (St Louis, MO, USA) with the highest degree of purity available, unless otherwise stated. The isobaric tags for relative and absolute quantitation (iTRAQ) Reagent-8Plex kit was supplied by Applied Biosystems (Foster City, CA, USA). Primary antibodies rabbit polyclonal anti-GAPH (ab9485), rabbit polyclonal anti-alpha 1 Sodium Potassium ATPase antibody (ab74945) and rabbit monoclonal anti-S100 alpha 6 antibody (ab134149) were supplied by Abcam (Cambridge, UK) and rabbit polyclonal anti-annexin A2 antibody (NBP1-19810) was supplied by Novus Biologicals (Littleton, CO, USA).

Animals

Forty 6-week-old male Wistar rats (Charles River Laboratories, Barcelona, Spain) were divided into two groups. The first group (diabetic, $n=20$) received an intraperitoneal injection of STZ (60 mg/kg in citrate buffer, pH 4.5) to induce diabetes, while the second (control, $n=20$) received an injection with the vehicle alone. Animals were considered diabetic if blood glucose was >200 mg/dl 3 days after the injection. Weekly measurements of blood glucose were performed during the first month to ensure that the hyperglycemia state was maintained. Animals were housed at constant temperature (21–24°C) on a daily light schedule of 12 h light versus dark. Food and water were provided *ad libitum*. Diabetic animals presented clear signs of polydipsia and polyuria. After 2 and 4 months, 10 rats from each group were sacrificed by cervical dislocation, resulting in four different groups: 2-month diabetic (D2M), 2-month control (C2M), 4-month diabetic (D4M) and 4-month control (C4M). SMGs were excised, weighted and frozen at −80°C until further processing. All procedures were performed in accordance with the Guide for the Care and Use of Laboratory Animals and after approval of the local ethics committee.

Preparation of SMG membrane fractions

Membrane-enriched fractions were prepared according to Feinstein and Schramm (*22*). In brief, both SMGs of two animals from each group ($n=2$) were homogenized in sucrose medium (0.25 M sucrose, 1 mM EDTA and pH 7.5) in a loose glass-Teflon homogenizer for 2 min at 700 rpm. The homogenate was centrifuged for 5 min at 250 × *g*, 4°C. The resulting supernatant was centrifuged for 10 min at 1,000 x *g* to obtain a pellet enriched in secretory granules and organelle membranes, which was resuspended in sucrose medium to a final concentration of 2–10 mg protein/ml. Protein concentration was estimated using the RC–DC method (Bio-Rad), according to the manufacturer's instructions.

Protein digestion and iTRAQ labelling

An in-solution digestion was performed for iTRAQ labelling. Briefly, 100 µg of protein was used for digestion which was performed according to the protocol provided by the manufacturer (Applied Biosystems). Briefly, samples were mixed with triethyl ammonium bicarbonate buffer (TEAB) (1 M and pH 8.5) and RapiGest (Waters) to a final concentration of 0.5 M and 0.1%, respectively. Samples were then reduced with 5 mM tris(2-carboxyethyl) phosphine for 1 h at 37°C and alkylated with 10 mM *S*-methyl methanethiosulfonate for 10 min at room temperature. Two micrograms of trypsin was added to each sample and the digestion was performed for 18 h at 37°C. Samples were dried in a SpeedVac (Thermo Savant).

Digested sample peptides were subsequently labelled with the iTRAQ reagents (8-plex) following the protocol provided by the manufacturer (Applied Biosystems). In brief, peptides were reconstituted in 70% ethanol/30% TEAB 500 mM, added to each label and incubated for 2 h at room temperature. The reaction was stopped by adding water and the labelled digests corresponding to each of the four 8-plex experiments were combined and dried using SpeedVac.

Protein identification and iTRAQ quantification by 2D-LC-MS/MS

Labelled peptides were separated by a multidimensional LC approach based on a first dimension with high pH reverse phase (as previously described (*23*)) and a second dimension with the acidic reverse-phase system. Sample loading was performed at 200 µl/min with buffers (A) 72 mM TEAB, 52 mM acetic acid in H_2O, pH 10 and (B) 72 mM TEAB, 52 mM acetic acid in acetonitrile (ACN), pH 10 (98% A:2% B). After 5 min of sample loading and washing, peptide fractionation was performed with linear gradient to 50% B over 35 min followed by a 100% B step. Sixteen fractions were collected, evaporated and resuspended in 2% ACN, 0.1% trifluoroacetic acid (TFA). Collected fractions were separated as previously described (*24*). Briefly, peptides loaded onto a C18 pre-column (5 µm particle size, 5 mm; Dionex) connected to an RP column PepMap100 C18 (150 mm × 75 µm i.d., 3 µm particle size). The flow rate was set at 300 nl/min. The mobile phases A and B were 2% ACN, 0.1% TFA in water and 95% ACN, 0.045% TFA, respectively. The gradient was started at 10 min and ramped to 60% B till 50 min and 100% B at 55 min and retained at 100% B till 65 min. The column was equilibrated with solvent A for 20 min before the next sample was injected. The separation was monitored at 214 nm using a UV detector (Dionex/LC Packings, Sunnyvale, CA, USA) equipped with a 3-nl flow cell. Using the micro-collector Probot (Dionex/LC Packings) and, after a lag time of 5 min, peptides eluting from the capillary column were mixed with a continuous flow of α-CHCA matrix solution (270 nl/min, 2 mg/ml in 70% ACN/0.3% TFA and internal standard Glu-Fib at 15 fmol) were directly deposited onto the LC-MALDI plates at 12 s intervals for each spot (150 nl/fraction). For every separation run, 208 fractions in total were collected.

The spectra were processed and analysed by the ProteinPilot software (v4.0 AB Sciex, USA), which uses paragon algorithm for protein/peptide identification based on MS/MS data against the SwissProt protein database (release date 01012011, all taxonomic categories). Default search parameters were used: trypsin as the digestion enzyme, methylthio on cysteine residue as fixed modification, iTRAQ 8Plex, biological modification with emphasis on phosphorylation and urea denaturation as the variable modification setting. Mass tolerances for precursor and fragments were default values for ProteinPilot®. Cut-off score value for accepting protein identification for ProteinPilot® was a ProteoScore of 1.3 (95% confidence). Data were normalized for loading error by bias correction, which is an algorithm in ProteinPilot that corrects for unequal mixing when combining the labelled samples of one experiment. It does so by calculating the median protein ratio for all proteins reported in each sample, adjusted to unity and assigning an autobias factor to it. The variation ratios were calculated individually against each of the individuals in the C2M group.

To ensure valid and statistically significant quantification, some exclusion criteria were developed and sequentially applied to the results obtained from the ProteinPilot software, selecting only the proteins that met the following conditions: (i) proteins were identified in all individuals, (ii) proteins could not present a variation >25% within the C2M, to eliminate individual variability; (iii) proteins presented at least two ratios with a P-value <0.05 and (iv) the standard deviation from the ratios selected was <30% of their average. Nevertheless, the quantification results were reviewed manually for all proteins found to be differentially expressed (iTRAQ ratio >1.25 or <0.75 according to (*25*)).

Western blot

Approximately 20 µg of protein from each fraction was electrophoresed on a 12.5% SDS–PAGE as described by Laemmli (*26*) and then blotted onto a nitrocellulose membrane (Millipore, Billerica, MA, USA). Nonspecific binding was blocked with 5% w/v dry non-fat milk in TBS-T (100 mM Tris, 1.5 mM NaCl, pH 8.0 and 0.05% Tween-20), followed by 3 h incubation with primary antibody (anti-GAPDH, anti-alpha 1 sodium potassium ATPase, anti-S100 alpha 6 and anti-annexin A2) diluted 1:1,000 in 5% w/v dry

non-fat milk in TBS-T, washed and incubated with horseradish peroxidase-conjugated anti-rabbit IgG secondary antibodies diluted 1:5,000 in 5% w/v dry non-fat milk in TBS-T, at room temperature. Immunoreactive bands were detected by enhanced chemiluminescence ECL (GE Healthcare, Buckinghamshire, UK) on X-ray films (Hyperfilm ECL, GE Healthcare) and digital images were obtained using a Molecular Imager Gel Doc XR system (Bio-Rad, Hercules, CA, USA) and analysed with QuantityOne Software (v 4.6.3, Bio-Rad). Results are presented as mean ± SD for each experimental group of at least three independent experiments with $n = 2$.

Statistical analysis

All statistical tests were performed using GraphPad Prism v5.00 (GraphPad Software, Inc.). General data from the animals involved in the study (weight, glycemia, HbA_{1c} and gland weight) were analysed using a two-way ANOVA with Bonferroni's post-tests to compare groups. Western blot data were analysed using one-way ANOVA followed by Dunnett's multiple comparison test to compare each group to C2M group. A P-value <0.05 was considered significant.

Results

The animals used in this work developed a hyperglycemic state within 2 days of the injection with STZ (Table I). It was observed a significant difference in body weight, with a higher increase in controls. Other classical symptoms of diabetes, such as polydipsia and polyuria, were also observed throughout the experimental period.

Protein identification in SMG fractions by 2D-LC-MS/MS

A total of 462 distinct proteins were identified by 2D-LC-MALDI-TOF/TOF mass spectrometry (Supplementary Table S1). To obtain a global view of the protein classes represented in our fractions enriched in organelle membranes, we have submitted the list of proteins identified to the 'Compare gene lists' tool in the PANTHER website (www.pantherdb.org), which retrieved a classification in protein classes and if the percentage of genes in each category would be lower or greater than expected, by comparing the list submitted with a list of all the *Rattus norvegicus* genes. The major protein classes with more gene hits were nucleic acid binding, oxidoreductase, cytoskeleton protein and transfer/carrier protein (Supplementary Table S2). However, to obtain a more physiologically relevant insight, we performed a similar analysis that retrieved the classification in GO biological processes. Some of the over-represented GO biological processes were the metabolic process, with the lowest P-value, as well as other processes that may be associated to intra-cellular vesicular transport, such as protein transport, cellular component organization, vesicle-mediated transport and endocytosis (Table II). A closer analysis on the proteins included in these processes reveals the presence of two clathrin subunits, five annexins (from a total of only seven entries in Uniprot), six ras-related proteins and four coatomer subunits, clearly indicating an enrichment of membranous structures such as secretory granules. Also, from a total of nine entries in the Uniprot database, we have identified eight glandular kallikreins, all of which with a high number of peptides above the threshold of 95% and a high degree of coverage (Supplementary Table S1).

iTRAQ quantitative analysis of proteome variations with hyperglycemia

To disclose how hyperglycemia affects protein expression, we have applied iTRAQ quantification to the fractions obtained from the SMG. As can be depicted from Fig. 1, the proteins that passed the exclusion criteria present a high correlation when we compared the ratios of each individual versus each of the controls, ensuring that only proteins with low individual variability were selected. Also, the time-matched control group (C4M) presented almost all of the proteins below the limits established to consider a protein up- or down-regulated (Fig. 1C).

A total 107 proteins passed the exclusion criteria in the D2M group. From these, 31 were considered up-regulated, 67 were down-regulated and 9 proteins presented no variation versus control. Within the D4M group, 48 proteins passed the exclusion criteria, 10 of which were up-regulated, 28 presented no variation and 10 other were down-regulated versus C2M (Table III). Regarding the C4M group, 31 proteins passed the exclusion criteria and only three of these presented variation versus C2M (two were up-regulated and one was down-regulated). iTRAQ quantification results were validated by western blot analysis of selected proteins, namely GAPDH, alpha 1 sodium potassium ATPase, annexin A2 and protein S100A6 (Fig. 2).

The lists of proteins selected for each of the treated groups were then submitted to the PANTHER database for a broader view of the GO biological processes altered with hyperglycemia. Table IV summarizes the distribution of the genes corresponding to those proteins by GO Biological Process. After 2 months of hyperglycemia, >50% of the identified proteins

Table I. Average values of weight, glycemia, HbA1c and SMG weight from the animals involved in the experimental protocol.

Group	C2M	D2M	C4M	D4M
Weight (g)	394.5 ± 32.4	233.7 ± 33.2***	437.1 ± 58.4	251.0 ± 43.1***
Glycemia (mg/dl)	71.0 ± 12.2	–[a]	66.3 ± 14.9	–[a]
HbA1c (%)	5.7 ± 0.6	8.4 ± 0.3***	3.9 ± 0.8	6.3 ± 1.1***
SMG weight (g)	0.351 ± 0.014	0.218 ± 0.018***	0.319 ± 0.014	0.256 ± 0.034**
Protein recovered in fractions (mg protein/g tissue)	14.14 ± 1.40	1.35 ± 0.51***	14.89 ± 3.32	5.25 ± 2.23***

Data are presented as mean ± SD. [a]The glycemia values in STZ-treated rats were above the detection limit of the device used for the readings (>600 mg/dl). **$P < 0.01$; ***$P < 0.001$.

Table II. Classification of the proteins identified by biological process.

Biological process	Number of gene hits: *Rattus norvegicus*—Reference list (27,758)	Number of gene hits: List of identified proteins (456)	Expected	Over-/under-representation in the list of identified proteins	*P*-value
Apoptosis	815	7	13.39	–	4.18E–02
Negative regulation of apoptosis	179	0	2.94	–	5.23E–02
Cell adhesion	962	8	15.8	–	2.27E–02
Cell–cell adhesion	484	3	7.95	–	4.25E–02
Cell communication	4,249	45	69.8	–	4.44E–04
Cell–cell signaling	869	6	14.28	–	1.11E–02
Signal transduction	4,065	43	66.78	–	5.90E–04
Cell surface receptor linked signal transduction	2,030	7	33.35	–	1.67E–08
G-protein coupled receptor protein signalling pathway	1,051	4	17.27	–	1.23E–04
Cytokine-mediated signalling pathway	272	0	4.47	–	1.12E–02
Transmembrane receptor protein tyrosine kinase signalling pathway	287	1	4.71	–	5.04E–02
Intracellular signalling cascade					
MAPKKK cascade	285	1	4.68	–	5.18E–02
Cell cycle	1,326	39	21.78	+	3.94E–04
Cellular component organization	1,215	50	19.96	+	4.12E–09
Cellular process					
Cell motion	469	18	7.7	+	9.48E–04
Chromosome segregation	153	6	2.51	+	4.25E–02
Cytokinesis	105	5	1.72	+	3.09E–02
Developmental process	2,381	57	39.11	+	2.86E–03
Anatomical structure morphogenesis	846	41	13.9	+	1.29E–09
Cellular component morphogenesis	846	41	13.9	+	1.29E–09
Embryonic development	181	0	2.97	–	5.06E–02
Pattern specification process	211	0	3.47	–	3.08E–02
System development					
Muscle organ development	192	9	3.15	+	5.05E–03
Generation of precursor metabolites and energy	401	41	6.59	+	4.82E–20
Oxidative phosphorylation	127	15	2.09	+	5.66E–09
Respiratory electron transport chain	376	29	6.18	+	1.43E–11
Tricarboxylic acid cycle	28	13	0.46	+	3.68E–15
Homeostatic process	87	6	1.43	+	3.47E–03
Cellular calcium ion homeostasis	45	6	0.74	+	1.18E–04
Immune system process					
Immune response	697	1	11.45	–	1.17E–04
B cell-mediated immunity	277	0	4.55	–	1.03E–02
Metabolic process	9,400	278	154.42	+	3.37E–32
Coenzyme metabolic process	90	10	1.48	+	3.36E–06
Nitrogen compound metabolic process	22	2	0.36	+	5.15E–02
Oxygen and reactive oxygen species metabolic process	51	7	0.84	+	2.68E–05
Primary metabolic process	8,928	252	146.67	+	2.68E–24
Carbohydrate metabolic process	784	46	12.88	+	2.08E–13
Monosaccharide metabolic process	232	20	3.81	+	3.51E–09
Gluconeogenesis	35	4	0.57	+	2.86E–03
Glycolysis	143	13	2.35	+	1.09E–06
Pentose-phosphate shunt	9	2	0.15	+	9.89E–03
Cellular amino acid and derivative metabolic process	297	15	4.88	+	1.57E–04
Cellular amino acid metabolic process	297	15	4.88	+	1.57E–04
Cellular amino acid biosynthetic process	82	6	1.35	+	2.60E–03
Cellular amino acid catabolic process	66	6	1.08	+	8.80E–04
Lipid metabolic process					
Fatty acid metabolic process	273	16	4.48	+	1.70E–05
Fatty acid beta-oxidation	26	6	0.43	+	5.69E–06
Phospholipid metabolic process	235	0	3.86	–	2.07E–02
Nucleobase, nucleoside, nucleotide and nucleic acid metabolic process					
DNA metabolic process					
DNA repair	200	0	3.29	–	3.70E–02
Purine base metabolic process	122	6	2	+	1.65E–02
Transcription	2,101	8	34.51	–	2.89E–08
Transcription from RNA polymerase II promoter	2,059	8	33.82	–	5.14E–08
Regulation of transcription from RNA polymerase II promoter	1,581	3	25.97	–	9.41E–09
Protein metabolic process	3,897	140	64.02	+	6.30E–20
Protein complex assembly	102	10	1.68	+	9.89E–06
Protein folding	253	19	4.16	+	7.30E–08

(continued)

Table II. Continued

Biological process	Number of gene hits: *Rattus norvegicus*—Reference list (27,758)	Number of gene hits: List of identified proteins (456)	Expected	Over-/under-representation in the list of identified proteins	*P*-value
Protein modification process					
Protein amino acid phosphorylation	804	1	13.21	−	2.21E−05
Translation	957	76	15.72	+	1.18E−29
tRNA aminoacylation for protein translation	49	6	0.8	+	1.86E−04
Sulphur metabolic process	123	5	2.02	+	5.41E−02
Vitamin metabolic process	46	4	0.76	+	7.42E−03
Vitamin biosynthetic process	23	3	0.38	+	6.76E−03
Reproduction	391	2	6.42	−	4.45E−02
Response to stimulus					
Cellular defense response	374	0	6.14	−	2.06E−03
Response to stress	304	13	4.99	+	1.87E−03
Response to toxin	116	7	1.91	+	3.42E−03
System process					
Muscle contraction	355	13	5.83	+	6.72E−03
Neurological system process	1,480	10	24.31	−	7.02E−04
Sensory perception	557	2	9.15	−	5.21E−03
Visual perception	286	1	4.7	−	5.11E−02
Transport	2,647	93	43.48	+	2.21E−12
Protein transport	1,344	64	22.08	+	4.01E−14
Intracellular protein transport	1,344	64	22.08	+	4.01E−14
Protein targeting	162	6	2.66	+	5.31E−02
Vesicle-mediated transport	848	38	13.93	+	4.05E−08
Endocytosis	367	19	6.03	+	1.57E−05
Receptor-mediated endocytosis	141	8	2.32	+	2.62E−03
Exocytosis	273	13	4.48	+	7.25E−04
Unclassified	1,1957	41	196.43	−	1.58E−58

This table lists the GO biological processes enriched in the fractions analysed, with a *P*-value <0.05 according to the PANTHER database (www.pantherdb.org).

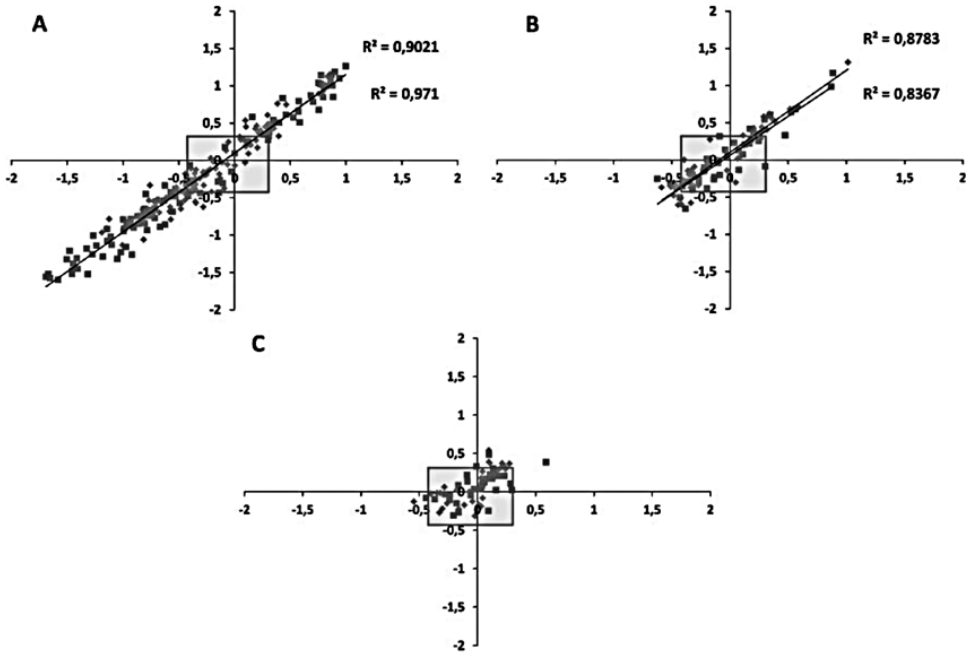

Fig. 1 Comparison of the protein variation ratios obtained for each animal in groups D2M (A), D4M (B) and C4M (C) versus each one of the control animals (*x*- and *y*-axis, respectively) from the C2M group. Filled squares and filled diamonds represent each one of the animals analysed in every group; each dot corresponds to a single protein, where the variation ratio versus each of the two animals of the C2M group can be read in the *x*- and *y*-axis, respectively. The shaded area in the centre delimits the area where it was considered that no variation occurred. It is observable a high correlation of the values for both animals in D2M (A) and D4M (B) groups, while almost all of the proteins in the C4M (C) group presented no significant variation.

Table III. Protein abundance ratios determined by iTRAQ quantification when compared with the C2M group.

Total	% Cov	Accession #		Name	Peptides (95%)	D2M	C4M	D4M
7.18	49.4	P68255	1433T_RAT	14-3-3 protein theta	6	1.618 ± 0.238		
19.92	52.1	P00507	AATM_RAT	Aspartate aminotransferase, mitochondrial	10	0.746 ± 0.072		
11.89	83.9	P11030	ACBP_RAT	Acyl-CoA-binding protein	9	1.466 ± 0.039		
24.27	43.1	Q9ER34	ACON_RAT	Aconitate hydratase, mitochondrial	13	0.74 ± 0.089		0.833 ± 0.039
74.6	89.9	P63259	ACTG_RAT	Actin, cytoplasmic 2	65			0.782 ± 0.024
27.03	67.1	Q09073	ADT2_RAT	ADP/ATP translocase 2	15	0.477 ± 0.153		
9.9	33.2	P07150	ANXA1_RAT	Annexin A1	9	1.473 ± 0.123	1.198 ± 0.065	1.246 ± 0.056
13.63	33.3	Q07936	ANXA2_RAT	Annexin A2	7	1.868 ± 0.113	1.176 ± 0.014	1.435 ± 0.105
14.74	42	P55260	ANXA4_RAT	Annexin A4	6	1.42 ± 0.192		1.229 ± 0.034
24.52	40.9	P48037	ANXA6_RAT	Annexin A6	14			1.204 ± 0.013
4.37	25.8	Q4V7C7	ARP3_RAT	Actin-related protein 3	2	2.031 ± 0.159		
59.89	57.2	P06685	AT1A1_RAT	Sodium/potassium-transporting ATPase subunit alpha-1	44	1.744 ± 0.522	1.102 ± 0.295	1.351 ± 0.146
28.16	57.2	P07340	AT1B1_RAT	Sodium/potassium-transporting ATPase subunit beta-1	16	1.797 ± 0.522	1.198 ± 0.14	1.378 ± 0.178
11.95	37.1	P18596	AT2A3_RAT	Sarcoplasmic/endoplasmic reticulum calcium ATPase 3	6	1.049 ± 0.45		
8.7	32.8	P19511	AT5F1_RAT	ATP synthase subunit b, mitochondrial	3	0.607 ± 0.047		1.056 ± 0.347
8.45	54	P31399	ATP5H_RAT	ATP synthase subunit d, mitochondrial	4	0.535 ± 0.002		
9.23	70.4	P29419	ATP5I_RAT	ATP synthase subunit e, mitochondrial	7	0.67 ± 0.109	1.213 ± 0.051	0.755 ± 0.035
13.58	75.9	P21571	ATP5J_RAT	ATP synthase-coupling factor 6, mitochondrial	8	0.54 ± 0.031		
38.1	72	P15999	ATPA_RAT	ATP synthase subunit alpha, mitochondrial	30	0.515 ± 0.163		0.792 ± 0.042
51.42	81.1	P10719	ATPB_RAT	ATP synthase subunit beta, mitochondrial	36	0.535 ± 0.137		0.794 ± 0.066
10	73.2	P35434	ATPD_RAT	ATP synthase subunit delta, mitochondrial	6	0.427 ± 0.167		
7.42	57.3	Q06647	ATPO_RAT	ATP synthase subunit O, mitochondrial	6	0.555 ± 0.181		0.705 ± 0.064
17.31	60.4	P27139	CAH2_RAT	Carbonic anhydrase 2	9			1.52 ± 0.073
21.74	87.3	P62161	CALM_RAT	Calmodulin	13	2.023 ± 0.362		1.4 ± 0.19
43.99	86.1	P18418	CALR_RAT	Calreticulin	27		0.815 ± 0.016	
10.87	26.4	P35565	CALX_RAT	Calnexin	5	0.536 ± 0.037		
19.02	42.1	P63039	CH60_RAT	60 kDa heat shock protein, mitochondrial	10	0.773 ± 0.049		
10.42	26.4	Q8VHF5	CISY_RAT	Citrate synthase, mitochondrial	6	0.536 ± 0.014		
2.79	20.2	P08081	CLCA_RAT	Clathrin light chain A	4	1.872 ± 0.293		
7.46	43.2	P10888	COX41_RAT	Cytochrome c oxidase subunit 4 isoform 1, mitochondrial	6	0.535 ± 0.015		0.776 ± 0.034
11.24	45.9	P11240	COX5A_RAT	Cytochrome c oxidase subunit 5A, mitochondrial	11	0.447 ± 0.124		0.72 ± 0.077
12.13	54.3	P12075	COX5B_RAT	Cytochrome c oxidase subunit 5B, mitochondrial	8	0.613 ± 0.077		1.025 ± 0.343
8.09	72.1	P10818	CX6A1_RAT	Cytochrome c oxidase subunit 6A1, mitochondrial	6	0.464 ± 0.016		
13.35	55.2	Q7M0E3	DEST_RAT	Destrin	6	1.646 ± 0.06		
12.58	36	P10860	DHE3_RAT	Glutamate dehydrogenase 1, mitochondrial	6	0.563 ± 0.001		
10.35	22.1	Q920L2	DHSA_RAT	Succinate dehydrogenase [ubiquinone] flavoprotein subunit, mitochondrial	8	0.501 ± 0.109		0.74 ± 0.051
5.95	22.3	P21913	DHSB_RAT	Succinate dehydrogenase [ubiquinone] iron-sulfur subunit, mitochondrial	3	0.456 ± 0.058		
11.6	21.4	Q6P6R2	DLDH_RAT	Dihydrolipoyl dehydrogenase, mitochondrial	6	0.593 ± 0.033		
2.21	8.9	Q9R0T3	DNJC3_RAT	DnaJ homolog subfamily C member 3	2	0.606 ± 0.095		
24.01	40	Q64428	ECHA_RAT	Trifunctional enzyme subunit alpha, mitochondrial	16	0.635 ± 0.142		
4.4	18.3	Q60587	ECHB_RAT	Trifunctional enzyme subunit beta, mitochondrial	4	0.485 ± 0.033		

(continued)

Table III. Continued

Total	% Cov	Accession #		Name	Peptides (95%)	D2M	C4M	D4M
6.41	37.9	P14604	ECHM_RAT	Enoyl-CoA hydratase, mitochondrial	3	0.645 ± 0.032		0.719 ± 0.035
18.74	60.2	P62630	EF1A1_RAT	Elongation factor 1-alpha 1	10		1.053 ± 0.248	1.022 ± 0.298
12	19.5	P85834	EFTU_RAT	Elongation factor Tu, mitochondrial	7	0.625 ± 0.023		
12.18	22.8	Q1JU68	EIF3A_RAT	Eukaryotic translation initiation factor 3 subunit A	7	0.732 ± 0.025	0.814 ± 0.022	0.767 ± 0.019
30.88	65.9	P04764	ENOA_RAT	Alpha-enolase	18	1.54 ± 0.265	1.148 ± 0.013	1.285 ± 0.052
30.4	45.5	Q66HD0	ENPL_RAT	Endoplasmin	16		0.782 ± 0.009	
11.36	52	P04797	G3P_RAT	Glyceraldehyde-3-phosphate dehydrogenase	7	1.863 ± 0.167		1.25 ± 0.135
8.19	21.1	P50399	GDIB_RAT	Rab GDP dissociation inhibitor beta	6	1.826 ± 0.025		
5.07	24.1	P09606	GLNA_RAT	Glutamine synthetase	3	1.771 ± 0.118		1.739 ± 0.211
17.33	37.7	P48721	GRP75_RAT	Stress-70 protein, mitochondrial	10	0.686 ± 0.112		
35.34	63.9	P06761	GRP78_RAT	78 kDa glucose-regulated protein	20	0.783 ± 0.086	0.855 ± 0.04	
48.41	96.8	P08462	GRPB_RAT	Submandibular gland secretory Glx-rich protein CB	33	1.868 ± 0.228		1.518 ± 0.125
16.69	62.4	P08010	GSTM2_RAT	Glutathione *S*-transferase Mu 2	8	1.615 ± 0.173		1.063 ± 0.27
15.1	51.7	O70351	HCD2_RAT	3-hydroxyacyl-CoA dehydrogenase Type-2	9	0.651 ± 0.042		
13.21	45.2	Q9WVK7	HCDH_RAT	Hydroxyacyl-coenzyme A dehydrogenase, mitochondrial	8	0.597 ± 0.017		0.782 ± 0.013
26.97	54.2	P63018	HSP7C_RAT	Heat shock cognate 71 kDa protein	12	1.369 ± 0.071		
18.97	40.3	Q63617	HYOU1_RAT	Hypoxia up-regulated protein 1	10		0.86 ± 0.032	
4.92	10.9	Q99NA5	IDH3A_RAT	Isocitrate dehydrogenase [NAD] subunit alpha, mitochondrial	4	0.442 ± 0.058		
24.36	49.1	P56574	IDHP_RAT	Isocitrate dehydrogenase [NADP], mitochondrial	14	0.742 ± 0.084	1.208 ± 0.081	
10.19	30.1	Q3KR86	IMMT_RAT	Mitochondrial inner membrane protein (Fragment)	5	0.611 ± 0.173		0.796 ± 0.004
35.05	61.5	P25809	KCRU_RAT	Creatine kinase U-type, mitochondrial	29	0.598 ± 0.14	1.178 ± 0.064	0.756 ± 0.044
105.3	92.7	P36375	KLK10_RAT	Glandular kallikrein-10	83	0.519 ± 0.085	0.993 ± 0.242	
41.11	93.1	P15950	KLK3_RAT	Glandular kallikrein-3, submandibular (fragment)	24	0.475 ± 0.051		
72.69	96.9	P36374	KLK6_RAT	Prostatic glandular kallikrein-6	55	0.692 ± 0.143	1.428 ± 0.037	1.116 ± 0.198
85.2	93.1	P07647	KLK9_RAT	Submandibular glandular kallikrein-9	71	0.598 ± 0.018	1.144 ± 0.028	
15.84	34.2	Q62902	LMAN1_RAT	Protein ERGIC-53	10	0.575 ± 0.02		
5.66	24.8	P97700	M2OM_RAT	Mitochondrial 2-oxoglutarate/ malate carrier protein	3	0.533 ± 0.164		
13.71	29.7	Q02253	MMSA_RAT	Methylmalonate-semialdehyde dehydrogenase [acylating], mitochondrial	7	0.736 ± 0.063		
6.46	41.3	P16036	MPCP_RAT	Phosphate carrier protein, mitochondrial	3	0.51 ± 0.013	1.205 ± 0.033	0.785 ± 0.027
65.09	37.7	Q62812	MYH9_RAT	Myosin-9	45	0.773 ± 0.048	1.148 ± 0.097	1.183 ± 0.25
12.5	51.7	Q5BK63	NDUA9_RAT	NADH dehydrogenase [ubiquinone] 1 alpha subcomplex subunit 9, mitochondrial	8	0.617 ± 0.026		0.756 ± 0.031
14.8	36.2	Q66HF1	NDUS1_RAT	NADH-ubiquinone oxidoreductase 75 kDa subunit, mitochondrial	7	0.57 ± 0.168		0.725 ± 0.03
11.96	35.4	Q641Y2	NDUS2_RAT	NADH dehydrogenase [ubiquinone] iron-sulfur protein 2, mitochondrial	7	0.49 ± 0.054		
4.05	21.4	P19234	NDUV2_RAT	NADH dehydrogenase [ubiquinone] flavoprotein 2, mitochondrial	4	0.325 ± 0.021		
22.2	47.6	Q9JI85	NUCB2_RAT	Nucleobindin-2	13			0.723 ± 0.024
6.64	24.3	Q5XI78	ODO1_RAT	2-Oxoglutarate dehydrogenase, mitochondrial	4	0.649 ± 0.097		
16.73	53.2	P49432	ODPB_RAT	Pyruvate dehydrogenase E1 component subunit beta, mitochondrial	11	0.721 ± 0.101		

(continued)

Table III. Continued

Total	% Cov	Accession #		Name	Peptides (95%)	D2M	C4M	D4M
4.58	14.7	P14882	PCCA_RAT	Propionyl-CoA carboxylase alpha chain, mitochondrial	2	0.53 ± 0.023		
9.84	34.9	P07633	PCCB_RAT	Propionyl-CoA carboxylase beta chain, mitochondrial	5	0.575 ± 0.044		
61.04	81.5	P04785	PDIA1_RAT	Protein disulphide-isomerase	36	1.272 ± 0.045	0.865 ± 0.039	1.02 ± 0.167
38.12	58	P11598	PDIA3_RAT	Protein disulphide-isomerase A3	24	1.32 ± 0.121	0.868 ± 0.026	
14.48	63.6	P31044	PEBP1_RAT	Phosphatidylethanolamine-binding protein 1	7	1.703 ± 0.319	1.129 ± 0.002	
5.12	29.4	P67779	PHB_RAT	Prohibitin	3	0.361 ± 0.004		
7.01	36.5	Q5XIH7	PHB2_RAT	Prohibitin-2	4	0.524 ± 0.187		
19.11	67.1	P10111	PPIA_RAT	Peptidyl-prolyl *cis–trans* isomerase A	16	1.613 ± 0.331		1.283 ± 0.105
4.49	27.9	P62963	PROF1_RAT	Profilin-1	3	1.875 ± 0.233		
5.08	52.9	P04550	PTMS_RAT	Parathymosin	2	2.005 ± 0.268		
6.27	12.1	P52873	PYC_RAT	Pyruvate carboxylase, mitochondrial	3	0.44 ± 0.087		
16.17	27.6	P53534	PYGB_RAT	Glycogen phosphorylase, brain form (Fragment)	12	1.75 ± 0.383	1.218 ± 0.028	
7.76	32.7	Q68FY0	QCR1_RAT	Cytochrome b-c1 complex subunit 1, mitochondrial	6	0.371 ± 0.008		
13.29	33	P32551	QCR2_RAT	Cytochrome b-c1 complex subunit 2, mitochondrial	10	0.45 ± 0.136		0.715 ± 0.001
10.83	44.9	Q5M9I5	QCR6_RAT	Cytochrome b-c1 complex subunit 6, mitochondrial	8	0.508 ± 0.176		
5.6	34.8	P62914	RL11_RAT	60S ribosomal protein L11	3	0.664 ± 0.086		
10.81	45.6	P61314	RL15_RAT	60S ribosomal protein L15	4	0.677 ± 0.056		0.696 ± 0.055
13.71	47.7	P21533	RL6_RAT	60S ribosomal protein L6	11	0.809 ± 0.024		
3.29	54.2	P62864	RS30_RAT	40S ribosomal protein S30	2			0.716 ± 0.076
7.78	40.7	P29314	RS9_RAT	40S ribosomal protein S9	4	0.694 ± 0.034		
16.81	71.5	P38983	RSSA_RAT	40S ribosomal protein SA	8	0.759 ± 0.016		
3.64	66.3	P05964	S10A6_RAT	Protein S100-A6	3	1.925 ± 0.229		2.15 ± 0.279
6.42	22	P10760	SAHH_RAT	Adenosylhomocysteinase	3		0.711 ± 0.035	
11.7	31.9	B2GV06	SCOT1_RAT	Succinyl-CoA:3-ketoacid-coenzyme A transferase 1, mitochondrial	7	0.623 ± 0.049		0.762 ± 0.065
21.5	75.3	P13432	SMR1_RAT	SMR1 protein	18	0.591 ± 0.03		
18.4	69.3	P18897	SMR2_RAT	SMR2 protein	8	1.718 ± 0.157		
22.14	39.8	Q66X93	SND1_RAT	Staphylococcal nuclease domain-containing protein 1	13	0.756 ± 0.02	0.825 ± 0.028	
33.79	25.6	P16086	SPTA2_RAT	Spectrin alpha chain, brain	16	1.238 ± 0.05		
3.33	25.7	Q7TPJ0	SSRA_RAT	Translocon-associated protein subunit alpha	4	0.463 ± 0.162		
27.41	48.1	Q6P9V9	TBA1B_RAT	Tubulin alpha-1B chain	19	1.454 ± 0.108		
18.71	54.7	P17764	THIL_RAT	Acetyl-CoA acetyltransferase, mitochondrial	12	0.718 ± 0.04	1.208 ± 0.073	
7.31	41.6	Q63584	TMEDA_RAT	Transmembrane emp24 domain-containing protein 10	4	0.539 ± 0.055		0.74 ± 0.054
4.4	19.7	P48500	TPIS_RAT	Triosephosphate isomerase	2	1.92 ± 0.138		
12.53	36.6	P04692	TPM1_RAT	Tropomyosin alpha-1 chain	7		1.407 ± 0.136	
11.62	24.4	P12346	TRFE_RAT	Serotransferrin	5	1.407 ± 0.129		
11.55	22.9	Q5U300	UBA1_RAT	Ubiquitin-like modifier-activating enzyme 1	7	1.495 ± 0.219		
4.14	36.1	P20788	UCRI_RAT	Cytochrome b-c1 complex subunit Rieske, mitochondrial	3	0.416 ± 0.155		

Ratios are presented as mean ± SD.

belong to processes that were down-regulated. From these, it is observable a clear down-regulation of the metabolic process and generation of precursor metabolites and energy proteins. From the processes found up-regulated, which corresponded to 37% of the proteins identified, the transport, cellular process and cell communication processes are worth of note, besides the metabolic process already mentioned in the down-regulated category. After 4 months of hyperglycemia, the majority of proteins (>60%) presented no variations, reflecting a tendency of adaptation to the chronic hyperglycemia. Nonetheless, within the up- and down-regulated processed, the distribution remained similar to the one observed in the C2M group. In general, it was noticed an up-regulation of annexins, calmodulin, sodium/potassium transporting ATPase subunits and SMG secretory Glx-rich protein CB associated with hyperglycemia, although these variations were attenuated with time (Fig. 3).

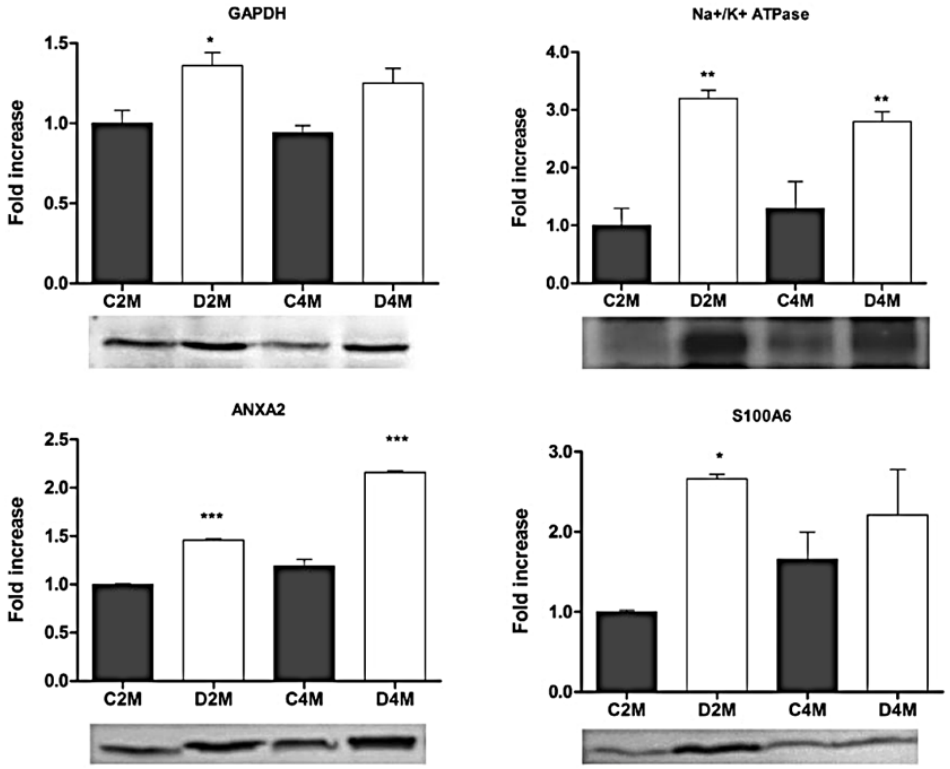

Fig. 2 Western blot analysis of GAPDH, alpha 1 sodium potassium ATPase, annexin A2 and protein S100A6 showing an up-regulation of these proteins in groups treated with STZ, confirming the tendency observed in iTRAQ quantification. A representative immunoblot image is presented below the histogram. Data are presented as mean ± SD. $*P<0.05$, $**P<0.01$, $***P<0.001$.

Table IV. Distribution of the genes corresponding to the proteins identified in the iTRAQ assay by GO Biological Process.

	D2M (189 genes)			D4M (90 genes)		
Biological process	↓	=	↑	↓	=	↑
Cell communication (GO:0007154)			4.8%		3.3%	3.3%
Cell cycle (GO:0007049)	3.2%		2.6%		2.2%	2.2%
Cellular component organization (GO:0016043)	0.5%	1.6%	1.6%		5.6%	
Cellular process (GO:0009987)	3.7%	1.6%	6.3%		10.0%	3.3%
Developmental process (GO:0032502)	2.6%	1.6%	3.2%		6.7%	2.2%
Generation of precursor metabolites and energy (GO:0006091)	12.2%			4.4%	5.6%	
Homeostatic process (GO:0042592)		0.5%	0.5%	1.1%		1.1%
Immune system process (GO:0002376)	0.5%	0.5%	1.6%		2.2%	1.1%
Metabolic process (GO:0008152)	22.8%	2.6%	8.5%	5.6%	15.6%	5.6%
Response to stimulus (GO:0050896)	0.5%	0.5%	1.1%		2.2%	
System process (GO:0003008)	0.5%		0.5%		1.1%	
Transport (GO:0006810)	6.9%	0.5%	6.3%	2.2%	8.9%	4.4%
Total	53.4%	9.5%	37.0%	13.3%	63.3%	23.3%

Each percentage was calculated by dividing the number of genes in each category by the total number of genes in the group.↓ down--regulated; = no variation; ↑ up-regulated.

Discussion

The influence of diabetes and hyperglycemia in the ultrastructure and protein activity of salivary glands has been demonstrated (*8*, *10*, *18*). However, a more in-depth proteomic analysis could provide important information regarding the intra-cellular changes that occur throughout a prolonged exposure to hyperglycemia.

STZ-induced destruction of pancreatic beta-cells has been extensively applied in the study of diabetes and hyperglycemia in animal models, including the study of its effects in salivary glands (*8*, *16*, *18*, *19*). Our goal was to apply a proteomic approach to SMG fractions, as major contributors for unstimulated saliva, and further disclose the molecular mechanisms responsible for the morphological alterations previously reported.

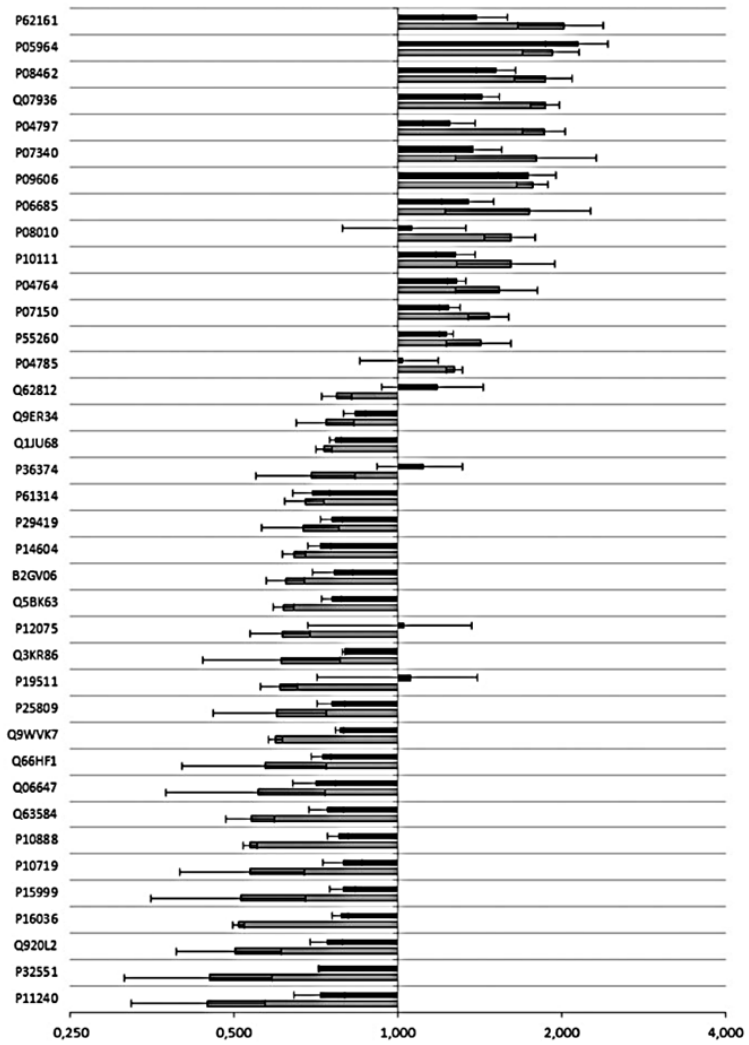

Fig. 3 Comparison of the variation values at two (grey bars) and four (black bars) months of hyperglycemia. It is observable a tendency to reduce the variation at 4 months, compared with the 2 months value. Proteins are identified by Uniprot ID on the left side. Data are presented as mean ± SD of the variation versus the C2M group.

We began by identifying the proteome constitution of our fractions. The presence of a high percentage of proteins classified as belonging to the GO biological processes of protein transport, cellular component organization, vesicle-mediated transport and exocytosis (Table II) clearly points towards enrichment in secretory granules and other vesicular structures, with some mitochondria contribution. The iTRAQ quantitative analysis provided an evaluation of the impact of STZ-induced diabetes in SMG and its evolution with the progressing of the disease.

Considering the ultrastructural changes reported for salivary glands in diabetes (*10*), it was not surprising to observe a down-regulation of the metabolic and energy production processes. However, the variations observed for proteins such as kallikreins and protein S100A6, for their role in inflammation and tissue regeneration, as well as annexins and clathrin, for their role in vesicular transport, are worth of a closer analysis.

Kallikreins play an important role in saliva production, namely in the activation of several proteins as proline-rich proteins (*27*) or matrix-metalloproteinases. Moreover, Chan *et al.* (*21*) have reported a decreased activity of kallikrein and kallikrein-like proteases in salivary glands of diabetic rats. Our sample was highly enriched in kallikreins and we describe the down-regulation of kallikreins 3, 6, 9 and 10 after 2 months of hyperglycemia (Table III). Kallikreins have been suggested to play a role in the maintenance of oral health either indirectly by proteolytic activation of proteins such as proline-rich protein

(*27*) that act in the protection and repair of dental enamel against dental caries (*28*) or directly as mediators of vasodilatation in injured areas of the oral mucosa, allowing a more efficient defense and faster healing (*29*). It has also been suggested an involvement in cell survival and proliferation, as kinins bind G-coupled receptors B1 and B2 may activate the pro-survival PI3K-Akt pathway, and salivary glands express these receptors (*30*, *31*). Since histochemical studies reported the predominance of glandular kallikreins in the striated ducts and ductal cells of SMGs of primates (*32*) and rodents (*33*), the down-regulation observed herein may, in one hand, compromise the regeneration ability of the gland, and in the other hand be justified by higher susceptibility of ductal cells to STZ-induced diabetes, as reported by Anderson *et al.* (*10*). It is also worth noting the extremely pronounced up-regulation of protein S100A6 after 2 months of hyperglycemia (Fig. 2). This protein is a trigger for apoptosis through the activation of JNK, a member of the mitogen-activated kinases mostly involved in stress response (*34*, *35*), and its up-regulation clearly suggests that apoptotic events are linked to the observed loss of glandular mass and function.

As stated above, another family of proteins that stands out from the list of identified proteins was the annexins family. Indeed, from a total of seven entries for rat annexins in Uniprot, we have identified five of them. Annexins are calcium-binding proteins that were shown to be involved in intracellular trafficking and organization of vesicles (*36*, *37*). Some of the members of this family, such as annexin A1, have been associated with an anti-inflammatory effect (*38*). Our iTRAQ-based quantitative analysis shows an up-regulation of annexins in diabetic rats, this tendency was further confirmed by western blot analysis of annexin A2 (Fig. 2), as well as an up-regulation of clathrin light chain A (Table III and Fig. 2). Considering that diabetes is often associated with an increased inflammatory state, namely in the oral cavity, the up-regulation of these proteins should be expected. However, one cannot exclude that annexins may play a role in granule fusion, which is another well-known ultrastructural modification in salivary gland associated with diabetes (*8*).

Regarding the temporal effect of hyperglycemia on the proteome constitution, our results suggest an adaptation of the tissue, with the reduction of the variation values at 4 months, when compared with the 2 months animals, as can be depicted from Fig. 3. This pattern indicates the presence of two kind of response to the stress caused by hyperglycemia. At 2 months, we have an early phase response with highly marked variations of several proteins, mostly down-regulations, while at 4 months, the variations are attenuated in a clear sign of adaptation to the chronic hyperglycemia, which is also evidenced in the biological processes altered (Table IV).

In overall, our results provide interesting evidence of the biochemical events underlying the morphological alterations previously reported, namely the loss of gland mass through apoptosis and loss of regeneration ability. Also, we observe an adaptation of the gland to the hyperglycemic state, through a more intense variation of some proteins at 2 months, which tend to normalize over time. As such, these results not only contribute to the comprehension of the morphological alterations but also open new pathways for the complete unravelling of the molecular mechanisms responsible for the link between diabetes mellitus and oral health decline.

Supplementary Data

Supplementary Data are available at *JB* Online.

Acknowledgements

The authors acknowledge the technical support of Celeste Resende in animal care.

Funding

This work was supported by the Foundation for Science and Technology of the Portuguese Ministry of Education and Science [PTDC/QUI/72903/2006 and PEst-C/QUI/UI0062/2011, PhD fellowship SFRH/BD/46829/2008 to RMPA].

Conflict of interest

None declared.

References

1. Wild, S., Roglic, G., Green, A., Sicree, R., and King, H. (2004) Global prevalence of diabetes: estimates for the year 2000 and projections for 2030. *Diabetes Care* **27**, 1047–1053
2. Narayan, K.M.V., Zhang, P., Kanaya, A.M., Williams, D.E., Engelgau, M.M., Imperatore, G., and Ramachandran, A. (2006) Diabetes: the pandemic and potential solutions in *Disease Control Priorities in Developing Countries* (Jamison, D.T., Breman, J.G., Measham, A.R., Alleyne, G., Claeson, M., Evans, D.B., Jha, P., Mills, A., and Musgrove, P., eds.), pp. 591–603, Washington, DC
3. Lakschevitz, F., Aboodi, G., Tenenbaum, H., and Glogauer, M. (2011) Diabetes and periodontal diseases: interplay and links. *Curr. Diabetes Rev.* **7**, 433–439
4. Moore, P.A., Guggenheimer, J., Etzel, K.R., Weyant, R.J., and Orchard, T. (2001) Type 1 diabetes mellitus, xerostomia, and salivary flow rates. *Oral Surg. Oral Med. Oral Pathol. Oral Radiol. Endod.* **92**, 281–291
5. Sreebny, L.M., Yu, A., Green, A., and Valdini, A. (1992) Xerostomia in diabetes mellitus. *Diabetes Care* **15**, 900–904
6. Navazesh, M. (1993) Methods for collecting saliva. *Ann. N.Y. Acad. Sci.* **694**, 72–77
7. Szkudelski, T. (2001) The mechanism of alloxan and streptozotocin action in B cells of the rat pancreas. *Physiol. Res.* **50**, 537–546
8. Cutler, L.S., Pinney, H.E., Christian, C., and Russotto, S.B. (1979) Ultrastructural studies of the rat submandibular gland in streptozotocin induced diabetes mellitus. *Virchows Arch. A Pathol. Anat. Hist.* **382**, 301–311
9. Anderson, L.C., Garrett, J.R., Suleiman, A.H., Proctor, G.B., Chan, K.M., and Hartley, R. (1993) In vivo secretory responses of submandibular glands in streptozotocin-diabetic rats to sympathetic and parasympathetic nerve stimulation. *Cell Tissue Res.* **274**, 559–566

10. Anderson, L.C., Suleiman, A.H., and Garrett, J.R. (1994) Morphological effects of diabetes on the granular ducts and acini of the rat submandibular gland. *Microsc. Res.Tech.* **27**, 61–70
11. Walz, A., Stuhler, K., Wattenberg, A., Hawranke, E., Meyer, H.E., Schmalz, G., Bluggel, M., and Ruhl, S. (2006) Proteome analysis of glandular parotid and submandibular-sublingual saliva in comparison to whole human saliva by two-dimensional gel electrophoresis. *Proteomics* **6**, 1631–1639
12. Caseiro, A., Vitorino, R., Barros, A.S., Ferreira, R., Calheiros-Lobo, M.J., Carvalho, D., Duarte, J.A., and Amado, F. (2012) Salivary peptidome in type 1 diabetes mellitus. *Biomed. Chromatogr.* **26**, 571–582
13. Vitorino, R., Alves, R., Barros, A., Caseiro, A., Ferreira, R., Lobo, M.C., Bastos, A., Duarte, J., Carvalho, D., Santos, L.L., and Amado, F.L. (2010) Finding new post-translational modifications in salivary proline-rich proteins. *Proteomics* **10**, 3732–3742
14. Vitorino, R., Lobo, M.J., Ferrer-Correira, A.J., Dubin, J.R., Tomer, K.B., Domingues, P.M., and Amado, F.M. (2004) Identification of human whole saliva protein components using proteomics. *Proteomics* **4**, 1109–1115
15. Denny, P., Hagen, F.K., Hardt, M., Liao, L., Yan, W., Arellanno, M., Bassilian, S., Bedi, G.S., Boontheung, P., Cociorva, D., Delahunty, C.M., Denny, T., Dunsmore, J., Faull, K.F., Gilligan, J., Gonzalez-Begne, M., Halgand, F., Hall, S.C., Han, X., Henson, B., Hewel, J., Hu, S., Jeffrey, S., Jiang, J., Loo, J.A., Ogorzalek Loo, R.R., Malamud, D., Melvin, J.E., Miroshnychenko, O., Navazesh, M., Niles, R., Park, S.K., Prakobphol, A., Ramachandran, P., Richert, M., Robinson, S., Sondej, M., Souda, P., Sullivan, M.A., Takashima, J., Than, S., Wang, J., Whitelegge, J.P., Witkowska, H.E., Wolinsky, L., Xie, Y., Xu, T., Yu, W., Ytterberg, J., Wong, D.T., Yates, J.R. 3rd, and Fisher, S.J. (2008) The proteomes of human parotid and submandibular/sublingual gland salivas collected as the ductal secretions. *J. Proteome Res.* **7**, 1994–2006
16. Ibuki, F.K., Simoes, A., and Nogueira, F.N. (2010) Antioxidant enzymatic defense in salivary glands of streptozotocin-induced diabetic rats: a temporal study. *Cell Biochem. Funct.* **28**, 503–508
17. Anderson, L.C. and Shapiro, B.L. (1979) The effect of alloxan diabetes and insulin in vivo on peroxidase activity in the rat submandibular gland. *Arch. Oral Biol.* **24**, 343–345
18. Mednieks, M.I., Szczepanski, A., Clark, B., and Hand, A.R. (2009) Protein expression in salivary glands of rats with streptozotocin diabetes. *Int. J. Exp. Pathol.* **90**, 412–422
19. Szczepanski, A., Mednieks, M.I., and Hand, A.R. (1998) Expression and distribution of parotid secretory proteins in experimental diabetes. *Eur. J. Morphol.* **36 (Suppl.)**, 240–246
20. Kasayama, S., Ohba, Y., and Oka, T. (1989) Epidermal growth factor deficiency associated with diabetes mellitus. *Proc. Natl Acad. Sci. USA* **86**, 7644–7648
21. Chan, K.M., Chao, J., Proctor, G.B., Garrett, J.R., Shori, D.K., and Anderson, L.C. (1993) Tissue kallikrein and tonin levels in submandibular glands of STZ-induced diabetic rats and the effects of insulin. *Diabetes* **42**, 113–117
22. Feinstein, H. and Schramm, M. (1970) Energy production in rat parotid gland. Relation to enzyme secretion and effects of calcium. *Eur. J. Biochem.* **13**, 158–163
23. Manadas, B., English, J.A., Wynne, K.J., Cotter, D.R., and Dunn, M.J. (2009) Comparative analysis of OFFGel, strong cation exchange with pH gradient, and RP at high pH for first-dimensional separation of peptides from a membrane-enriched protein fraction. *Proteomics* **9**, 5194–5198
24. Vitorino, R., Barros, A., Caseiro, A., Domingues, P., Duarte, J., and Amado, F. (2009) Towards defining the whole salivary peptidome. *Proteom Clin. Appl.* **3**, 528–540
25. Gan, C.S., Chong, P.K., Pham, T.K., and Wright, P.C. (2007) Technical, experimental, and biological variations in isobaric tags for relative and absolute quantitation (iTRAQ). *J. Proteome Res.* **6**, 821–827
26. Laemmli, U.K. (1970) Cleavage of structural proteins during the assembly of the head of bacteriophage T4. *Nature* **227**, 680–685
27. Wong, R.S., Madapallimattam, G., and Bennick, A. (1983) The role of glandular kallikrein in the formation of a salivary proline-rich protein A by cleavage of a single bond in salivary protein C. *Biochem. J.* **211**, 35–44
28. Levine, M. (2011) Susceptibility to dental caries and the salivary proline-rich proteins. *Int. J. Dent.* **2011**, 953412
29. Fábián, T.K., Fejérdy, P., and Csermely, P. (2008) Saliva in health and disease (chemical biology of) *Wiley Encyclopedia of Chemical Biology* (Begley, T.P., ed.), pp. 1–9, John Wiley and Sons, Inc
30. Dlamini, Z. and Bhoola, K.D. (2005) Upregulation of tissue kallikrein, kinin B1 receptor, and kinin B2 receptor in mast and giant cells infiltrating oesophageal squamous cell carcinoma. *J. Clin. Pathol.* **58**, 915–922
31. Bader, M. (2009) Kallikrein-kinin system in neovascularization. *Arterioscler. Thromb. Vasc. Biol.* **29**, 617–619
32. Yahiro, J. and Miyoshi, S. (1996) Immunohistochemical localization of kallikrein in salivary glands of the Japanese monkey, Macaca fuscata. *Arch. Oral Biol.* **41**, 225–228
33. Garrett, J.R., Smith, R.E., Kidd, A., Kyriacou, K., and Grabske, R.J. (1982) Kallikrein-like activity in salivary glands using a new tripeptide substrate, including preliminary secretory studies and observations on mast cells. *Histochem. J.* **14**, 967–979
34. Leclerc, E., Fritz, G., Weibel, M., Heizmann, C.W., and Galichet, A. (2007) S100B and S100A6 differentially modulate cell survival by interacting with distinct RAGE (receptor for advanced glycation end products) immunoglobulin domains. *J. Biol. Chem.* **282**, 31317–31331
35. Schaeffer, H.J. and Weber, M.J. (1999) Mitogen-activated protein kinases: specific messages from ubiquitous messengers. *Mol. Cell. Biol.* **19**, 2435–2444
36. Gerke, V., Creutz, C.E., and Moss, S.E. (2005) Annexins: linking Ca2+ signalling to membrane dynamics. *Nat. Rev. Mol. Cell Biol.* **6**, 449–461
37. Donnelly, S.R. and Moss, S.E. (1997) Annexins in the secretory pathway. *Cell. Mol. Life Sci.* **53**, 533–538
38. Lim, L.H. and Pervaiz, S. (2007) Annexin 1: the new face of an old molecule. *FASEB J.* **21**, 968–975

Supplementary tables for:

iTRAQ-based quantitative proteomic analysis of submandibular glands from rats with STZ-induced hyperglycemia

Renato M. P. Alves[1], Rui Vitorino[1], Ana I. Padrão[1], Daniel Moreira-Gonçalves[2], José A. Duarte[2], Rita M. P. Ferreira[1], Francisco Amado[1]

[1]QOPNA, Department of Chemistry, University of Aveiro, Aveiro, Portugal

[2]CIAFEL, Faculty of Sports, University of Porto, Porto, Portugal

Supplementary Table 1 – List of proteins identified in the granule-enriched fractions from rat submandibular gland by nLC-MS/MS, in alphabetical order.

Total (ProtScore)
A measure of the total amount of evidence for a detected protein. The Total ProtScore is calculated using all of the peptides detected for the protein, as described in About the Total ProtScore and the Unused ProtScore. The Total ProtScore does not indicate anything about the confidence that a protein has been detected, because some or even all of the spectra contributing to the Total ProtScore may be better explained by higher ranked proteins.
Peptides (95%)
The number of distinct peptides having at least 95% confidence. Multiple modified and cleaved states of the same underlying peptide sequence are considered distinct peptides because they have different molecular formulas. Multiple spectra of the same peptide, due to replicate acquisition or different charge states, only count once.

Name	Uniprot Accession #	% Cov	# of peptides (95%)	Total protscore
14-3-3 protein beta/alpha	P35213	34.6	4	4.11
14-3-3 protein epsilon	P62260	32.9	9	8.88
14-3-3 protein eta	P68511	22.8	3	2.04
14-3-3 protein gamma	P61983	28.3	4	4.8
14-3-3 protein theta	P68255	49.4	6	7.18
14-3-3 protein zeta/delta	P63102	54.7	7	8.22
2,4-dienoyl-CoA reductase, mitochondrial	Q64591	22.7	4	7.57
26S protease regulatory subunit 7	Q63347	17.3	2	4
26S proteasome non-ATPase regulatory subunit 1	O88761	12.5	3	4.94
26S proteasome non-ATPase regulatory subunit 2	Q4FZT9	12.7	2	3.44
2-oxoglutarate dehydrogenase, mitochondrial	Q5XI78	12.3	6	7.81
2-oxoisovalerate dehydrogenase subunit alpha, mitochondrial (Fragment)	P11960	11.3	3	3.11
3-alpha-hydroxysteroid dehydrogenase	P23457	11.8	4	6.12
3-hydroxyacyl-CoA dehydrogenase type-2	O70351	51.7	9	15.1
3-hydroxyisobutyrate dehydrogenase, mitochondrial	P29266	41.5	5	6.08
40S ribosomal protein S10	P63326	48.5	4	6.2
40S ribosomal protein S11	P62282	44.9	5	4.98
40S ribosomal protein S12	P63324	34.9	2	2.72
40S ribosomal protein S14	P13471	45	3	3.32
40S ribosomal protein S15	P62845	51	5	9.65
40S ribosomal protein S15a	P62246	33.9	3	4.97
40S ribosomal protein S16	P62250	44.5	3	5.64

Name	Uniprot Accession #	% Cov	# of peptides (95%)	Total protscore
40S ribosomal protein S17	P04644	36.3	5	6.71
40S ribosomal protein S18	P62271	45.4	7	9.14
40S ribosomal protein S19	P17074	43.5	3	6.1
40S ribosomal protein S2	P27952	21.8	2	2.4
40S ribosomal protein S23	P62268	44.8	5	3.71
40S ribosomal protein S26	P62856	40	3	4.84
40S ribosomal protein S28	P62859	30.4	3	2.26
40S ribosomal protein S3	P62909	64.6	6	10.39
40S ribosomal protein S30	P62864	42.4	3	5.94
40S ribosomal protein S3a	P49242	38.3	9	11.96
40S ribosomal protein S4, X isoform	P62703	43	11	18.13
40S ribosomal protein S5	P24050	35.3	2	3.76
40S ribosomal protein S6	P62755	34.5	5	8.95
40S ribosomal protein S7	P62083	37.1	7	11.69
40S ribosomal protein S8	P62243	53.9	10	16.29
40S ribosomal protein S9	P29314	48.5	6	10.51
40S ribosomal protein SA	P38983	71.5	8	16.81
4-trimethylaminobutyraldehyde dehydrogenase	Q9JLJ3	17.2	3	4.98
60 kDa heat shock protein, mitochondrial	P63039	35.1	11	19.03
60S acidic ribosomal protein P0	P19945	28.4	5	10.29
60S acidic ribosomal protein P1	P19944	36.8	3	3.65
60S acidic ribosomal protein P2	P02401	71.3	9	8.51
60S ribosomal protein L10	Q6PDV7	45.8	13	12.13
60S ribosomal protein L11	P62914	40.5	5	8.62
60S ribosomal protein L13	P41123	42.7	8	14.49
60S ribosomal protein L13a	P35427	31.5	3	3.34
60S ribosomal protein L14	Q63507	31.8	5	4.23
60S ribosomal protein L15	P61314	55.4	6	12.08
60S ribosomal protein L17	P24049	34.8	5	7.08
60S ribosomal protein L18	P12001	18.1	3	2.58

Name	Uniprot Accession #	% Cov	# of peptides (95%)	Total protscore
60S ribosomal protein L18a	P62718	32.4	4	6.35
60S ribosomal protein L19	P84100	40.8	3	4.96
60S ribosomal protein L21	P20280	38.8	5	5.9
60S ribosomal protein L22	P47198	16.4	2	2
60S ribosomal protein L23	P62832	25	2	3.73
60S ribosomal protein L23a	P62752	19.9	2	2.88
60S ribosomal protein L24	P83732	28.7	3	5.55
60S ribosomal protein L26	P12749	24.8	3	5.54
60S ribosomal protein L27	P61354	23.5	2	2.37
60S ribosomal protein L27a	P18445	34.5	2	4.04
60S ribosomal protein L29	P25886	46.8	3	4.94
60S ribosomal protein L3	P21531	29.5	8	15.54
60S ribosomal protein L30	P62890	35.7	7	4
60S ribosomal protein L31	P62902	33.6	6	7.87
60S ribosomal protein L32	P62912	26.7	3	4.55
60S ribosomal protein L34	P11250	19.7	2	0.72
60S ribosomal protein L35	P17078	39.8	4	6.59
60S ribosomal protein L36a	P83883	28.3	4	2.97
60S ribosomal protein L4	P50878	41.1	12	11.53
60S ribosomal protein L5	P09895	45.5	8	11.98
60S ribosomal protein L6	P21533	53.7	15	17.91
60S ribosomal protein L7	P05426	38.5	3	5.77
60S ribosomal protein L7a	P62425	33.5	4	6.85
60S ribosomal protein L8	P62919	32.7	2	3.27
60S ribosomal protein L9	P17077	16.7	3	5.17
6-phosphofructokinase, muscle type	P47858	8.7	2	2.92
6-phosphogluconolactonase	P85971	20.2	2	4
78 kDa glucose-regulated protein	P06761	63.9	20	35.34
Acetyl-CoA acetyltransferase, mitochondrial	P17764	39.9	15	19.54
Aconitate hydratase, mitochondrial	Q9ER34	34.7	15	25.59

Name	Uniprot Accession #	% Cov	# of peptides (95%)	Total protscore
Actin, aortic smooth muscle	P62738	65.3	39	30.92
Actin, cytoplasmic 1	P60711	89.9	63	74.6
Actin, cytoplasmic 2	P63259	88.8	74	53.08
Actin-related protein 3	Q4V7C7	16.3	3	4.75
Acyl-CoA-binding protein	P11030	83.9	9	11.89
Adenine phosphoribosyltransferase	P36972	29.4	4	6.36
Adenosylhomocysteinase	P10760	22	3	6.42
Adenylate kinase 2, mitochondrial	P29410	36	3	5.57
Adenylyl cyclase-associated protein 1	Q08163	11.6	3	4.49
ADP/ATP translocase 1	Q05962	46	12	18.77
ADP/ATP translocase 2	Q09073	57.4	17	29.2
ADP-ribosylation factor 3	P61206	24.9	2	3.53
ADP-ribosylation factor 4	P61751	12.2	2	2.75
ADP-ribosylation factor-like protein 1	P61212	29.3	2	4
Aflatoxin B1 aldehyde reductase member 2	Q8CG45	4.4	2	2
Alcohol dehydrogenase [NADP+]	P51635	9.5	2	4
Aldehyde dehydrogenase, mitochondrial	P11884	8.3	6	5.64
Alpha-actinin-1	Q9Z1P2	26.2	14	15.44
Alpha-actinin-4	Q9QXQ0	22.8	16	20.37
Alpha-aminoadipic semialdehyde dehydrogenase	Q64057	19.5	3	4.34
Alpha-aminoadipic semialdehyde synthase, mitochondrial	A2VCW9	11.8	3	4.51
Alpha-enolase	P04764	57.1	20	30.59
Alpha-soluble NSF attachment protein	P54921	13.9	3	4.23
Aminopeptidase N	P15684	14.7	2	4
Amyloid beta A4 protein	P08592	7.4	3	3.64
Annexin A1	P07150	40.2	10	11.01
Annexin A2	Q07936	33.3	7	13.63
Annexin A4	P55260	43.9	8	15.68
Annexin A5	P14668	40.1	9	12.82
Annexin A6	P48037	47	20	30.66

Name	Uniprot Accession #	% Cov	# of peptides (95%)	Total protscore
AP-2 complex subunit alpha-2	P18484	7.8	2	2.67
Arginase-1	P07824	14.9	2	3.2
Asparagine synthetase [glutamine-hydrolyzing]	P49088	12.8	4	6.54
Aspartate aminotransferase, mitochondrial	P00507	52.1	10	19.92
Aspartate--tRNA ligase, cytoplasmic	P15178	15	2	3.64
ATP synthase subunit alpha, mitochondrial	P15999	72	30	38.1
ATP synthase subunit b, mitochondrial	P19511	36.3	7	9.89
ATP synthase subunit beta, mitochondrial	P10719	64.8	37	47.87
ATP synthase subunit d, mitochondrial	P31399	54	4	8.45
ATP synthase subunit delta, mitochondrial	P35434	73.2	6	10
ATP synthase subunit e, mitochondrial	P29419	81.7	9	11.83
ATP synthase subunit gamma, mitochondrial	P35435	27.1	5	6.85
ATP synthase subunit O, mitochondrial	Q06647	49.8	9	9.64
ATP synthase-coupling factor 6, mitochondrial	P21571	75.9	8	13.58
ATPase inhibitor, mitochondrial	Q03344	38.3	3	2.5
ATP-binding cassette sub-family F member 1	Q6MG08	8.9	2	3.66
ATP-citrate synthase	P16638	5.7	2	1.37
ATP-dependent RNA helicase DDX1	Q641Y8	9.9	3	4.77
Band 3 anion transport protein	P23562	6.4	2	3.78
Beta-hexosaminidase subunit beta	Q6AXR4	16.4	2	4.13
Brain protein 44	P38718	42.5	3	5.35
Branched-chain-amino-acid aminotransferase, mitochondrial	O35854	27.7	3	6.16
Calmodulin	P62161	87.3	13	21.74
Calmodulin-like protein 3	Q5U206	45	4	7
Calnexin	P35565	20.5	6	10.55
Calpain small subunit 1	Q64537	17.8	2	2.48
Calreticulin	P18418	80.1	28	41.78
Carbonic anhydrase 2	P27139	60.4	9	17.31
Catenin beta-1	Q9WU82	9	3	5.55
Cationic trypsin-3	P08426	30.4	2	0.68

Name	Uniprot Accession #	% Cov	# of peptides (95%)	Total protscore
Chloride intracellular channel protein 1	Q6MG61	9.1	2	2
Citrate synthase, mitochondrial	Q8VHF5	35.6	8	12.07
Clathrin heavy chain 1	P11442	12.6	8	13.06
Clathrin light chain A	P08081	20.2	4	2.79
Coatomer subunit beta	P23514	11.2	2	4
Coatomer subunit beta'	O35142	6.3	4	5.25
Coatomer subunit delta	Q66H80	8.6	3	3.51
Coatomer subunit gamma	Q4AEF8	18.9	6	6.85
Collagen alpha-1(I) chain	P02454	54.6	51	21.4
Collagen alpha-1(III) chain	P13941	36	34	10.55
Collagen alpha-2(I) chain	P02466	30.7	17	2.25
Complement component 1 Q subcomponent-binding protein, mitochondrial	O35796	41.2	5	8.83
Core histone macro-H2A.1	Q02874	26.7	8	6.08
Creatine kinase B-type	P07335	35.7	19	14.74
Creatine kinase S-type, mitochondrial	P09605	20.8	14	6.68
Creatine kinase U-type, mitochondrial	P25809	62	34	35.03
Cullin-associated NEDD8-dissociated protein 1	P97536	7.5	3	6.04
Cytochrome b-c1 complex subunit 1, mitochondrial	Q68FY0	23.8	8	10.66
Cytochrome b-c1 complex subunit 2, mitochondrial	P32551	33	10	13.29
Cytochrome b-c1 complex subunit 6, mitochondrial	Q5M9I5	44.9	8	10.83
Cytochrome b-c1 complex subunit Rieske, mitochondrial	P20788	36.1	3	4.14
Cytochrome c oxidase subunit 2	P00406	19.4	4	5.96
Cytochrome c oxidase subunit 4 isoform 1, mitochondrial	P10888	43.2	6	7.46
Cytochrome c oxidase subunit 5A, mitochondrial	P11240	45.9	11	11.24
Cytochrome c oxidase subunit 5B, mitochondrial	P12075	54.3	8	12.13
Cytochrome c oxidase subunit 6A1, mitochondrial	P10818	72.1	6	8.09
Cytochrome c oxidase subunit 6C-2	P11951	61.8	4	3.57
Cytochrome c, somatic	P62898	42.9	4	7.76
Cytoplasmic aconitate hydratase	Q63270	6.7	2	2.05
Cytoplasmic dynein 1 heavy chain 1	P38650	8.9	7	15.68

Name	Uniprot Accession #	% Cov	# of peptides (95%)	Total protscore
Cytosol aminopeptidase	Q68FS4	14.3	3	5.31
Cytosolic 10-formyltetrahydrofolate dehydrogenase	P28037	10.9	2	2.01
D-3-phosphoglycerate dehydrogenase	O08651	18.2	3	6
Decorin	Q01129	8.5	4	2.73
Delta(3,5)-Delta(2,4)-dienoyl-CoA isomerase, mitochondrial	Q62651	17.7	2	3.81
Delta-aminolevulinic acid dehydratase	P06214	14.9	6	8
Destrin	Q7M0E3	53.9	8	14.82
Dihydrolipoyl dehydrogenase, mitochondrial	Q6P6R2	21.4	6	11.6
Dihydrolipoyllysine-residue acetyltransferase component of pyruvate dehydrogenase complex, mitochondrial	P08461	7.6	3	2.75
Dihydrolipoyllysine-residue succinyltransferase component of 2-oxoglutarate dehydrogenase complex, mitochondrial	Q01205	7.3	3	3.59
Dipeptidyl peptidase 3	O55096	9.6	4	5.24
DnaJ homolog subfamily C member 3	Q9R0T3	10.1	3	3.77
Dolichyl-diphosphooligosaccharide--protein glycosyltransferase 48 kDa subunit	Q641Y0	13.2	3	2.23
Dolichyl-diphosphooligosaccharide--protein glycosyltransferase subunit 1	P07153	12.4	4	7.35
Dolichyl-diphosphooligosaccharide--protein glycosyltransferase subunit 2	P25235	15.5	2	4
Dynactin subunit 1	P28023	13.1	2	4.02
Dynamin-1-like protein	O35303	5.7	2	2.04
Dynamin-like 120 kDa protein, mitochondrial	Q2TA68	13.4	2	4
Dynein light chain 2, cytoplasmic	Q78P75	40.5	2	4.03
EH domain-containing protein 2	Q4V8H8	10.1	2	2
EH domain-containing protein 3	Q8R491	12.2	2	4
Electron transfer flavoprotein subunit alpha, mitochondrial	P13803	18.6	6	3.23
Electron transfer flavoprotein subunit beta	Q68FU3	39.6	4	7.21
Electron transfer flavoprotein-ubiquinone oxidoreductase, mitochondrial	Q6UPE1	9.9	4	3.32
Elongation factor 1-alpha 1	P62630	54.8	13	24.53
Elongation factor 1-gamma	Q68FR6	36.4	12	14.48
Elongation factor 2	P05197	31	17	32.45
Elongation factor Tu, mitochondrial	P85834	19.5	7	12
Endoplasmic reticulum resident protein 29	P52555	28.9	2	3.94
Endoplasmin	Q66HD0	37.9	20	33.49

Name	Uniprot Accession #	% Cov	# of peptides (95%)	Total protscore
Enoyl-CoA delta isomerase 1, mitochondrial	P23965	15.2	2	2.73
Enoyl-CoA hydratase, mitochondrial	P14604	31	5	7.61
Erlin-2	B5DEH2	10.3	2	2.68
ERO1-like protein alpha	Q8R4A1	10.1	2	3.89
Ester hydrolase C11orf54 homolog	Q5U2Q3	9.8	2	2.73
Eukaryotic initiation factor 4A-II	Q5RKI1	19.4	7	6.89
Eukaryotic translation initiation factor 3 subunit A	Q1JU68	24.5	9	14.65
Eukaryotic translation initiation factor 3 subunit B	Q4G061	23.7	2	4.08
Eukaryotic translation initiation factor 3 subunit C	B5DFC8	13.2	2	1.66
Eukaryotic translation initiation factor 3 subunit E	Q641X8	6.7	2	2.74
Eukaryotic translation initiation factor 3 subunit J	A0JPM9	22.4	4	6.12
Eukaryotic translation initiation factor 5A-1	Q3T1J1	58.4	5	9.55
Ezrin	P31977	26.1	5	9
F-actin-capping protein subunit alpha-2	Q3T1K5	18.5	2	3.44
Far upstream element-binding protein 2	Q99PF5	10.4	2	2.56
Fructose-bisphosphate aldolase A	P05065	50.3	5	10.9
Gamma-enolase	P07323	20.7	4	4.92
General vesicular transport factor p115	P41542	8.9	2	1.2
Glandular kallikrein-10	P36375	85.7	100	90.35
Glandular kallikrein-12, submandibular/renal	P36376	48.3	26	24.92
Glandular kallikrein-3, submandibular (Fragment)	P15950	86.7	32	40.67
Glandular kallikrein-7, submandibular/renal	P36373	85.1	52	57.31
Glia maturation factor beta	Q63228	35.2	3	6.1
Glucosamine--fructose-6-phosphate aminotransferase [isomerizing] 1	P82808	10.3	3	4
Glucose-6-phosphate 1-dehydrogenase	P05370	5.8	2	2
Glucose-6-phosphate isomerase	Q6P6V0	22.9	6	7.85
Glutamate dehydrogenase 1, mitochondrial	P10860	27.4	8	13.09
Glutamine synthetase	P09606	23.3	4	6.13
Glutathione peroxidase 1	P04041	32.8	4	6.74
Glutathione S-transferase Mu 1	P04905	19.3	3	2.21

Name	Uniprot Accession #	% Cov	# of peptides (95%)	Total protscore
Glutathione S-transferase Mu 2	P08010	64.7	11	19.6
Glutathione S-transferase P	P04906	33.8	7	4.15
Glutathione synthetase	P46413	9.3	2	0.71
Glyceraldehyde-3-phosphate dehydrogenase	P04797	44.7	8	13.4
Glycogen phosphorylase, brain form (Fragment)	P53534	22.8	13	17.18
Golgi integral membrane protein 4	Q5BJK8	9.6	2	3.48
Golgi phosphoprotein 3	Q9ERE4	15.8	2	3.42
Golgi reassembly-stacking protein 2	Q9R064	7.9	2	2.64
GTP-binding protein 1	D2XV59	9.3	2	2.9
Guanine nucleotide-binding protein G(I)/G(S)/G(T) subunit beta-1	P54311	10.6	2	3.59
Guanine nucleotide-binding protein G(I)/G(S)/G(T) subunit beta-2	P54313	9.4	2	3.61
Guanine nucleotide-binding protein subunit beta-2-like 1	P63245	39.1	10	10.74
Heat shock 70 kDa protein 1A/1B	Q07439	36	8	16.83
Heat shock 70 kDa protein 4	O88600	6.3	3	4.89
Heat shock cognate 71 kDa protein	P63018	43.8	14	26.71
Heat shock protein HSP 90-alpha	P82995	26.6	8	12.82
Heat shock protein HSP 90-beta	P34058	30.4	13	12.4
Hemoglobin subunit alpha-1/2	P01946	82.4	20	22.91
Hemoglobin subunit beta-1	P02091	83.7	29	32.17
Hemoglobin subunit beta-2	P11517	71.4	25	28.04
Hemopexin	P20059	6.7	3	5.06
Heterogeneous nuclear ribonucleoprotein A3	Q6URK4	22.2	3	4.76
Heterogeneous nuclear ribonucleoprotein H2	Q6AY09	9.8	2	2
Heterogeneous nuclear ribonucleoprotein K	P61980	34.1	7	8.04
Heterogeneous nuclear ribonucleoprotein M	Q62826	10	2	3.28
Heterogeneous nuclear ribonucleoprotein Q	Q7TP47	15.2	2	4.05
Heterogeneous nuclear ribonucleoproteins A2/B1	A7VJC2	43.6	4	6.65
Hexokinase-1	P05708	9.4	4	7.37
High mobility group nucleosome-binding domain-containing protein 3	Q66H40	31.6	2	1.01
High mobility group protein B1	P63159	45.6	5	7.11

Name	Uniprot Accession #	% Cov	# of peptides (95%)	Total protscore
Histone H1.2	P15865	68.5	9	17.53
Histone H2A type 1	P02262	69.2	14	12.94
Histone H2A type 2-A	P0CC09	73.1	10	9.76
Histone H2A.Z	P0C0S7	35.9	2	1.31
Histone H2B type 1	Q00715	76.8	21	12.95
Histone H3.3	P84245	78.7	7	8.26
Histone H4	P62804	64.1	5	9.27
Hydroxyacyl-coenzyme A dehydrogenase, mitochondrial	Q9WVK7	40.1	9	12.89
Hydroxymethylglutaryl-CoA lyase, mitochondrial	P97519	13.9	2	4
Hypoxia up-regulated protein 1	Q63617	22.7	13	21.25
Importin subunit beta-1	P52296	2.9	2	2.82
Isocitrate dehydrogenase [NAD] subunit alpha, mitochondrial	Q99NA5	10.9	4	4.92
Isocitrate dehydrogenase [NAD] subunit beta, mitochondrial	Q68FX0	14	2	3.83
Isocitrate dehydrogenase [NADP] cytoplasmic	P41562	13.5	3	3.22
Isocitrate dehydrogenase [NADP], mitochondrial	P56574	38.9	15	26.9
Junction plakoglobin	Q6P0K8	11.5	2	4
Kallikrein-1	P00758	90.8	94	97.53
Kinesin-1 heavy chain	Q2PQA9	11.9	4	5.54
LETM1 and EF-hand domain-containing protein 1, mitochondrial	Q5XIN6	10.2	2	4
Leucine-rich repeat-containing protein 59	Q5RJR8	28.3	5	6.15
L-lactate dehydrogenase A chain	P04642	47.9	7	13.36
L-lactate dehydrogenase B chain	P42123	12	3	4.07
Lon protease homolog, mitochondrial	Q924S5	12.8	2	3.58
Macrophage migration inhibitory factor	P30904	39.1	2	3.59
Macrophage-capping protein	Q6AYC4	28.9	6	10.74
Major vault protein	Q62667	7.4	3	5.62
Malate dehydrogenase, cytoplasmic	O88989	32	11	16.72
Malate dehydrogenase, mitochondrial	P04636	41.1	7	8.92
Malonyl-CoA decarboxylase, mitochondrial	Q920F5	16.9	2	2.89
Mannose-1-phosphate guanyltransferase alpha	Q5XIC1	20.5	3	4.94

Name	Uniprot Accession #	% Cov	# of peptides (95%)	Total protscore
Mesencephalic astrocyte-derived neurotrophic factor	P0C5H9	12.3	4	7.57
Methylcrotonoyl-CoA carboxylase subunit alpha, mitochondrial	Q5I0C3	12	2	4
Methylmalonate-semialdehyde dehydrogenase [acylating], mitochondrial	Q02253	29.7	7	13.71
Mitochondrial 2-oxoglutarate/malate carrier protein	P97700	24.8	3	5.66
Mitochondrial import inner membrane translocase subunit Tim13	P62076	19	2	2
Mitochondrial import receptor subunit TOM22 homolog	Q75Q41	38	2	4
Mitochondrial inner membrane protein (Fragment)	Q3KR86	21.2	8	15.73
Moesin	O35763	22.4	4	6.59
Multiple coagulation factor deficiency protein 2 homolog	Q8K5B3	35.2	2	4
Myosin light chain 3	P16409	27	2	2.14
Myosin light polypeptide 6	Q64119	66.2	6	8
Myosin regulatory light chain RLC-A	P13832	33.1	4	7.44
Myosin regulatory light polypeptide 9	Q64122	17.5	2	3.17
Myosin-10	Q9JLT0	18	7	5.95
Myosin-11 (Fragments)	Q63862	25.5	14	23.09
Myosin-4	Q29RW1	12.4	3	2.25
Myosin-9	Q62812	36.4	54	67.33
Myosin-Ic	Q63355	11.5	2	4.18
N(G),N(G)-dimethylarginine dimethylaminohydrolase 1	O08557	19	2	1.38
NADH dehydrogenase [ubiquinone] 1 alpha subcomplex subunit 10, mitochondrial	Q561S0	26.2	5	5.82
NADH dehydrogenase [ubiquinone] 1 alpha subcomplex subunit 9, mitochondrial	Q5BK63	44.6	13	14.56
NADH dehydrogenase [ubiquinone] flavoprotein 2, mitochondrial	P19234	21.4	4	4.05
NADH dehydrogenase [ubiquinone] iron-sulfur protein 2, mitochondrial	Q641Y2	35.4	7	11.96
NADH-cytochrome b5 reductase 1	Q5EB81	19.7	2	4
NADH-ubiquinone oxidoreductase 75 kDa subunit, mitochondrial	Q66HF1	23.3	8	15.97
Niban-like protein 1	B4F7E8	13.8	4	6.05
Non-specific lipid-transfer protein	P11915	4.6	2	1.59
Nuclease-sensitive element-binding protein 1	P62961	46.6	4	8
Nucleobindin-2	Q9JI85	51.7	14	23.19
Nucleolin	P13383	18.1	2	4.24

Name	Uniprot Accession #	% Cov	# of peptides (95%)	Total protscore
Nucleoside diphosphate kinase B	P19804	34.9	4	7.1
Nucleosome assembly protein 1-like 4	Q5U2Z3	7.3	2	3.44
Obg-like ATPase 1	A0JPJ7	17.2	2	4
Ornithine aminotransferase, mitochondrial	P04182	22.8	5	7.68
Parathymosin	P04550	65.7	5	5.31
Peptidyl-prolyl cis-trans isomerase A	P10111	67.1	16	19.11
Peptidyl-prolyl cis-trans isomerase B	P24368	31.5	3	2.51
Peroxiredoxin-1	Q63716	25.6	3	5.3
Peroxiredoxin-2	P35704	30.3	3	5.63
Peroxiredoxin-5, mitochondrial	Q9R063	41.8	5	9.12
Phenylalanine--tRNA ligase alpha chain	Q505J8	10.6	4	4.47
Phosphate carrier protein, mitochondrial	P16036	22.5	4	5.9
Phosphatidylethanolamine-binding protein 1	P31044	63.1	9	16.84
Phosphoglycerate kinase 1	P16617	27.3	3	5.41
Phosphoglycerate mutase 1	P25113	24	5	7.97
Plasma membrane calcium-transporting ATPase 1	P11505	8.3	2	3.05
Platelet-activating factor acetylhydrolase IB subunit gamma	O35263	23.3	3	5.21
Plectin	P30427	14.2	3	6.96
Polyadenylate-binding protein 1	Q9EPH8	23.9	8	11.17
Polymerase I and transcript release factor	P85125	17.6	2	4
Polypyrimidine tract-binding protein 1	Q00438	14.2	3	3.07
Potassium-transporting ATPase alpha chain 1	P09626	13.8	3	6.13
Prelamin-A/C	P48679	24.4	3	6.06
Pro-epidermal growth factor	P07522	12.4	6	8.64
Profilin-1	P62963	27.9	3	4.49
Programmed cell death 6-interacting protein	Q9QZA2	11	2	4
Prohibitin	P67779	37.5	5	8.69
Prohibitin-2	Q5XIH7	36.5	4	7.01
Prolactin-inducible protein homolog	O70417	40.4	2	4
Propionyl-CoA carboxylase alpha chain, mitochondrial	P14882	14.3	3	4.42

Name	Uniprot Accession #	% Cov	# of peptides (95%)	Total protscore
Propionyl-CoA carboxylase beta chain, mitochondrial	P07633	29	8	11.72
Prostaglandin E synthase 3	P83868	20	2	0.74
Prostatic glandular kallikrein-6	P36374	89.7	58	63.77
Proteasome activator complex subunit 1	Q63797	22.1	3	2.89
Proteasome subunit alpha type-5	P34064	5	2	3.77
Proteasome subunit beta type-2	P40307	19.9	2	3.36
Proteasome subunit beta type-4	P34067	13.3	2	3.62
Protein disulfide-isomerase	P04785	83.3	42	67.96
Protein disulfide-isomerase A3	P11598	53.1	25	34.57
Protein disulfide-isomerase A4	P38659	17.7	5	4.53
Protein disulfide-isomerase A6	Q63081	35	10	11.43
Protein DJ-1	O88767	20.6	2	3.06
Protein ERGIC-53	Q62902	34.2	10	15.84
Protein phosphatase 1 regulatory subunit 1B	Q6J4I0	49.3	7	12
Protein S100-A1	P35467	62.8	7	10.56
Protein S100-A11	Q6B345	52	2	4.18
Protein S100-A6	P05964	66.3	4	0.94
Protein transport protein Sec31A	Q9Z2Q1	9	2	4
Protein-arginine deiminase type-2	P20717	8.4	2	2
Prothymosin alpha	P06302	43.8	8	11.24
Purine nucleoside phosphorylase	P85973	37	5	9.73
Purkinje cell protein 4	P63055	59.7	2	2.62
Putative 60S ribosomal protein L37a	P61515	37	4	4.27
Pyruvate carboxylase, mitochondrial	P52873	12.1	3	6.27
Pyruvate dehydrogenase E1 component subunit alpha, somatic form, mitochondrial	P26284	15.6	2	3.1
Pyruvate dehydrogenase E1 component subunit beta, mitochondrial	P49432	53.2	11	16.73
Pyruvate kinase isozymes M1/M2	P11980	23.2	9	10.36
Rab GDP dissociation inhibitor alpha	P50398	14.3	4	5.4
Rab GDP dissociation inhibitor beta	P50399	24.7	7	10.83
Ras-related protein Rab-11A	P62494	10.7	2	1.62

Name	Uniprot Accession #	% Cov	# of peptides (95%)	Total protscore
Ras-related protein Rab-1A	Q6NYB7	18.5	2	0.56
Ras-related protein Rab-1B	P10536	16.9	2	1.39
Ras-related protein Rab-27A	P23640	24.9	3	3.72
Ras-related protein Rab-27B	Q99P74	12.8	2	2
Ras-related protein Rap-1b	Q62636	20.7	3	4
Retinal dehydrogenase 1	P51647	11	2	1.64
Rho GDP-dissociation inhibitor 1	Q5XI73	50.5	5	6.83
Sarcoplasmic/endoplasmic reticulum calcium ATPase 2	P11507	19.9	3	6.62
Sarcoplasmic/endoplasmic reticulum calcium ATPase 3	P18596	18.2	7	14.71
Scaffold attachment factor B1	O88453	10.2	2	3.48
Serine/threonine-protein phosphatase 2A 65 kDa regulatory subunit A beta isoform	Q4QQT4	8.3	2	4
Serine--tRNA ligase, cytoplasmic	Q6P799	17.2	4	4.97
Serotransferrin	P12346	13.6	7	12.34
Short-chain specific acyl-CoA dehydrogenase, mitochondrial	P15651	17.7	2	2.86
SMR1 protein	P13432	75.3	18	21.5
SMR2 protein	P18897	55.5	12	18.03
Sodium/potassium-transporting ATPase subunit alpha-1	P06685	40.6	49	55.54
Sodium/potassium-transporting ATPase subunit beta-1	P07340	57.2	16	28.16
Sorting nexin-3	Q5U211	11.1	2	2
Spectrin alpha chain, brain	P16086	22.2	17	34.82
Spectrin beta chain, brain 2	Q9QWN8	20.2	6	11.14
Spliceosome RNA helicase Ddx39b	Q63413	16.4	3	3.19
Staphylococcal nuclease domain-containing protein 1	Q66X93	33	14	22.61
STE20-like serine/threonine-protein kinase	O08815	11.7	2	4.02
Stress-70 protein, mitochondrial	P48721	25	11	17.42
Submandibular gland secretory Glx-rich protein CB	P08462	96.8	33	48.41
Submandibular glandular kallikrein-9	P07647	88.4	80	82.53
Succinate dehydrogenase [ubiquinone] flavoprotein subunit, mitochondrial	Q920L2	20.6	9	9.49
Succinate dehydrogenase [ubiquinone] iron-sulfur subunit, mitochondrial	P21913	13.5	4	3.88
Succinate-semialdehyde dehydrogenase, mitochondrial	P51650	7.6	2	4

Name	Uniprot Accession #	% Cov	# of peptides (95%)	Total protscore
Succinyl-CoA ligase [ADP/GDP-forming] subunit alpha, mitochondrial	P13086	33.8	5	9.69
Succinyl-CoA:3-ketoacid-coenzyme A transferase 1, mitochondrial	B2GV06	31.9	7	11.7
Sulfotransferase 1C1	P50237	50.3	9	11.99
Superoxide dismutase [Cu-Zn]	P07632	29.2	3	4.3
Superoxide dismutase [Mn], mitochondrial	P07895	30.2	4	6
Syntaxin-7	O70257	17.2	2	0.69
T-complex protein 1 subunit epsilon	Q68FQ0	22.2	5	10
Thioredoxin	P11232	22.9	2	1.57
Thioredoxin-like protein 1	Q920J4	13.5	2	3.36
Thiosulfate sulfurtransferase	P24329	20.2	3	5.35
Threonine--tRNA ligase, cytoplasmic	Q5XHY5	12.5	2	2.96
Thymosin beta-4	P62329	77.3	9	13.54
Tonin	P00759	74.5	59	68.02
Transaldolase	Q9EQS0	16.9	3	5.75
Transforming protein RhoA	P61589	35.2	4	7.24
Transgelin	P31232	15.4	2	1.05
Transgelin-2	Q5XFX0	57.3	8	8.6
Transitional endoplasmic reticulum ATPase	P46462	35.5	17	26.96
Transketolase	P50137	33.7	6	11.51
Translationally-controlled tumor protein	P63029	48.3	3	5.95
Translocon-associated protein subunit alpha	Q7TPJ0	16.3	6	3.31
Translocon-associated protein subunit gamma	Q08013	21.6	4	4
Transmembrane emp24 domain-containing protein 10	Q63584	41.1	5	6.55
Transmembrane emp24 domain-containing protein 9	Q5I0E7	16.2	4	4.02
Trifunctional enzyme subunit alpha, mitochondrial	Q64428	34.2	18	21.93
Trifunctional enzyme subunit beta, mitochondrial	Q60587	18.3	4	4.4
Triosephosphate isomerase	P48500	14.9	4	6.3
Tripeptidyl-peptidase 1	Q9EQV6	5	4	2.99
Tropomyosin alpha-1 chain	P04692	42.6	9	17.97
Tropomyosin alpha-3 chain	Q63610	39.5	6	11.16

Name	Uniprot Accession #	% Cov	# of peptides (95%)	Total protscore
Tropomyosin beta chain	P58775	44.4	8	15.07
Tubulin alpha-1B chain	Q6P9V9	30.2	20	19.73
Tubulin alpha-1C chain	Q6AYZ1	31.6	19	18.9
Tubulin alpha-4A chain	Q5XIF6	37.7	17	22.46
Tubulin beta-2B chain	Q3KRE8	38	21	29.03
Tubulin beta-4B chain	Q6P9T8	47	23	34.11
Tubulin-specific chaperone A	Q6PEC1	21.3	2	2.58
Tumor protein D54	Q6PCT3	18.6	3	3.01
Ubiquitin-conjugating enzyme E2 variant 2	Q7M767	13.8	2	3.8
Ubiquitin-like modifier-activating enzyme 1	Q5U300	22.9	7	11.55
Ubiquitin-like modifier-activating enzyme 5	Q5M7A4	16.6	3	3.61
UDP-glucose:glycoprotein glucosyltransferase 1	Q9JLA3	8.1	2	3.91
UMP-CMP kinase	Q4KM73	14.8	2	2.6
Vacuolar protein sorting-associated protein 29	B2RZ78	14.8	3	6
Valine--tRNA ligase	Q04462	12.4	5	8.7
Vesicle-trafficking protein SEC22b	Q4KM74	13.5	2	3.55
Vimentin	P31000	23.2	3	5.86
Vinculin	P85972	4.8	2	2.97
Voltage-dependent anion-selective channel protein 1	Q9Z2L0	22.6	3	5.04
V-type proton ATPase subunit B, brain isoform	P62815	15.1	2	3

Supplementary table 2 - Classification of the proteins identified by PANTHER Protein Class. This table lists the PANTHER Protein Classes enriched in the fractions analyzed, with a p-value below 0.05 according to the PANTHER database (www.pantherdb.org)

PANTHER Protein Class	Number of gene hits				
	Rattus norvegicus - reference list (27758)	List of identified proteins (456)	Expected	Over-/ Under-representation in the list of identified proteins	P-value
calcium-binding protein	313	23	5.07	+	6.49E-07
intracellular calcium-sensing protein	197	12	3.19	+	2.11E-02
calmodulin	197	12	3.19	+	2.11E-02
chaperone	262	21	4.25	+	7.13E-07
Hsp70 family chaperone	22	6	.36	+	3.68E-04
cytoskeletal protein	974	46	15.79	+	3.16E-08
actin family cytoskeletal protein	447	29	7.25	+	9.91E-08
actin binding motor protein	60	8	.97	+	1.44E-03
tubulin	22	5	.36	+	6.32E-03
defense/immunity protein	778	1	12.61	-	7.00E-03
enzyme modulator					
G-protein	284	15	4.60	+	1.51E-02
small GTPase	210	12	3.40	+	3.77E-02
isomerase	224	15	3.63	+	1.03E-03
kinase					
amino acid kinase	5	3	.08	+	1.49E-02
protein kinase	658	1	10.67	-	4.40E-02
ligase	502	20	8.14	+	4.83E-02
lyase	178	15	2.89	+	6.42E-05
hydratase	20	7	.32	+	9.71E-06
membrane traffic protein	373	20	6.05	+	8.44E-04
vesicle coat protein	44	9	.71	+	1.17E-05
nucleic acid binding	3434	95	55.67	+	2.41E-05
RNA binding protein	1631	85	26.44	+	3.54E-19
ribosomal protein	777	60	12.60	+	6.92E-21
translation factor	112	10	1.82	+	3.51E-03
oxidoreductase	862	66	13.97	+	5.75E-23
dehydrogenase	305	40	4.94	+	2.61E-21
reductase	229	16	3.71	+	2.97E-04
receptor	1857	4	30.10	-	2.68E-07
G-protein coupled receptor	642	0	10.41	-	4.81E-03
transcription factor	1977	5	32.05	-	3.04E-07
zinc finger transcription factor	671	0	10.88	-	2.97E-03
transfer/carrier protein	470	25	7.62	+	6.41E-05
transporter					
cation transporter	217	15	3.52	+	7.09E-04
ATP synthase	59	9	.96	+	1.32E-04
Unclassified	11977	47	194.17	-	3.47E-50

v. POST-TRANSLATIONAL MODIFICATIONS OF PROLINE-RICH PROTEINS AS BIOMARKERS OF SUSCEPTIBILITY TO ORAL DISEASE

The results presented in this chapter were published as a rapid communication:

Vitorino R, Alves R, Barros A, Caseiro A, Ferreira R, Lobo MC, Bastos A, Duarte J, Carvalho D, Santos LL, Amado FL. Finding new posttranslational modifications in salivary proline-rich proteins. Proteomics. 2010 Oct;10(20):3732-42. doi: 10.1002/pmic.201000261.

1. Introduction

Saliva is a body fluid particularly enriched in several low-molecular weight protein species, where peptides up to 20 kDa represent about 40% of total secreted proteins (Amado, Vitorino et al. 2005). Salivary proline-rich proteins form a protein family that represents approximately 20-30% of salivary protein content and up to 60% of proteins secreted by submandibular and sublingual glands (Levine 2011). Two major subgroups are considered in the PRP family: acidic proline-rich proteins (aPRP) and basic proline-rich proteins (bPRP).

aPRPs have a distinctive 30 amino acids N-terminus rich in aspartate, glutamate, and containing a few serine phosphate residues, giving it acidic properties and are exclusively found in salivary glands secretions (Schenkels, Veerman et al. 1995). This N-terminus binds strongly to recently cleaned teeth surfaces, inducing a conformational change that exposes the C-terminal domain bearing a binding site for bacteria (Elangovan, Margolis et al. 2007). For this reason, it is of particular relevance in the formation of acquired enamel pellicle (Li, Helmerhorst et al. 2004). Acidic PRPs are encoded by two genes *PRH1* and *PRH2*, with 3 and 2 alleles, respectively. These are responsible for up to 18 possible polymorphisms from the possible combinations of the alleles *Db*, *Pa*, *Pif* from *PRH1* gene with the *PRP1* and *PRP2* of the *PRH2* gene (Levine 2011). Besides this variability, the proteins may undergo post-translational processing either by proteolytic cleavage or amino acid modification. The cleavage at Arg^{123} originates the salivary peptides Db-F, Pif-F, PRP-3 and PRP-4, from the N-terminus of Db, Pif, PRP1 and PRP2,

respectively, while the C-terminal fragment is known as peptide P-C. The *Pa* allele form is not proteolytically cleaved. Additionally, phosphorylations of Ser^{24}, Ser^{33}, Ser^{38}, as well as O-linked addition of glucuronic acid on Ser^{33}, were already described (Jonsson, Griffiths et al. 2000; Inzitari, Cabras et al. 2005; The UniProt Consortium 2012).

bPRPs are also found in other glands secretions (Schenkels, Veerman et al. 1995). Although not adhering to teeth, they play an important role binding bacteria and tannins. Because they bind to several oral bacteria, they are important in the protection against dental caries (Vitorino, de Morais Guedes et al. 2006). However, caries-free individuals do not have increased content of bPRPs in whole saliva. Instead, it appears to be less fragmentation (Ayad, Van Wuyckhuyse et al. 2000; Vitorino, Lobo et al. 2005). Binding to tannins indicates that bPRPs also have a role in astringency. Interestingly, larger bPRPs have higher affinity to bind tannins than smaller bPRPs (Charlton, Baxter et al. 1996). This is of particular importance as individuals lacking larger forms of bPRPs tend to follow a sucrose-rich diet, because sucrose reduces the astringency feeling but further increases the risk of developing caries (Ishikawa and Noble 1995; Levine 2011). These proteins are encoded by four genes *PRB1*, *PRB2*, *PRB3* and *PRB4*. Greater allele variations, in addition to alternative splice variants, proteolytic cleavage and post-translational modifications, is responsible for the large number of bPRPs found (Maeda, Kim et al. 1985; Levine 2011). Splice variants of the different alleles originates several proteins with deletions in certain areas of the primary sequence. bPRP1 has deletions of amino acids 93-153 in allele M, 106-319 in clone CP5, 106-299 in clone CP-4, 134-255 in allele S; bPRP3 has a deletion of amino acids 158-220 in allele S; and bPRP4 has deletions of 113-154 in allele M and 113-154 plus 164-184 in allele S (Maeda, Kim et al. 1985; The UniProt Consortium 2012>Entries P04280, P02812, Q04118 and P10163). Proteolytic cleavage may occur before secretion during granule maturation (Messana, Cabras et al. 2008), and originates peptides II-2, IB-6 and P-H from bPRP1; IB-1, IB-4, IB-7, IB-8c and PE from bPRP2; and

protein N1, glycosylated protein A and peptide P-D from bPRP4 (Kauffman, Bennick et al. 1991; Vitorino, Barros et al. 2009; The UniProt Consortium 2012). Like aPRPs, bPRPs may undergo amino acid post-translational modifications. Glycosylation is one of the major modifications detected in bPRPs, suggesting they have a role in oral lubrication (Hatton, Loomis et al. 1985). Moreover, phosphorylation and conversion of N-terminal Gln residues to pyroglutamate were also detected (Inzitari, Cabras et al. 2005).

Thus, it is clear that both acidic and basic proline-rich proteins are essential in the maintenance of oral health, but the presence or absence of certain PTMs may enhance or reduce such properties. As diabetic patients have higher incidence of oral complications, this study proposes to apply state of the art mass spectrometry techniques to identify novel PTMs in salivary PRPs and compare their frequency against control individuals. Because alterations in glycosylation are common biomarkers in cancer, a group of head and neck cancer patients was also analysed.

2. Methods

2.1. Sample collection

Unstimulated whole saliva from 20 individuals (aged 23-54) was collected at 10:00 a.m. by direct draining into a saliva collection tube, after a fasting period of at least 2 hours. The donors were grouped, according to their clinical evaluation, in diabetic (T1DM) – 5 individuals with type 1 DM; head and neck cancer (HNC) – 10 individuals with head and neck cancer not undergoing radiation treatment; and control (C) – 5 individuals with no evidence of oral pathologies or inflammation. This study was approved by the local ethics committee and all participating individuals gave their informed consent.

2.2. Sample preparation

Salivary peptide isolation was performed as described by Vitorino, Barros et al. (2009). Protease activity was blocked with the addition of 10 µl of PMSF 0.1 M, 1 µl of peptstatin 1 mM and 20 µl of anti-protease

cocktail (aprotinin, E-64, EDTA, AEBSF and leupeptin)(P2714, Sigma, USA) to 1 ml of whole saliva. Samples were acidified with 0.2% trifluoracetic acid (TFA) in a proportion 1:1 and centrifuged at 12,000x *g*, 30 min, 4ºC, to remove bacteria, insoluble material and precipitated protein. Next, samples were filtered through a sequence of filters with cut-offs of 100 kDa, 50 kDa and 10 kDa (Centricom, Millipore, USA).

Peptide enriched fractions were separated by nano-LC using an Ultimate 3000 (Dionex, Thermo Fisher Scientific, USA) onto a 150 mm x 75 μm Pepmap100 capillary analytical C18 column with a 3 μm particle size (Dionex, Thermo Fisher Scientific, USA) at a flow rate of 300 nl/min. A linear gradient of 5% to 50% of buffer B (85% ACN, 5% 2-propanol, 0.04% TFA) was run over a period of 35 minutes. Peptides eluted from the capillary column were mixed with a continuous flow of alpha-CHCA matrix solution (270 nl/min, 2 mg/ml in 70% ACN/0.1% TFA and internal standard Glu-Fib at 15 fmol) and were directly deposited onto a LC-MALDI plate at 20 second intervals for each spot (100 nl/fraction). For every separation run, 156 fractions were collected.

2.3. Mass spectrometry analysis

MALDI-TOF/TOF MS analysis was performed using a 4800 MALDI-TOF/TOF Analyser (Applied Biosystems, USA). A signal-to-noise ratio threshold of 50 was applied to select peaks for MS/MS analyses. A fragmentation voltage of 2 kV was used throughout the automatic runs. Spectra were processed and analysed with the Global Protein Server (GPS) Workstation (Applied Biosystems, USA), which uses an internal MASCOT software (v.2.1.0.4, Matrix Science, UK) for protein/peptide identification based on peptide mass fingerprints and MS/MS data.

An initial search was performed against the SwissProt database (March 2009, 428,650 entries) for Homo sapiens. An MS tolerance of 30 ppm was considered for precursor ions and of 0.3 Da for fragment ions.

Protein identifications were considered reliable if the MASCOT score was >70.

For post-translation modifications (PTM) analyses, spectra were reprocessed against an internal database including all PRP variants as described in literature (Stubbs, Chan et al. 1998) and Uniprot (Apweiler, Bairoch et al. 2004). In order to estimate the false positive rate (FDR) and considering the repetitive PRP motif, a random decoy database was created for all SwissProt and internal database entries, resulting in 12% and 5% of FDR, respectively. Unique peptides from FDR search were considered for PTM characterization. The PTMs used in the search are listed in Table 4. The presence of the PTM was considered reliable when the program indicated a significant MASCOT score and the ion score was above 20. Each PTM was then validated by the manual analysis of spectra through the analysis of a, b and/or y fragmentation ions series.

Table 4 – List of post-translational modifications searched in the GPS workstation.

Modification	Monoisotopic mass variation (Da)
Galactosyl (K)	178,05
Glucosylgalactosyl (K)	340,10
dHex (S)	146,06
Hex (N-term)	162,05
HexNAc (S,N)	203,08
Phospho (S; T; Y)	79,97
Pro->pyro-Glu (Pyroglutamic) (P)	13,98
Gln->pyro-Glu (N-term-Q)	-17,03
Glucuronyl (S)	17,60
Sulfo (Sulfation) (S; T; Y)	79,96
Nmethylmaleimide (K)	111,03
Oxidation (K, R, P, G, C, H, F, V, L, N)	15,99
Dioxidation (K, R, P, G, C, H, F, V, L, N)	31,99
Pro to pyrrolidone	-27,99
Pro to pyro-Glu	-30,01

2.4. Statistical analysis

Statistical analysis of frequency tables was performed using GraphPad Prism v5.00 (GraphPad Software, Inc., USA). An one-way ANOVA analysis followed by the Tukey-Kramer test to all the column pairs was used. A p value <0.05 was considered significant.

3. Results

A total of 1391 fragments from proline-rich proteins were identified. The more represented family was aPRPs with 498 fragments, while bPRP1, bPRP2, bPRP3 and bPRP4 had 334, 298, 122 and 139 fragments identified, respectively (Figure 25). The mining for 38 different PTMs (Table 4), allowed the identification of 69 unique peptides with 12 different modifications mainly due to glycosylation, phosphorylation and conversion of N-terminal Gln to pyroglytamate.

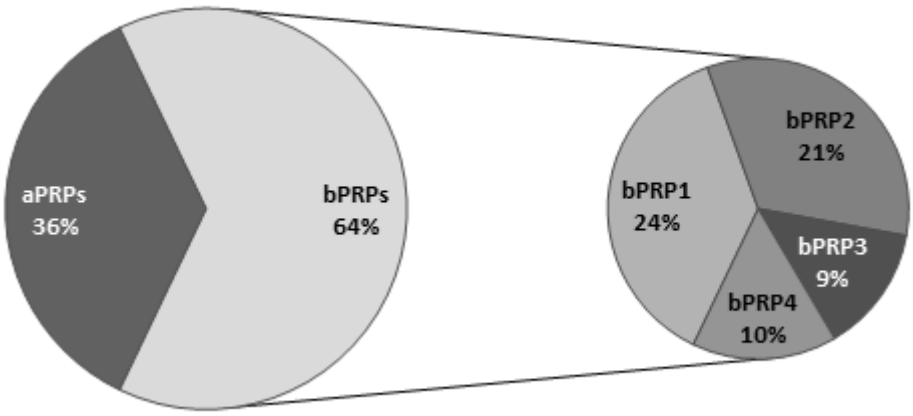

Figure 25 – Distribution of the identified fragments by the several proline-rich proteins.

All PRPs presented at least one phosphorylated Ser residue, with the exception of bPRP4, but aPRPs presented the higher number of phosphopeptides (Table 5). Apart from the already identified phosphorylated residues in Uniprot, a survey for potential phosphorylation sites was conducted using NetPhos v2.0 (Blom,

Gammeltoft et al. 1999) (Supplementary table 1). So, in addition to the already described phosphorylation of Ser^{8} from bPRP1, we have identified the phosphorylation of Ser^{134} from bPRP2 and Ser^{8} from bPRP3 (Figure 26). In aPRPs, despite the high number of phosphorylated peptides identified, all contained the same phosphorylated residue: Ser^{22}.

Table 5 – List of peptides found with post-translational modifications. (*) denotes modifications presently indicated in Uniprot and attributed after the publication this study (Vitorino, Alves et al. 2010).

Specie (Uniprot acession number)	Sequence	Residue Modified	Modification	Nº Individuals (20)	Group (Nº Individual)		
					Control (5)	Diabetes (5)	Cancer (10)
bPRP1 (P04280)	PGKPQGPPAQGGS	Ser314*	HexNAc (S)[13]	7	1	1	5
	GPPPQGGNKPQGPPPPGKPQGPPPQGDKSR	Ser71*	HexNAc (S)[29]	3	0	1	2
	GPPPPGKPQGPPPQGDKSR	Ser71*	HexNAc (S)[18]	7	2	1	4
	GKPQGPPPQGDKSQS	Ser134*	dHex (S)[15]	4	1	2	1
	SPQGGNKPQGPPPPPGKPQ	Ser24*	Hex (S)[1]	1	0	0	1
	GPPPPGKPQGPPPQGDKS	Lys70	Glucosylgalactosyl (K)[17]	3	0	0	3
	KPQGPPPQGDKSQSPRSPPGK	Lys131	Galacotsyl (K)[11]	3	0	0	3
	GPPPQGGNKPQGPPPPGKPQGPPPQGDKS	Lys70	Glucosylgalactosyl (K)[28]	4	0	1	3
	GPPPQGGNKPQGPPPPGKPQGPPAQGGSKS	Lys313	Glucosylgalactosyl (K)[29]	4	0	1	3
	QGGNKPQGPPPPPGKPQ	Gln25	Gln->pyro-Glu (N-term Q)[0]	9	2	2	5
	QNLNEDVSQEESPSLIAGNPQGPSPQGGNKPQ	Gln1*,Ser8*	Gln->pyro-Glu (N-term Q)[0], Phospho (ST)[8]	3	0	1	2
	PQGPPPQGDKSRSPRSPPGKPQ	Ser76*	Phospho (ST)[16]	6	3	2	1
	QGPPPQGDKSQSPRSPPGKPQGPPPQ	Ser134*	Phospho (ST)[12]	6	3	1	2
bPRP2 (P02812)	GPPPQGGNKSQGPPPPGKPQ	Asn256*	HexNAc (N)[8]	5	0	0	5
	GPPPPGKPQGPPPQGDNKSQ	Asn214*	HexNAc (N)[17]	6	1	1	4
	GPPPQGDNKSQSARSPPGKPQ	Asn214*	HexNAc (N)[8]	2	0	0	2
	GPPPPGKPQGPPPQGDNKSQ	Ser232*	dHex (S)[19]	4	0	2	2
	GPPPQGGNKPQGPPPPGKPQGPPPQGDKS	Lys107	Glucosylgalactosyl (K)[28]	2	0	0	2
	QPQGPPRPPQ	Gln397	Gln->pyro-Glu (N-term Q)[0]	4	1	2	1
	QGPPRPPQGGRPS	Gln399	Gln->pyro-Glu (N-term Q)[0]	8	2	2	4
	QAPPAGQPQGPPRPPQ	Gln391	Gln->pyro-Glu (N-term Q)[0]	6	2	3	1
	QGGNQPQGPPPPPGKPQ	Gln62	Gln->pyro-Glu (N-term Q)[0]	6	1	1	4

Specie (Uniprot acession number)	Sequence	Residue Modified	Modification	Nº Individuals (20)	Group (Nº Individual)		
					Control (5)	Diabetes (5)	Cancer (10)
	QPQAPPAGQPQGPPRPPQ	Gln389	Gln->pyro-Glu (N-term Q)[0]	2	0	0	2
	QGGNQPQGPPPPPGKPQGPPPQGGNKPQ	Gln62	Gln->pyro-Glu (N-term Q)[0]	5	0	4	1
	QQEGNNPQGPPPPAGGNPQQPQAPPAGQPQGPPRPP	Gln370	Gln->pyro-Glu (N-term Q)[0]	1	0	0	1
	QEESPSLIAGNPQGAPPQGGNKPQGPPSP	Ser36*	Phospho (ST) (S)[36]	6	3	1	2
bPRP3 (Q04118)	KPQGPPPQEGNKPQ	Asn239*	Hex (N)[11]	5	1	1	3
	GPPPRPGKPEGPPPQGGNQS	Ser72*	dHex (S)[20]	6	2	3	1
	SQGPPPRPGKPEGPPPQGGNQ	Asn71	HexNAc (N)[20]	6	1	1	4
	QPLPPPAGKPQ	Gln277	Gln->pyro-Glu (N-term Q)[0]	6	1	4	1
	QGPPPRPGKPE	Gln47	Gln->pyro-Glu (N-term Q)[0]	3	0	2	1
	QSQGPPPRPGKPE	Gln45	Gln->pyro-Glu (N-term Q)[0]	11	2	4	5
	QGGRPHRPPQGQPP	Gln294	Gln->pyro-Glu (N-term Q)[0]	5	2	2	1
	QGGRPHRPPQGQPPQ	Gln294	Gln->pyro-Glu (N-term Q)[0]	6	2	3	1
	QSQGPPPRPGKPEGSPS	Gln213	Gln->pyro-Glu (N-term Q)[0]	3	0	2	1
	QSQGPPPRPGKPEGQPPQ	Gln66	Gln->pyro-Glu (N-term Q)[0]	6	2	3	1
	QSLNEDVSQEESPSVISGKPEGR	Gln1*	Gln->pyro-Glu (N-term Q)[0]	3	0	1	2
	QSLNEDVSQEESPSVISGKPEGR	Gln1*,Ser8*	Gln->pyro-Glu (N-term Q)[0], Phospho (ST)[8]	4	0	2	2
bPRP4 (P10163)	GPPPPPGKPEGRPPQGGNQ	Asn71*	HexNAc (N)[18]	8	2	2	4
	QRPPPPP	Gln32	Gln->pyro-Glu (N-term Q)[0]	2	0	0	2
	QPQRPPPPP	Gln30	Gln->pyro-Glu (N-term Q)[0]	6	0	2	4
	QGPPPHPGKPE	Gln74	Gln->pyro-Glu (N-term Q)[0]	6	1	4	1
	QGPPPPPQGGRPP	Gln272	Gln->pyro-Glu (N-term Q)[0]	1	0	0	1
	QSQGPPPHPGKPE	Gln72	Gln->pyro-Glu (N-term Q)[0]	4	0	1	3
	QSHRPPPPPGKPE	Gln177	Gln->pyro-Glu (N-term Q)[0]	2	0	0	2
	QSQGPPPPPGKPEGRPP	Gln51	Gln->pyro-Glu (N-term Q)[0]	3	1	1	1
	QSQGPPPHPGKPERPPP	Gln72	Gln->pyro-Glu (N-term Q)[0]	1	0	0	1
	QSQGPPPHPGKPEGPPPQ	Gln197	Gln->pyro-Glu (N-term Q)[0]	1	0	0	1
	QSQGPPPHPGKPEGPPPQEGNKS	Gln197	Gln->pyro-Glu (N-term Q)[0]	1	0	0	1
	QSQGPPPHPGKPEGPPPQEGNKSR	Gln197	Gln->pyro-Glu (N-term Q)[0]	2	0	0	2
aPRP (P02810)	DSEQFIDEER	Ser22*	Glucuronyl (S)[2]	5	2	2	1
	DSEQFIDEERQGPPLGGQQSQPS	Ser22*	Glucuronyl (S)[2]	6	3	2	1

Specie (Uniprot acession number)	Sequence	Residue Modified	Modification	Nº Individuals (20)	Group (Nº Individual)		
					Control (5)	Diabetes (5)	Cancer (10)
	DSEQFIDEERQGPPLGGQQ	Ser22*	Glucuronyl (S)[2]	6	3	2	1
	GGDSEQFIDEER	Ser22	Phospho (ST) (S)[4]	16	4	2	10
	DGGDSEQFIDEER	Ser22	Phospho (ST) (S)[5]	12	4	4	4
	GGDSEQFIDEERQ	Ser22	Phospho (ST) (S)[4]	11	4	3	4
	DGGDSEQFIDEERQ	Ser22	Phospho (ST) (S)[5]	8	2	4	2
	VISDGGDSEQFIDEER	Ser22	Phospho (ST) (S)[8]	1	0	0	1
	GGDSEQFIDEERQGPPL	Ser22	Phospho (ST) (S)[4]	7	2	4	1
	VISDGGDSEQFIDEERQ	Ser22	Phospho (ST) (S)[8]	1	0	0	1
	GGDSEQFIDEERQGPPLG	Ser22	Phospho (ST) (S)[4]	4	1	2	1
	GGDSEQFIDEERQGPPLGG	Ser22	Phospho (ST) (S)[4]	17	3	5	9
	GGDSEQFIDEERQGPPLGGQ	Ser22	Phospho (ST) (S)[4]	9	1	4	4
	DVPLVISDGGDSEQFIDEER	Ser22	Phospho (ST) (S)[12]	4	0	2	2
	GGDSEQFIDEERQGPPLGGQQ	Ser22	Phospho (ST) (S)[4]	15	5	4	6
	DGGDSEQFIDEERQGPPLGGQQ	Ser22	Phospho (ST) (S)[5]	9	1	4	4
	GGDSEQFIDEERQGPPLGGQQSQPS	Ser22	Phospho (ST) (S)[4]	7	2	4	1
	VISDGGDSEQFIDEERQGPPLGGQQ	Ser22	Phospho (ST) (S)[8]	3	0	2	1
	DGGDSEQFIDEERQGPPLGGQQSQPS	Ser22	Phospho (ST) (S)[5]	4	1	2	1

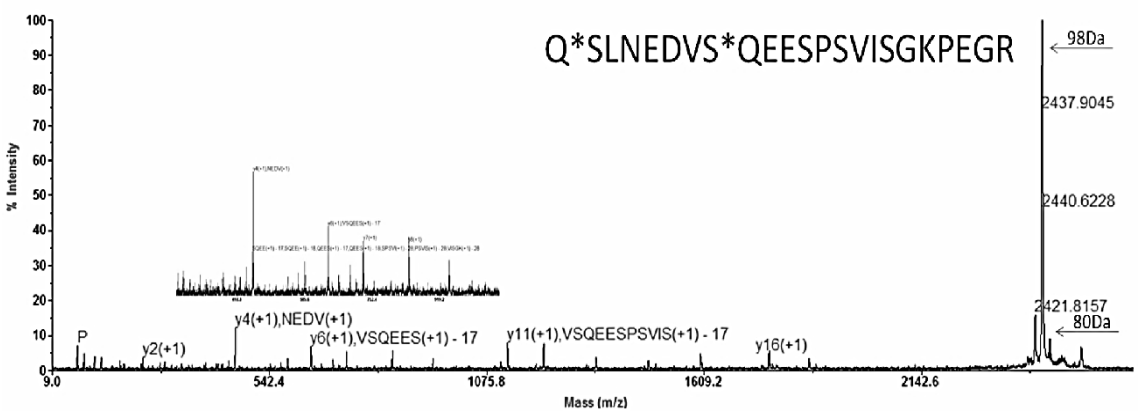

Figure 26 – Representative MS/MS spectrum of a peptide with m/z 2535.11 from bPRP3. Phosphorylation of Ser[8] and simultaneous cyclization of N-terminal Gln[1] to pyroglutamate may be observed in the fragmentation pattern.

Along with phosphorylation, a special emphasis was also given to glycosylation. It was possible to identify 21 unique peptides containing monosaccharide units in bPRPs fragments. Most of the glycosylated peptides contained Ser O-glycosylation or Asn N-glycosylation to N-acetyl hexosamine (HexNAc). As in phosphorylation, bioinformatics prediction of glycosylation sites was also conducted with YinOYang v1.2 (Gupta and Brunak 2002) and NetNGlyc v1.0 (Gupta, Jung et al. 2004), revealing several potential glycosylation sites: three on bPRP2, eight on bPRP3 and eight on bPRP4. It was detected N-HexNAc at Asn^{214} and Asn^{256} (Figure 27) on bPRP2, Asn^{71} on bPRP3 and Asn^{71} on bPRP4; on bPRP1, only O-HexNAc on Ser^{71} (Figure 27) and Ser^{314} was detected (Table 5). The losses of terminal sugars fucose or hexose were also identified in some fragments by the neutral-loss of 146 Da and 162 Da, respectively, on residues Ser^{24} and Ser^{134} from bPRP1, Ser^{232} from bPRP2 and Ser^{232} and Asn^{239} from bPRP3. The PTM mining also allowed the identification of numerous bPRPs fragments with cyclisation of N-terminal Gln to pyroglutamate (Table 5 and Figure 26).

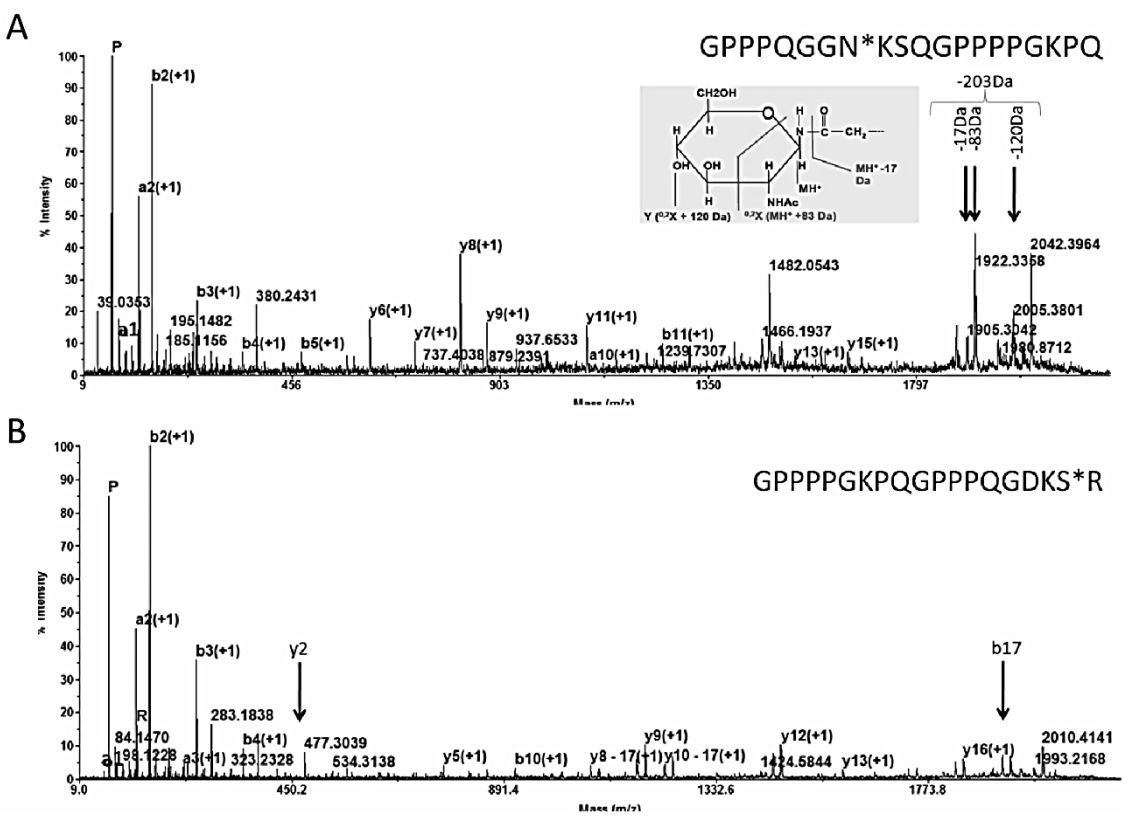

Figure 27 – Representative MS/MS spectra of glycosylated bPRP fragments.
A: Identification of N-HexNAc at Asn^{256} in a peptide with m/z 2125.04 from bPRP2. B: Identification of O-HexNAc at Ser^{71} in a peptide with m/z 2097.08 from bPRP1.

Regarding the frequency of the PTMs in each group, modifications were grouped in O-glycosylation, N-glycosylation, Gln->pyroGlu, phosphorylation and both O- and N-HexNAc for their apparently high occurrence. The distribution of frequencies in each group is graphically presented in (Figure 28) as box and whiskers Tukey plots, which allow the visualization of outliers. Significant increased frequencies were found for N-glycosylation and O-/N-HexNAc in cancer patients, while diabetic patients had a very significant increase in the frequency of N-terminal cyclised fragments (Figure 28).

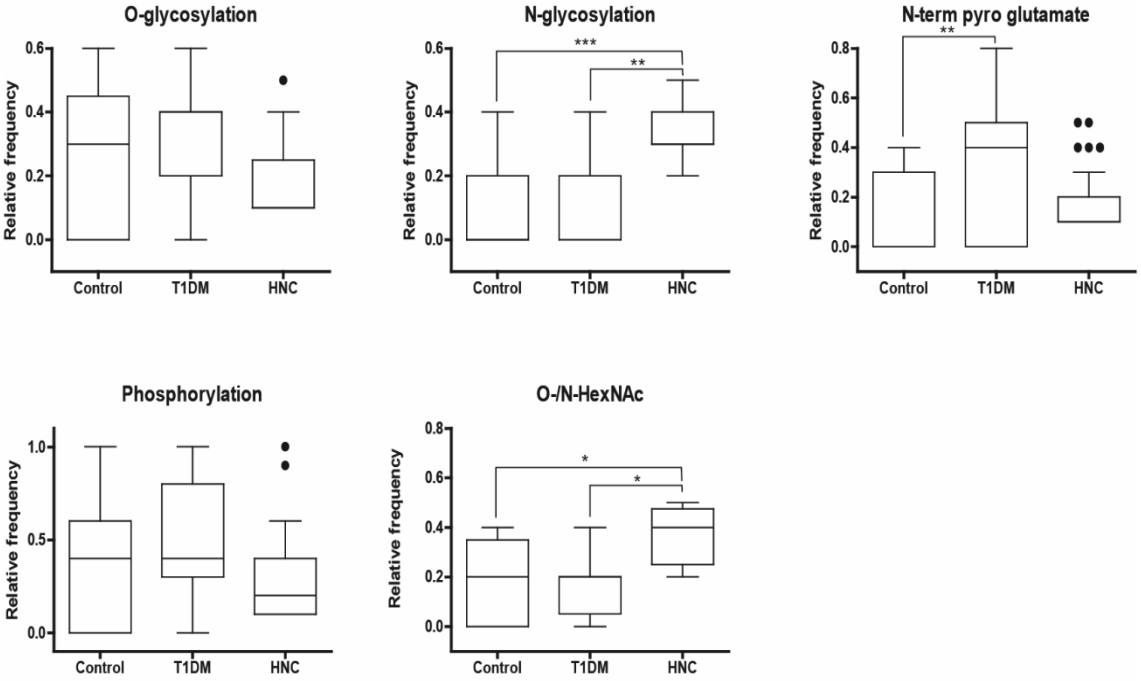

Figure 28 – Frequency distribution of selected PTMs in control, diabetic (T1DM) and head and neck cancer (HNC) patients.

4. Discussion

There is a direct link between diabetes and oral pathologies, being diabetic patients more susceptible to periodontal diseases (Lakschevitz, Aboodi et al. 2011). Proline-rich proteins, not only are one of the major family of proteins found in saliva, but have been suggested to play important roles in oral protection against demineralization and bacteria responsible for dental caries (Vitorino, Lobo et al. 2005; Vitorino, Calheiros-Lobo et al. 2006; Vitorino, de Morais Guedes et al. 2006). The protective role of PRP is directly associated to their ability to adhere to the teeth surface and to bind bacterial antigens. These properties depend of two main factors: proteolytic cleavage of PRPs and post-translational modification of amino acid residues.

Acidic PRPs strongly interact with calcium in a phosphorylation-dependant manner, so it has been proposed that they play a role in keeping Ca^{2+} and PO_4^{2-} ions supersaturate in saliva, preventing hydroxyapatite precipitation (Moreno, Varughese et al. 1979;

Moreno and Zahradnik 1979; Bennick, Cannon et al. 1981). Moreover, because the N-terminus binds to teeth surface and the C-terminus binds to antigens on the surface of bacteria, they have been implied in the formation of enamel pellicle (Vitorino, Lobo et al. 2005). In accordance, it was observed a high number of aPRPs phosphopeptides. bPRPs phosphorylated fragments were identified for the first time on residues Ser^{134} of bPRP2 and Ser^{8} of bPRP3. Despite that, no significant differences were found among groups (Figure 28 and Table 5).

Regarding the glycosylation of bPRPs, several residues were also identified, for the first time, linked to carbohydrate moieties (Table 5). Interestingly, it was observed a significant increase of the frequency of O-/N-HexNAc in cancer patients, which is in agreement with the observed accumulation of O-GlcNAcylation in other types of cancer, such as lung cancer (Satomaa, Heiskanen et al. 2009). Salivary proteins glycosylation is linked to the lubricant properties of saliva, which would seem contradictory with the results presented herein, as diabetic patients frequently complaint of reduction in oral lubrication. However, unstimulated saliva is mainly secreted by submandibular glands, whereas bPRPs are mainly secreted by parotid glands, suggesting that lubrication is not on the main functions attributed to bPRPs.

An interesting finding was the significantly higher frequency of fragments with N-terminal Gln residues cyclized to pyroglutamate. This modification is performed enzymatically by glutaminyl cyclase and has been suggested to have a protective role against proteolytic activity (Schilling, Wasternack et al. 2008; Rink, Arkema-Meter et al. 2010). Diabetic patients were shown to have increased proteolytic activity in saliva, namely by matrix-metalloproteases (MMPs), but also by kallikrein 1, whose PRPs have long been described as a substrate (Wong, Madapallimattam et al. 1983; Caseiro, Ferreira et al. 2012). Moreover, it was also described a significant increase of N-terminal pyroglutamate-bearing peptides from all PRPs in type 1 diabetes with complications (Caseiro, Ferreira et al. 2013). As such, one may conclude

that the increased proteolytic activity will increase the relative amount of N-terminal pyroglutamate-bearing peptides, by degrading unmodified peptides. This will certainly contribute to diminish the protective functions of PRP, as their size is intimately linked to their ability to regulate astringency and may lead patients to follow a cariogenic diet (Charlton, Baxter et al. 1996).

In conclusion, this study presented the discovery of several modified residues in salivary PRPs never described before, as well as an enrichment of fragments protected against proteolytic activity in diabetic patients, probably as a result of the degradation of unprotected peptides through the increased proteolytic activity of saliva.

5. References

Amado, F. M., R. M. Vitorino, P. M. Domingues, M. J. Lobo and J. A. Duarte (2005). "Analysis of the human saliva proteome." Expert Rev Proteomics **2**(4): 521-539.

Apweiler, R., A. Bairoch, C. H. Wu, W. C. Barker, B. Boeckmann, S. Ferro, E. Gasteiger, H. Huang, R. Lopez, M. Magrane, M. J. Martin, D. A. Natale, C. O'Donovan, N. Redaschi and L. S. Yeh (2004). "UniProt: the Universal Protein knowledgebase." Nucleic Acids Res **32**(Database issue): D115-119.

Ayad, M., B. C. Van Wuyckhuyse, K. Minaguchi, R. F. Raubertas, G. S. Bedi, R. J. Billings, W. H. Bowen and L. A. Tabak (2000). "The association of basic proline-rich peptides from human parotid gland secretions with caries experience." J Dent Res **79**(4): 976-982.

Bennick, A., M. Cannon and G. Madapallimattam (1981). "Factors affecting the adsorption of salivary acidic proline-rich proteins to hydroxyapatite." Caries Res **15**(1): 9-20.

Blom, N., S. Gammeltoft and S. Brunak (1999). "Sequence and structure-based prediction of eukaryotic protein phosphorylation sites." J Mol Biol **294**(5): 1351-1362.

Caseiro, A., R. Ferreira, A. Padrao, C. Quintaneiro, A. Pereira, R. Marinheiro, R. Vitorino and F. Amado (2013). "Salivary Proteome and Peptidome Profiling in Type 1 Diabetes Mellitus Using a Quantitative Approach." J Proteome Res.

Caseiro, A., R. Ferreira, C. Quintaneiro, A. Pereira, R. Marinheiro, R. Vitorino and F. Amado (2012). "Protease profiling of different biofluids in type 1 diabetes mellitus." Clinical Biochemistry **45**(18): 1613-1619.

Charlton, A. J., N. J. Baxter, T. H. Lilley, E. Haslam, C. J. McDonald and M. P. Williamson (1996). "Tannin interactions with a full-length human salivary proline-rich protein display a stronger affinity than with single proline-rich repeats." FEBS Lett **382**(3): 289-292.

Elangovan, S., H. C. Margolis, F. G. Oppenheim and E. Beniash (2007). "Conformational changes in salivary proline-rich protein 1 upon adsorption to calcium phosphate crystals." Langmuir **23**(22): 11200-11205.

Gupta, R. and S. Brunak (2002). "Prediction of glycosylation across the human proteome and the correlation to protein function." Pac Symp Biocomput: 310-322.

Gupta, R., E. Jung and S. Brunak. (2004). "NetNGlyc 1.0 Server." from http://www.cbs.dtu.dk/services/NetNGlyc/.

Hatton, M. N., R. E. Loomis, M. J. Levine and L. A. Tabak (1985). "Masticatory lubrication. The role of carbohydrate in the lubricating property of a salivary glycoprotein-albumin complex." Biochem J **230**(3): 817-820.

Inzitari, R., T. Cabras, G. Onnis, C. Olmi, A. Mastinu, M. T. Sanna, M. G. Pellegrini, M. Castagnola and I. Messana (2005). "Different isoforms and post-translational modifications of human salivary acidic proline-rich proteins." Proteomics **5**(3): 805-815.

Ishikawa, T. and A. C. Noble (1995). "Temporal perception of astringency and sweetness in red wine." Food Quality and Preference **6**(1): 27-33.

Jonsson, A. P., W. J. Griffiths, P. Bratt, I. Johansson, N. Stromberg, H. Jornvall and T. Bergman (2000). "A novel Ser O-glucuronidation in acidic proline-rich proteins identified by tandem mass spectrometry." FEBS Lett **475**(2): 131-134.

Kauffman, D. L., A. Bennick, M. Blum and P. J. Keller (1991). "Basic proline-rich proteins from human parotid saliva: relationships of the covalent structures of ten proteins from a single individual." Biochemistry **30**(14): 3351-3356.

Lakschevitz, F., G. Aboodi, H. Tenenbaum and M. Glogauer (2011). "Diabetes and periodontal diseases: interplay and links." Curr Diabetes Rev **7**(6): 433-439.

Levine, M. (2011). "Susceptibility to Dental Caries and the Salivary Proline-Rich Proteins." Int J Dent **2011**.

Li, J., E. J. Helmerhorst, R. F. Troxler and F. G. Oppenheim (2004). "Identification of in vivo pellicle constituents by analysis of serum immune responses." J Dent Res **83**(1): 60-64.

Maeda, N., H. S. Kim, E. A. Azen and O. Smithies (1985). "Differential RNA splicing and post-translational cleavages in the human salivary proline-rich protein gene system." J Biol Chem **260**(20): 11123-11130.

Messana, I., T. Cabras, E. Pisano, M. T. Sanna, A. Olianas, B. Manconi, M. Pellegrini, G. Paludetti, E. Scarano, A. Fiorita, S. Agostino, A. M. Contucci, L. Calo, P. M. Picciotti, A. Manni, A. Bennick, A. Vitali, C. Fanali, R. Inzitari and M. Castagnola (2008). "Trafficking and postsecretory events responsible for the formation of secreted human salivary peptides: a proteomics approach." Mol Cell Proteomics **7**(5): 911-926.

Moreno, E. C., K. Varughese and D. I. Hay (1979). "Effect of human salivary proteins on the precipitation kinetics of calcium phosphate." Calcif Tissue Int **28**(1): 7-16.

Moreno, E. C. and R. T. Zahradnik (1979). "Demineralization and remineralization of dental enamel." J Dent Res **58**(Spec Issue B): 896-903.

Rink, R., A. Arkema-Meter, I. Baudoin, E. Post, A. Kuipers, S. A. Nelemans, M. H. Akanbi and G. N. Moll (2010). "To protect peptide pharmaceuticals against peptidases." J Pharmacol Toxicol Methods **61**(2): 210-218.

Satomaa, T., A. Heiskanen, I. Leonardsson, J. Angstrom, A. Olonen, M. Blomqvist, N. Salovuori, C. Haglund, S. Teneberg, J. Natunen, O. Carpen and J. Saarinen (2009). "Analysis of the human cancer glycome identifies a novel group of tumor-associated N-acetylglucosamine glycan antigens." Cancer Res **69**(14): 5811-5819.

Schenkels, L. C. P. M., E. C. I. Veerman and A. V. Nieuw Amerongen (1995). "Biochemical Composition of Human Saliva in Relation To Other Mucosal Fluids." Critical Reviews in Oral Biology & Medicine **6**(2): 161-175.

Schilling, S., C. Wasternack and H. U. Demuth (2008). "Glutaminyl cyclases from animals and plants: a case of functionally convergent protein evolution." Biol Chem **389**(8): 983-991.

Stubbs, M., J. Chan, A. Kwan, J. So, U. Barchynsky, M. Rassouli-Rahsti, R. Robinson and A. Bennick (1998). "Encoding of human basic and glycosylated proline-rich proteins by the PRB gene complex and proteolytic processing of their precursor proteins." Arch Oral Biol **43**(10): 753-770.

The UniProt Consortium (2012). "Reorganizing the protein space at the Universal Protein Resource (UniProt)." Nucleic Acids Res **40**(D1): D71-D75.

Vitorino, R., R. Alves, A. Barros, A. Caseiro, R. Ferreira, M. C. Lobo, A. Bastos, J. Duarte, D. Carvalho, L. L. Santos and F. L. Amado (2010). "Finding new posttranslational modifications in salivary proline-rich proteins." Proteomics **10**(20): 3732-3742.

Vitorino, R., A. Barros, A. Caseiro, P. Domingues, J. Duarte and F. Amado (2009). "Towards defining the whole salivary peptidome." Proteomics Clinical Applications **3**(5): 528-540.

Vitorino, R., M. J. Calheiros-Lobo, J. A. Duarte, P. Domingues and F. Amado (2006). "Salivary clinical data and dental caries susceptibility: is there a relationship?" Bull Group Int Rech Sci Stomatol Odontol **47**(1): 27-33.

Vitorino, R., S. de Morais Guedes, R. Ferreira, M. J. Lobo, J. Duarte, A. J. Ferrer-Correia, K. B. Tomer, P. M. Domingues and F. M. Amado (2006). "Two-dimensional electrophoresis study of in vitro pellicle formation and dental caries susceptibility." Eur J Oral Sci **114**(2): 147-153.

Vitorino, R., M. J. Lobo, J. R. Duarte, A. J. Ferrer-Correia, P. M. Domingues and F. M. Amado (2005). "The role of salivary peptides in dental caries." Biomed Chromatogr **19**(3): 214-222.

Wong, R. S., G. Madapallimattam and A. Bennick (1983). "The role of glandular kallikrein in the formation of a salivary proline-rich protein A by cleavage of a single bond in salivary protein C." Biochem J **211**(1): 35-44.

6. Supplementary table

Supplementary table 1 – Detailed listing of the modified fragments identified with indication of prediction sites retrieved from bioinformatics analysis.

Specie (Uniprot acession number)	Sequence	Calc Mass	Obs Mass	Match Error Da	Match Error PPM	Start Seq Pos	Residue Modified	End Seq Pos	Modification	Ion Score (C.I.%)	Nº Individuals (20)	Group (Nº Individual) Cancer (10)	Diabetes (5)	Control (5)	Uniprot indication	Prediction site
bPRP1 (P04280)	PGKPQGPPAQGGS	1380,68	1380,72	-0,04	-29,41	302	Ser314	314	HexNAc (S)[13]	34 (98)	7	5	1	1		YinOYang prediction hSer8, hSer71, hSer132, hSer193, hSer254, hSer259, hSer314
	GPPPQGGNKPQGPPPPGKPQGPPPQGDKSR	3154,6	3154,61	0	-0,92	43	Ser71	72	HexNAc (S)[29]	39 (99)	3	2	1	0		
	GPPPPGKPQGPPPQGDKSR	2097,07	2097,08	-0,01	-3,72	54	Ser71	72	HexNAc (S)[18]	63 (100)	7	4	1	2		
	GKPQGPPPQGDKSQS	1653,81	1653,86	-0,05	-30,05	120	Ser134	134	dHex (S)[15]	27 (91)	4	1	2	1		
	SPQGGNKPQGPPPPPGKPQ	2027,02	2026,97	0,05	26,02	24	Ser25	42	Hex (S)[1]	43 (98)	1	1	0	0		
	GPPPPGKPQGPPPQGDKS	2077,99	2077,94	0,06	26,8	54	Lys70	71	Glucosylgalactosyl (K)[17]	34 (98)	3	3	0	0		
	KPQGPPPQGDKSQSPRSPPGK	2220,09	2220,07	0,02	7,48	121	Lys131	141	Galacotsyl (K)[11]	32 (97)	3	3	0	0		
	GPPPQGGNKPQGPPPPGKPQGPPPQGDKS	3135,52	3135,59	-0,06	-20,25	43	Lys70	71	Glucosylgalactosyl (K)[28]	73 (100)	4	3	1	0		
	GPPPQGGNKPQGPPPPGKPQGPPAQGGSKS	3138,53	3138,56	-0,03	-8,32	287	Lys313	316	Glucosylgalactosyl (K)[29]	35 (98)	4	3	1	0		
	QGGNKPQGPPPPPGKPQ	1663,86	1663,84	0,01	7,92	26	Gln25	42	Gln->pyro-Glu (N-term Q)[0]	50 (100)	9	5	2	2		
	QNLNEDVSQEESPSLIAGNPQGPSPQGGNKPQ	3379,51	3379,51	0	0,29	1	Gln1,Ser8	32	Gln->pyro-Glu (N-term Q)[0], Phospho (ST)[8]	34 (97)	3	2	1	0	pSer8	NetPhos prediction pSer8, pSer73, pSer76, pSer134, pSer137, pSer195, pSer198, pSer254, pSer256, pSer259, pSer318
	PQGPPPQGDKSRSPRSPPGKPQ	2375,16	2375,22	-0,06	-24,27	61	Ser76	82	Phospho (ST)[16]	65 (99)	6	1	2	3		
	QGPPPQGDKSQSPRSPPGKPQGPPPQ	2726,3	2726,38	-0,08	-29,19	123	Ser134	148	Phospho (ST)[12]	43 (99)	6	2	1	3		

Specie (Uniprot acession number)	Sequence	Calc Mass	Obs Mass	Match Error Da	Match Error PPM	Start Seq Pos	Residue Modified / End Seq Pos	Modification / Ion Score (C.I.%)	N° Individuals (20)	Group (N° Individual) Cancer (10)	Diabetes (5)	Control (5)	Uniprot indication	Prediction site
bPRP2 (P02812	GPPPQGGNKSQGPPPPGKPQ	2125,07	2125,04	0,03	12,94	249	Asn256 / 268	HexNAc (N)[8] / 83 (100)	5	5	0	0	Asn152, Asn214, Asn256	NetNGlyc prediction hAsn152, hAsn214, hAsn256
	GPPPPGKPQGPPPQGDNKSQ	2183,07	2183,04	0,03	13,24	198	Asn214 / 217	HexNAc (N)[17] / 31 (95)	6	4	1	1		
	GPPPQGDNKSQSARSPPGKPQ	2333,15	2333,15	0	-1,71	207	Asn214 / 227	HexNAc (N)[8] / 36 (99)	2	2	0	0		
	GPPPPGKPQGPPPQGDNKSQ	2126,05	2126,03	0,02	10,58	198	Ser232 / 217	dHex (S)[19] / 34 (95)	4	2	2	0		
	GPPPQGGNKPQGPPPPGKPQGPPPQGDKS	3135,52	3135,59	-0,06	-20,25	64	Lys107 / 92	Glucosylgalactosyl (K)[28] / 73 (100)	2	2	0	0		
	QPQGPPRPPQ	1084,55	1084,54	0,02	14,52	382	Gln397 / 391	Gln->pyro-Glu (N-term Q)[0] / 45 (100)	4	1	2	1	pyro-Gln1	
	QGPPRPPQGGRPS	1313,67	1313,66	0,02	11,52	384	Gln399 / 396	Gln->pyro-Glu (N-term Q)[0] / 38 (99)	8	4	2	2		
	QAPPAGQPQGPPRPPQ	1605,81	1605,8	0,01	5,78	376	Gln391 / 391	Gln->pyro-Glu (N-term Q)[0] / 30 (95)	6	1	3	2		
	QGGNQPQGPPPPPGKPQ	1663,82	1663,85	-0,04	-21,42	47	Gln62 / 63	Gln->pyro-Glu (N-term Q)[0] / 98 (100)	6	4	1	1		
	QPQAPPAGQPQGPPRPPQ	1830,92	1830,81	0,11	29	374	Gln389 / 391	Gln->pyro-Glu (N-term Q)[0] / 36 (99)	2	2	0	0		
	QGGNQPQGPPPPPGKPQGPPPQGGNKPQ	2721,35	2721,32	0,03	10,23	47	Gln62 / 74	Gln->pyro-Glu (N-term Q)[0] / 50 (100)	5	1	4	0		
	QQEGNNPQGPPPPAGGNPQQPQAPPAGQPQGPPRPP	3567,71	3567,46	0,25	70,62	355	Gln370 / 390	Gln->pyro-Glu (N-term Q)[0] / 34 (98)	1	1	0	0		
	QEESPSLIAGNPQGAPPQGGNKPQGPPSP	2916,35	2916,38	-0,03	-10,75	9	Ser36 / 37	Phospho (ST) (S)[36] / 36 (100)	6	2	1	3		
bPRP3 Q04118	KPQGPPPQEGNKPQ	1663,83	1663,85	-0,03	-15,48	229	Asn239 / 242	Hex (N)[11] / 38 (100)	5	3	1	1		
	GPPPRPGKPEGPPPQGGNQS	2097,04	2097,08	-0,04	-21,08	54	Ser72 / 73	dHex (S)[20] / 36 (100)	6	1	3	2		

Specie (Uniprot acession number)	Sequence	Calc Mass	Obs Mass	Match Error Da	Match Error PPM	Start Seq Pos	Residue Modified / End Seq Pos	Modification / Ion Score (C.I.%)	Nº Individuals (20)	Group (Nº Individual) Cancer (10)	Diabetes (5)	Control (5)	Uniprot indication	Prediction site
	SQGPPPRPGKPEGPPPQGGNQ	2282,12	2282,1	0,01	5,78	52	**Asn71** / 72	**HexNAc (N)[20]** / 51 (100)	6	4	1	1	hAsn50, hAsn71, hAsn92, hAsn113, hAsn134, hAsn155, hAsn176, hAsn197	NetNGlyc prediction hAsn50, hAsn71, hAsn92, hAsn113, hAsn134, hAsn155, hAsn176, hAsn197
	QPLPPPAGKPQ	1112,61	1112,6	0,01	6,14	262	**Gln277** / 272	**Gln->pyro-Glu (N-term Q)[0]** / 43 (100)	6	1	4	1		
	QGPPPRPGKPE	1142,6	1142,58	0,01	10,04	32	**Gln47** / 42	**Gln->pyro-Glu (N-term Q)[0]** / 36 (99)	3	1	2	0		
	QSQGPPPRPGKPE	1357,69	1357,68	0	1,8	30	**Gln45** / 42	**Gln->pyro-Glu (N-term Q)[0]** / 61 (100)	11	5	4	2		
	QGGRPHRPPQGQPP	1491,76	1491,75	0,01	6,63	279	**Gln294** / 292	**Gln->pyro-Glu (N-term Q)[0]** / 29 (94)	5	1	2	2		
	QGGRPHRPPQGQPPQ	1619,81	1619,78	0,03	21,55	279	**Gln294** / 293	**Gln->pyro-Glu (N-term Q)[0]** / 57 (100)	6	1	3	2		
	QSQGPPPRPGKPEGSPS	1685,82	1685,82	0,01	4,05	198	**Gln213** / 214	**Gln->pyro-Glu (N-term Q)[0]** / 49 (100)	3	1	2	0		
	QSQGPPPRPGKPEGQPPQ	1864,93	1864,92	0,01	5,11	51	**Gln66** / 68	**Gln->pyro-Glu (N-term Q)[0]** / 49 (100)	6	1	3	2		
	QSLNEDVSQEESPSVISGKPEGR	2455,16	2455,16	0	-0,3	1	**Gln1** / 23	**Gln->pyro-Glu (N-term Q)[0]** / 67 (100)	3	2	1	0		
	QSLNEDVSQEESPSVISGKPEGR	2535,12	2535,11	0,01	4,62	1	**Gln1,Ser8** / 23	**Gln->pyro-Glu (N-term Q)[0], Phospho (ST)[8]** / 44 (100)	4	2	2	0		NetPhos prediction pSer8, pSer12, pSer14, pSer17, pSer212, pSer214
bPRP4 P10163	**GPPPPPGKPEGRPPQGGNQ**	2067,03	2067,02	0	2,03	70	**Asn71** / 88	**HexNAc (N)[18]** / 52 (100)	8	4	2	2		NetNGlyc prediction hAsn50, hAsn71, hAsn92, hAsn134, hAsn155, hAsn176, hAsn197, hAsn218
	QRPPPPP	771,41	771,4	0,01	14,8	32	**Gln32** / 38	**Gln->pyro-Glu (N-term Q)[0]** / 52 (100)	2	2	0	0		
	QPQRPPPPP	996,53	996,55	-0,03	-26,85	30	**Gln30** / 38	**Gln->pyro-Glu (N-term Q)[0]** / 62 (100)	6	4	2	0		

Specie (Uniprot acession number)	Sequence	Calc Mass	Obs Mass	Match Error Da	Match Error PPM	Start Seq Pos	Residue Modified / End Seq Pos	Modification / Ion Score (C.I.%)	N° Individuals (20)	Group (N° Individual) Cancer (10)	Diabetes (5)	Control (5)	Uniprot indication	Prediction site
	QGPPPHPGKPE						**Gln74**	**Gln->pyro-Glu (N-term Q)[0]**	6	1	4	1		
		1123,55	1123,54	0,02	14,56	74	84	37 (99)						
	QGPPPPPQGGRPP						**Gln272**	**Gln->pyro-Glu (N-term Q)[0]**	1	1	0	0		
		1264,64	1264,63	0,01	8,49	272	284	51 (100)						
	QSQGPPPHPGKPE						**Gln72**	**Gln->pyro-Glu (N-term Q)[0]**	4	3	1	0		
		1338,64	1338,64	0,01	6,11	72	84	73 (100)						
	QSHRPPPPPGKPE						**Gln177**	**Gln->pyro-Glu (N-term Q)[0]**	2	2	0	0		
		1406,72	1406,71	0,01	3,82	177	189	46 (100)						
	QSQGPPPPPGKPEGRPP						**Gln51**	**Gln->pyro-Glu (N-term Q)[0]**	3	1	1	1		
		1705,87	1705,84	0,03	16,64	51	67	62 (100)						
	QSQGPPPHPGKPERPPP						**Gln72**	**Gln->pyro-Glu (N-term Q)[0]**	1	1	0	0		
		1785,9	1785,85	0,05	27,76	72	88	55 (100)						
	QSQGPPPHPGKPEGPPPQ						**Gln197**	**Gln->pyro-Glu (N-term Q)[0]**	1	1	0	0		
		1814,88	1814,83	0,05	28,25	197	214	36 (99)						
	QSQGPPPHPGKPEGPPPQEGNKS						**Gln197**	**Gln->pyro-Glu (N-term Q)[0]**	1	1	0	0		
		2330,12	2330,09	0,03	12,24	197	219	29 (96)						
	QSQGPPPHPGKPEGPPPQEGNKSR						**Gln197**	**Gln->pyro-Glu (N-term Q)[0]**	2	2	0	0		
		2486,22	2486,2	0,02	7,27	197	220	33 (98)						
aPRP P02810	**DSEQFIDEER**						**Ser22**	**Glucuronyl (S)[2]**	5	1	2	2	pSer8, pSer17, pSer22	NetPhos prediction pSer8, pSer22, pSer43
		1443,58	1443,61	-0,03	-20,84	21	30	45 (100)						
	DSEQFIDEERQGPPLGGQQSQPS						**Ser22**	**Glucuronyl (S)[2]**	6	1	2	3		
		2705,18	2705,10	0,08	29,33	21	43	48 (100)						
	DSEQFIDEERQGPPLGGQQ						**Ser22**	**Glucuronyl (S)[2]**	6	1	2	3		
		2306,01	2305,97	0,03	14,50	21	39	52 (100)						
	GGDSEQFIDEER						**Ser22**	**Phospho (ST) (S)[4]**	16	10	2	4		
		1461,54	1461,55	0,00	-2,67	19	30	70 (100)						
	DGGDSEQFIDEER						**Ser22**	**Phospho (ST) (S)[5]**	12	4	4	4		
		1576,57	1576,57	0,00	2,92	18	30	64 (100)						
	GGDSEQFIDEERQ						**Ser22**	**Phospho (ST) (S)[4]**	11	4	3	4		
		1589,60	1589,60	0,01	4,40	19	31	50 (100)						

	DGGDSEQFIDEERQ					**Ser22**	**Phospho (ST) (S)[5]**	8	2	4	2		
	1704,63	1704,63	0,00	0,70	18	31	63 (100)						
	VISDGGDSEQFIDEER					**Ser22**	**Phospho (ST) (S)[8]**	1	1	0	0		
	1875,75	1875,74	0,01	5,38	15	30	47 (100)						
	GGDSEQFIDEERQGPPL					**Ser22**	**Phospho (ST) (S)[4]**	7	1	4	2		
	1953,81	1953,83	-0,01	-7,57	19	35	78 (100)						
	VISDGGDSEQFIDEERQ					**Ser22**	**Phospho (ST) (S)[8]**	1	1	0	0		
	2003,81	2003,82	-0,01	-3,54	15	31	72 (100)						
	GGDSEQFIDEERQGPPLG					**Ser22**	**Phospho (ST) (S)[4]**	4	1	2	1		
	2010,83	2010,85	-0,01	-6,32	19	36	78 (100)						
	GGDSEQFIDEERQGPPLGG					**Ser22**	**Phospho (ST) (S)[4]**	17	9	5	3		
	2067,86	2067,85	0,01	3,82	19	37	80 (100)						
	GGDSEQFIDEERQGPPLGGQ					**Ser22**	**Phospho (ST) (S)[4]**	9	4	4	1		
	2195,91	2195,88	0,03	13,93	19	38	69 (100)						
	DVPLVISDGGDSEQFIDEER					**Ser22**	**Phospho (ST) (S)[12]**	4	2	2	0		
	2299,99	2300,01	-0,02	-9,65	11	30	66 (100)						
	GGDSEQFIDEERQGPPLGGQQ					**Ser22**	**Phospho (ST) (S)[4]**	15	6	4	5		
	2323,97	2323,91	0,06	25,09	19	39	82 (100)						
	DGGDSEQFIDEERQGPPLGGQQ					**Ser22**	**Phospho (ST) (S)[5]**	9	4	4	1		
	2439,00	2438,99	0,01	2,99	18	39	51 (100)						
	GGDSEQFIDEERQGPPLGGQQSQPS					**Ser22**	**Phospho (ST) (S)[4]**	7	1	4	2		
	2723,15	2723,07	0,08	28,06	19	43	28 (100)						
	VISDGGDSEQFIDEERQGPPLGGQQ					**Ser22**	**Phospho (ST) (S)[8]**	3	1	2	0		
	2738,18	2738,19	-0,01	-3,10	15	39	50 (100)						
	DGGDSEQFIDEERQGPPLGGQQSQPS					**Ser22**	**Phospho (ST) (S)[5]**	4	1	2	1		
	2838,18	2838,10	0,08	27,87	18	43	38 (100)						

VI. GENERAL DISCUSSION

1. General discussion

Diabetes mellitus is one of the fastest growing causes of death in Portugal and the European Union (Pordata 2012). The key symptom of the disease is hyperglycemia, which is the basis for the clinical diagnosis of DM (World Health Organization. 2006; Gardner, Shoback et al. 2011). The regulation of glycemia is orchestrated by the endocrine pancreas, mainly through the secretion of glucagon and insulin. In diabetic patients, there is a disturbance of glycemic control either by the impairment of insulin production and/or the development of resistance to insulin in its key targets: adipose and muscle tissues. However, despite the common symptoms, the aetiology of DM is diverse and several types have been defined.

A common set of complications is usually present in every type of DM, namely neuropathy, nephropathy, retinopathy and a series of cardiovascular problems. Most of these complications share a close relation to vascular dysfunction. It has been described a relation between hyperglycemia and endothelial dysfunction, which justifies an in-depth study of the endothelium response to the imbalances present in DM (Bakker, Eringa et al. 2009; Bucciarelli, Pollreisz et al. 2009; Abebe and Mozaffari 2010; Avogaro, Albiero et al. 2011). However, because of the systemic effects observed in DM, the use of cell culture approaches fails to adequately reproduce the systemic response that contains numerous stimuli from the diverse organs affected by hyperglycemia (Chavakis, Bierhaus et al. 2004; Schalkwijk and Stehouwer 2005; Son 2007; Packard and Libby 2008; Maugeri, Rovere-Querini et al. 2009). It is thus necessary to perform direct analyses of the endothelium to unravel the underlying mechanisms of hyperglycemia-associated endothelial dysfunction.

Another frequent complication of DM is the elevated incidence of oral diseases (Sreebny, Yu et al. 1992; Ryan, Carnu et al. 2003; Lamster, Lalla et al. 2008; Yeh, Harris et al. 2012). Diabetic patients regularly

complain from a sensation of dry-mouth, which is termed xerostomia, and is associated with a decrease in the flow rates of salivary secretion (Sreebny, Yu et al. 1992; Anderson, Garrett et al. 1993). This suggests that hyperglycemia is somehow affecting salivary gland secretion, and it has been described a loss of tissue integrity and leucocytic infiltrations in the salivary glands of hyperglycemic animal models (Cutler, Pinney et al. 1979; Anderson, Suleiman et al. 1994). Additionally, diabetic patients often suffer from gingivitis, progressing to periodontitis, which affects also the connective tissues underneath gingiva and could progress to severe loss of connective tissue, alveolar bone and teeth. These complications are suggested to be connected to an increased inflammatory response of the organism to the bacteria present in the bacterial biofilm overlaying the oral cavity as a consequence of impaired wound healing and neutrophil chemotaxis, also associated to endothelial dysfunction (Lakschevitz, Aboodi et al. 2011).

The first challenge of every study, such as the present one, is the choice of an adequate model to study the effects intended. The choice of an animal model allows a tighter control of the variables and provides more meaningful results with a smaller sample size. In the field of diabetes, there are several animal models in use (Shafrir and Sima 2003; Rees and Alcolado 2005). A careful weighting of the pros and cons of several models was conducted (Table 3), and it was selected a streptozotocin-induced hyperglycemia model, which is also one of the more frequent models used. Considering that the direct study of endothelial cells would require a rather large number of cells, and in vitro proliferation was not a viable choice for the loss of the systemic stimuli, given the alternatives of using a mouse or rat model, it was selected the rat for its larger size and potential larger number of endothelial cells. Having chosen the animal model, an experimental plan had to be designed. A preliminary study was conducted with a small number of animals to verify the feasibility of endothelial cell isolation and the assessment of endothelial damage and repair ability by flow cytometry.

The endothelial cell isolation was performed with magnetic beads and was successfully confirmed by fluorescence microscopy. With only one month of hyperglycemia, it was also observable significant changes in the levels of circulating EPC and CEC, confirming the adequateness of the chosen model. However, it was also intended to study salivary glands and existing literature indicated that morphological changes in salivary glands only occurred after 3 months of hyperglycemia (Anderson, Suleiman et al. 1994). As such, it was chosen to design an experimental plan with time points at 2 and 4 months.

Despite the successful isolation of endothelial cells achieved in the preliminary study, the number of isolated cells was probably not enough to conduct proteomic studies and it was not possible to analyse the proteins involved in cell proliferation and impairment, nor the direct binding of MBL from the complement system to endothelial cells. Nonetheless, it was possible to observe a highly significant increase of CEC, which suggests a strong endothelial damage. Moreover, despite a lower number of circulating EPC, there was a stimulus to cell proliferation by the increased levels of VEGF and BrdU incorporation in aortic endothelial cells. Additionally, an increased specific-activity of the MBL pathway of activation of the complement system, still suggests that complement activation and endothelial dysfunction are linked, as suggested by some other reports (Hansen, Tarnow et al. 2004; Hovind, Hansen et al. 2005; Ostergaard, Hansen et al. 2005; Saraheimo, Forsblom et al. 2005; Ostergaard, Thiel et al. 2007; Elawa, AoudAllah et al. 2011; Ostergaard, Bjerre et al. 2012; Pavlov, La Bonte et al. 2012; Ostergaard, Bjerre et al. 2013).

Regarding the effects on salivary glands, it was observed that there is a distinct effect in short- and long-term exposure to hyperglycemia in the submandibular. An acute response in the short-term shows more pronounced variations of the proteome composition, which is attenuated in the long-term, suggesting a mechanism of adaptation to the chronic hyperglycemia. Interestingly, it was observed an increase of proteins

related to vesicular transport and secretion despite the reported decrease in salivary flow-rate. This suggests the lower flow is somehow stimulating the gland to increase the secretory activity, although it is not yet possible to fully understand why such stimulus fails to produce results. A possible link between the decrease of kallikrein expression, increased inflammation and reduced proliferation stimuli may be related to this impairment. Kallikreins are mostly secreted by duct cells, which are the first to be affected by hyperglycemia (Anderson, Suleiman et al. 1994), and are responsible by the release of the kinin peptide from kininogen, which may have a proliferative effect, as salivary glands express kinin receptors (Mahabeer, Naidoo et al. 2000; Dlamini and Bhoola 2005). A decreased expression of kallikreins may be responsible for the impairment in salivary gland regeneration, which is further enhanced by the lack of the proliferative effect of insulin. Moreover, the extremely pronounced increase of the apoptosis-trigger protein S100A6 is certainly related to the loss of glandular mass and function.

Because the pathogenesis of periodontal disease is linked to an hyper-inflammatory response, impaired neutrophil activity and the formation of advanced glycation endproducts (Lakschevitz, Aboodi et al. 2011), an analysis of post-translational modifications in the major family of salivary proteins was also conducted. However, rodents do not normally secrete of proline-rich proteins as do humans (Carlson 1993). So, this study was conducted using human saliva from 3 test groups: control, diabetic and head and neck cancer patients. A higher frequency of N-glycosylated PRP fragments was observed in cancer patients in accordance to the literature (Satomaa, Heiskanen et al. 2009). However, it was observed an increased frequency of pyroglutamate-modified fragments in diabetic patients, which taken together with posterior reports from our group where increased proteolytic activity and pyroglutamate modification of bPRP3 and bPRP4 fragments in diabetic patients with vascular complications were shown (Caseiro, Ferreira et al. 2012; Caseiro, Ferreira

et al. 2013), may suggest it as a potential biomarker for oral complications.

In conclusion, it is reported that different epithelial-derived tissues have distinct responses to hyperglycemia. The endothelium presents a progressive damage and a shift of the repair mechanisms towards an angiogenic process, while salivary glands present an acute and a chronic response that suggests an adaptation to chronic hyperglycemia in terms of protein expression. Moreover, the analysis of post-translational modifications in human proline-rich proteins, suggests that the increase of pyroglutamate-modified fragments may be a potential biomarker for diabetic susceptibility to oral complications.

2. References

Abebe, W. and M. Mozaffari (2010). "Endothelial dysfunction in diabetes: potential application of circulating markers as advanced diagnostic and prognostic tools." EPMA J **1**(1): 32-45.

Anderson, L. C., J. R. Garrett, A. H. Suleiman, G. B. Proctor, K. M. Chan and R. Hartley (1993). "In vivo secretory responses of submandibular glands in streptozotocin-diabetic rats to sympathetic and parasympathetic nerve stimulation." Cell Tissue Res **274**(3): 559-566.

Anderson, L. C., A. H. Suleiman and J. R. Garrett (1994). "Morphological effects of diabetes on the granular ducts and acini of the rat submandibular gland." Microsc Res Tech **27**(1): 61-70.

Avogaro, A., M. Albiero, L. Menegazzo, S. de Kreutzenberg and G. P. Fadini (2011). "Endothelial dysfunction in diabetes: the role of reparatory mechanisms." Diabetes Care **34 Suppl 2**: S285-290.

Bakker, W., E. C. Eringa, P. Sipkema and V. W. van Hinsbergh (2009). "Endothelial dysfunction and diabetes: roles of hyperglycemia, impaired insulin signaling and obesity." Cell Tissue Res **335**(1): 165-189.

Bucciarelli, L. G., A. Pollreisz, M. Kebschull, A. Ganda, A. Z. Kalea, B. I. Hudson, Y. S. Zou, E. Lalla, R. Ramasamy, P. C. Colombo, A. M. Schmidt and S. F. Yan (2009). "Inflammatory stress in primary venous and aortic endothelial cells of type 1 diabetic mice." Diab Vasc Dis Res **6**(4): 249-261.

Carlson, D. M. (1993). "Salivary proline-rich proteins: biochemistry, molecular biology, and regulation of expression." Crit Rev Oral Biol Med **4**(3-4): 495-502.

Caseiro, A., R. Ferreira, A. Padrao, C. Quintaneiro, A. Pereira, R. Marinheiro, R. Vitorino and F. Amado (2013). "Salivary Proteome and Peptidome Profiling in Type 1 Diabetes Mellitus Using a Quantitative Approach." J Proteome Res.

Caseiro, A., R. Ferreira, C. Quintaneiro, A. Pereira, R. Marinheiro, R. Vitorino and F. Amado (2012). "Protease profiling of different biofluids in type 1 diabetes mellitus." Clinical Biochemistry **45**(18): 1613-1619.

Chavakis, T., A. Bierhaus and P. P. Nawroth (2004). "RAGE (receptor for advanced glycation end products): a central player in the inflammatory response." Microbes Infect **6**(13): 1219-1225.

Cutler, L. S., H. E. Pinney, C. Christian and S. B. Russotto (1979). "Ultrastructural studies of the rat submandibular gland in streptozotocin induced diabetes mellitus." Virchows Arch A Pathol Anat Histol **382**(3): 301-311.

Dlamini, Z. and K. D. Bhoola (2005). "Upregulation of tissue kallikrein, kinin B1 receptor, and kinin B2 receptor in mast and giant cells infiltrating oesophageal squamous cell carcinoma." J Clin Pathol **58**(9): 915-922.

Elawa, G., A. M. AoudAllah, A. E. Hasaneen and A. M. El-Hammady (2011). "The predictive value of serum mannan-binding lectin levels for diabetic control and renal complications in type 2 diabetic patients." Saudi Med J **32**(8): 784-790.

Gardner, D. G., D. M. Shoback and F. S. Greenspan (2011). Greenspan's basic & clinical endocrinology. New York, McGraw-Hill Medical.

Hansen, T. K., L. Tarnow, S. Thiel, R. Steffensen, C. D. Stehouwer, C. G. Schalkwijk, H. H. Parving and A. Flyvbjerg (2004). "Association between mannose-binding lectin and vascular complications in type 1 diabetes." Diabetes **53**(6): 1570-1576.

Hovind, P., T. K. Hansen, L. Tarnow, S. Thiel, R. Steffensen, A. Flyvbjerg and H. H. Parving (2005). "Mannose-binding lectin as a predictor of microalbuminuria in type 1 diabetes: an inception cohort study." Diabetes **54**(5): 1523-1527.

Lakschevitz, F., G. Aboodi, H. Tenenbaum and M. Glogauer (2011). "Diabetes and periodontal diseases: interplay and links." Curr Diabetes Rev **7**(6): 433-439.

Lamster, I. B., E. Lalla, W. S. Borgnakke and G. W. Taylor (2008). "The relationship between oral health and diabetes mellitus." J Am Dent Assoc **139 Suppl**: 19S-24S.

Mahabeer, R., S. Naidoo and D. M. Raidoo (2000). "Detection of Tissue Kallikrein and Kinn B1 and B2 Receptor mRNAs in Human Brain by In Situ RT-PCR." Metabolic Brain Disease **15**(4): 325-335.

Maugeri, N., P. Rovere-Querini, M. Baldini, M. G. Sabbadini and A. A. Manfredi (2009). "Translational mini-review series on immunology of vascular disease: mechanisms of vascular inflammation and remodelling in systemic vasculitis." Clin Exp Immunol **156**(3): 395-404.

Ostergaard, J., T. K. Hansen, S. Thiel and A. Flyvbjerg (2005). "Complement activation and diabetic vascular complications." Clin Chim Acta **361**(1-2): 10-19.

Ostergaard, J., S. Thiel, M. Gadjeva, T. K. Hansen, R. Rasch and A. Flyvbjerg (2007). "Mannose-binding lectin deficiency attenuates renal changes in a streptozotocin-induced model of type 1 diabetes in mice." Diabetologia **50**(7): 1541-1549.

Ostergaard, J. A., M. Bjerre, F. Dagnaes-Hansen, T. K. Hansen, S. Thiel and A. Flyvbjerg (2013). "Diabetes-induced changes in mannan-binding lectin levels and complement activation in a mouse model of type 1 diabetes." Scand J Immunol **77**(3): 187-194.

Ostergaard, J. A., M. Bjerre, S. P. RamachandraRao, K. Sharma, J. R. Nyengaard, T. K. Hansen, S. Thiel and A. Flyvbjerg (2012). "Mannan-binding lectin in diabetic kidney disease: the impact of mouse genetics in a type 1 diabetes model." Exp Diabetes Res **2012**: 678381.

Packard, R. R. and P. Libby (2008). "Inflammation in atherosclerosis: from vascular biology to biomarker discovery and risk prediction." Clin Chem **54**(1): 24-38.

Pavlov, V. I., L. R. La Bonte, W. M. Baldwin, M. M. Markiewski, J. D. Lambris and G. L. Stahl (2012). "Absence of mannose-binding lectin prevents hyperglycemic cardiovascular complications." Am J Pathol **180**(1): 104-112.

Pordata (2012). Pordata - Base de dados Portugal contemporâneo. Lisboa, Portugal, Fundação Francisco Manuel dos Santos.

Rees, D. A. and J. C. Alcolado (2005). "Animal models of diabetes mellitus." Diabet Med **22**(4): 359-370.

Ryan, M. E., O. Carnu and A. Kamer (2003). "The influence of diabetes on the periodontal tissues." J Am Dent Assoc **134 Spec No**: 34S-40S.

Saraheimo, M., C. Forsblom, T. K. Hansen, A. M. Teppo, J. Fagerudd, K. Pettersson-Fernholm, S. Thiel, L. Tarnow, P. Ebeling, A. Flyvbjerg and P. H. Groop (2005). "Increased levels of mannan-binding lectin in type 1 diabetic patients with incipient and overt nephropathy." Diabetologia **48**(1): 198-202.

Satomaa, T., A. Heiskanen, I. Leonardsson, J. Angstrom, A. Olonen, M. Blomqvist, N. Salovuori, C. Haglund, S. Teneberg, J. Natunen, O. Carpen and J. Saarinen (2009). "Analysis of the human cancer glycome identifies a novel group of tumor-associated N-acetylglucosamine glycan antigens." Cancer Res **69**(14): 5811-5819.

Schalkwijk, C. G. and C. D. Stehouwer (2005). "Vascular complications in diabetes mellitus: the role of endothelial dysfunction." Clin Sci (Lond) **109**(2): 143-159.

Shafrir, E. and A. A. F. Sima (2003). Animal Models in Diabetes: A Primer, Taylor & Francis.

Son, S. M. (2007). "Role of vascular reactive oxygen species in development of vascular abnormalities in diabetes." Diabetes Res Clin Pract **77 Suppl 1**: S65-70.

Sreebny, L. M., A. Yu, A. Green and A. Valdini (1992). "Xerostomia in diabetes mellitus." Diabetes Care **15**(7): 900-904.

World Health Organization. (2006). Definition and diagnosis of diabetes mellitus and intermediate hyperglycemia: report of a WHO/IDF consultation. Geneva, Switzerland, World Health Organization.

Yeh, C. K., S. E. Harris, S. Mohan, D. Horn, R. Fajardo, Y. H. Chun, J. Jorgensen, M. Macdougall and S. Abboud-Werner (2012). "Hyperglycemia and xerostomia are key determinants of tooth decay in type 1 diabetic mice." Lab Invest **92**(6): 868-882.